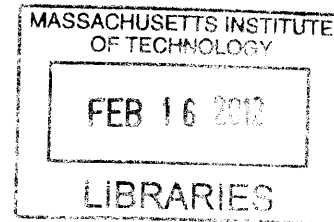


Development of a Floating Piston Expander Control Algorithm for a Collins-Type Cryocooler

by

Jake Hogan



B.S., Mechanical Engineering, Electrical Engineering
Colorado School of Mines, Colorado, 2009

ARCHIVES

Submitted to the Department of Mechanical Engineering in Partial
Fulfillment of the Requirements for the Degree of Master of Science in
Mechanical Engineering


at the

Massachusetts Institute of Technology

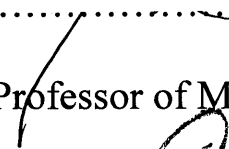
February 2012

©2012 Massachusetts Institute of Technology
All Rights Reserved

Signature of Author.....

 Jake Hogan
Department of Mechanical Engineering
November 21, 2011

Certified by.....

 John G. Brisson
Professor of Mechanical Engineering
Thesis Supervisor

Accepted by.....

 David E. Hardt
Chairman, Department Committee on Graduate Students

Development of a Floating Piston Expander Control Algorithm for a Collins-Type Cryocooler

by

Jake Hogan

Submitted to the Department of Mechanical Engineering on November 21, 2011 in Partial Fulfillment of the Requirements for the Degree of Master of Science in Mechanical Engineering

ABSTRACT

The multi-stage Collins-type cryocooler uses a floating piston design for the working fluid expansion in each stage. The piston floats between a cold volume, where the working fluid is expanded, and a warm volume. The piston's motion is controlled by opening and closing valves connecting several reservoirs at various pressures to the warm volume. Ideally, these pressures should be distributed between the high and low system pressure to gain good control of the piston motion. In past prototypes, helium flow through the piston-cylinder gap resulted in a loss of pressure in the reservoirs causing the piston to become immobile. A more complex control algorithm is required to maintain a net zero helium flow through this gap to allow for steady expander operation.

A numerical quasi-steady thermodynamic model is developed for the piston cycle. The model determines the steady state pressure distribution of the reservoirs for an ideal expander with no helium flow through the piston-cylinder gap. This pressure distribution is dependent on the total mass of helium in pressure reservoirs as well as the points at which the warm helium intake as well as the cold helium exhaust end. The pressures in the pressure reservoirs show varying levels of dependence on the lengths of the intake and exhaust strokes.

The model is extended to include helium flow through the gap and the inertia of the piston. The model is then used to determine how helium can be added to or removed from the reservoirs in the case that there is too much helium flow through the gap. These results are then integrated into a control algorithm that maintains zero net mass flow through the gap in each expander stage.

Thesis Supervisor: John G. Brisson
Title: Professor of Mechanical Engineering

ACKNOWLEDGEMENTS

I would like to thank Professor Brisson for his support and guidance throughout my research. He always made himself available and taught me so much. I would also like to thank Chuck Hannon and AMTI for their support of this research. Chuck was a great resource throughout the project.

I would also like to thank my lab mates for their friendship and support over the last couple of years. It was great to have a group of people to ask for help with a problem. I'll always remember our Friday tradition. A special thank you goes to Kevin and Cristi for graciously giving up their second bedroom to me while I was finishing up this thesis.

Lastly, I must thank my family for all of their support. They were constantly there with words of encouragement to keep me going. Most of all I have to thank my wife, Keri. You were always there for me when I thought I couldn't make it and for that I will always be grateful.

TABLE OF CONTENTS

Chapter 1: Introduction and Background	9 -
1.1 Background	9 -
1.2 The Collins Cycle.....	10 -
1.3 The floating piston expander.....	13 -
1.4 Previous Work.....	15 -
1.5 Motivation	16 -
1.6 About this thesis	17 -
Chapter 2: Expander Modeling.....	18 -
2.1 Expander Cycle Description.....	18 -
2.2 Development of an ideal model for each process	21 -
2.3 Cutoff and Recompression volume study	27 -
2.4 Total warm helium mass study	34 -
2.5 Valve Flow	37 -
2.6 Reservoir Volume Size.....	41 -
2.7 Chapter 2 summary	46 -
Chapter 3: Floating Piston Expander Control Algorithm	48 -
3.1 Expander model with helium blow-by	48 -
3.2 Steady State operation of the expander	61 -
3.3 Adding mass to the warm volume.....	64 -
3.4 Removing mass from the warm volume	73 -
3.5 Controlling steady state expander operation	81 -
3.6 Expander startup and shut down	87 -
3.7 Chapter 3 Summary.....	91 -
Chapter 4: Conclusion	93 -
Bibliography	96 -
Appendix A.....	97 -
Appendix B	104 -
Appendix C	108 -
Appendix D.....	109 -

LIST OF FIGURES

Figure 1.1 The standard Collins-type helium liquefier.....	- 10 -
Figure 1.2 Collins cycle T-s diagram.....	- 11 -
Figure 1.3 Modified Collins cryocooler for current design.....	- 12 -
Figure 1.4 Expander schematic with pressure reservoirs.....	- 13 -
Figure 1.5 Expander used by Hannon et al with bleed line throttles.....	- 16 -
Figure 2.1 Expander cycle dimensionless indicator diagram.....	- 19 -
Figure 2.2 Ideal Expander Cycle Samples.....	- 29 -
Figure 2.3 High V_{rec} expander cycle samples.....	- 30 -
Figure 2.4 Low V_{co} expander cycle samples.....	- 30 -
Figure 2.5 Reservoir pressure vs. cutoff volume.....	- 31 -
Figure 2.6 Reservoir pressure vs. recompression volume.....	- 32 -
Figure 2.7 Average reservoir pressure vs. steady state reservoir pressure.....	- 34 -
Figure 2.8 Average pressure indicator diagrams.....	- 36 -
Figure 2.9 Cold Valve Schematics.....	- 38 -
Figure 2.10 Reservoir Volume Flow.....	- 42 -
Figure 3.1 Gap flow model.....	- 50 -
Figure 3.2 Effect of friction force coefficient on net blow-by mass flow rate.....	- 57 -
Figure 3.3 Sample first stage expander model with piston inertia.....	- 58 -
Figure 3.4 First stage acceleration and velocity during intake.....	- 59 -
Figure 3.5 Sample second stage expander model with piston inertia.....	- 60 -
Figure 3.6 First stage expander model with no touchdown after 100 cycles.....	- 62 -
Figure 3.7 Second stage expander after 100 iterations.....	- 63 -
Figure 3.8 First stage indicator diagram for low mean reservoir pressure.....	- 66 -
Figure 3.9 Second stage indicator diagram for no addition with low mean pressure.....	- 67 -
Figure 3.10 First stage indicator diagram for early helium addition.....	- 68 -
Figure 3.11 Second stage indicator diagram for early helium addition.....	- 68 -
Figure 3.12 First stage indicator diagram for helium addition near target pressure.....	- 69 -
Figure 3.13 Second stage indicator diagram for helium addition near target pressure.....	- 70 -
Figure 3.14 First stage indicator diagram after helium addition.....	- 71 -
Figure 3.15 Second stage indicator diagram after helium addition.....	- 71 -
Figure 3.16 First stage reservoir pressures plotted over time.....	- 72 -
Figure 3.17 Second stage reservoir pressures plotted over time.....	- 73 -
Figure 3.18 First stage high pressure model.....	- 75 -
Figure 3.19 Second stage high pressure model.....	- 76 -
Figure 3.20 First stage helium reduction expander model.....	- 77 -
Figure 3.21 Second stage helium reduction expander model.....	- 77 -
Figure 3.22 First stage helium reduction normal operation.....	- 78 -
Figure 3.23 Second stage helium reduction normal operation.....	- 79 -

Figure 3.24 First stage reservoir pressures plotted over time - 80 -

Figure 3.25 Second stage reservoir pressures plotted over time..... - 80 -

Figure 3.26 Indicator diagram for the switch state constants.. - 81 -

Figure 3.27 Indicator diagram for switch states when two reservoir pressures are switched. - 83 -

Figure 3.28 The reservoir pressures plotted over time.. - 84 -

Figure 3.29 Control diagram for steady state expander operation..... - 86 -

Figure 3.30 First cycle of expander start up.. - 89 -

Figure 3.31 Expander startup after 10 cycles..... - 89 -

Figure 3.32 Expander startup after 20 cycles..... - 90 -

Figure 3.33 The reservoir pressures plotted over time for startup..... - 90 -

LIST OF TABLES

Table 2.1 Reservoir Temperature Results.....	- 45 -
Table 3.1 Simple control scheme for expander model.	- 61 -
Table 3.2 Reservoir switch conditions for expansion and recompression.....	- 62 -
Table 3.3 Switch states for expander operation.	- 87 -
Table B.1 The nondimensional cutoff and recompression volumes.....	- 104 -
Table B.2 Reservoir A pressures and corresponding recompression and cutoff volumes.....	- 104 -
Table B.3 Reservoir B pressures and corresponding recompression and cutoff volumes.....	- 105 -
Table B.4 Reservoir C pressures and corresponding recompression and cutoff volumes.....	- 106 -
Table B.5 Reservoir D pressures and corresponding recompression and cutoff volumes.....	- 107 -
Table C.1 Assumptions applying to the pressure reservoirs.....	- 108 -
Table C.2 Assumptions applying to the expander intake, expander exhaust, the warm volume, and the cold volume.	- 108 -

Chapter 1: Introduction and Background

1.1 Background

NASA's future plans include long distance missions that will require the storage of cryogenic fuels (liquid oxygen and liquid hydrogen) in low earth orbit. Temperatures in low earth orbit can be as high as 250 K [1], well above the atmospheric boiling points of oxygen (90 K) and hydrogen (20 K). It becomes apparent then that the long term storage of cryogenic fuels in low earth orbit will require active cooling and management.

The modified Collins cryocooler, discussed in this work, is being developed by AMTI and MIT in response to this need. The most significant innovation in this machine over previous Collins-type machines is the use of a floating piston in the expander. The floating piston design eliminates the mechanical linkages in the expander and utilizes electronic "smart valves" for piston actuation. In previous work on this type of expander gas flow around the floating piston reduced the performance of the expander and, on occasion, contributed to the stopping of the expander's cyclic operation. In this work expander models have been developed to investigate the effects of leakage across the piston and to develop control algorithms to permit steady operation of the expander.

In what follows, the differences between the Collins cycle and the modified Collins cycle as well as the benefits of using a modified Collins machine over a traditional Collins machine are clarified. The significance of the floating piston expander design is also explained.

Additionally, previous work on the modified Collins cryocooler and the performance of the previous prototype are discussed.

1.2 The Collins Cycle

In 1946, Dr. Samuel C. Collins developed an efficient cryostat that, for the first time, produced liquid helium in a safe and cost effective manner [2]. The machine is safer because it eliminates the need to use hazardous cryogenic hydrogen as a precooling fluid. Additionally, hydrogen has a freezing point at roughly 14 Kelvin so helium is the only feasible working fluid below this temperature. The Collins liquefier uses multiple stages of heat exchangers and expanders to cool high pressure helium as shown in Figure 1.1. High pressure helium is passed through a series of heat exchangers that are in counter flow with low temperature and low pressure helium. At each expander stage, some of the helium in the high pressure line is expanded and re-circulated into the low pressure helium return. This increases the pre-cooling of

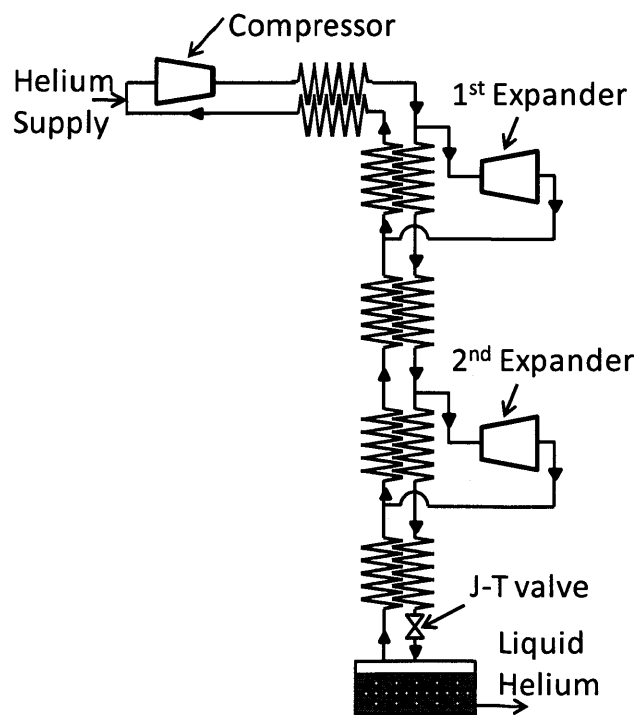


Figure 1.1 The standard Collins-type helium liquefier.

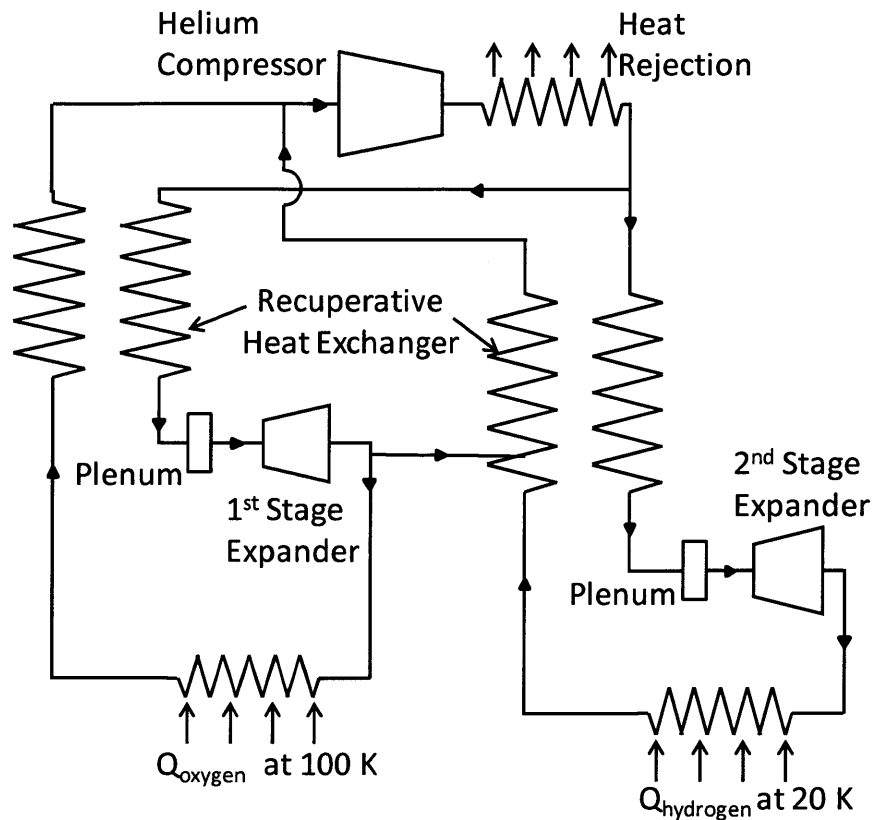


Figure 1.3 Modified Collins cryocooler for current design. The first stage is designed for 100 W at 100 K with a liquid oxygen based heat load and the second stage is designed for 25 W at 20 K with a liquid hydrogen based heat load.

compressor in parallel (as opposed to the traditional Collins machine shown in Figure 1.1 where all cooling stages are connected in series) with a small pre-cooling flow from the high temperature stage to the low temperature stage. Additional stages can be added for new heat loads or to achieve lower temperatures. Segado et. al. [3] showed that adding a second expander to each stage could increase the efficiency of the machine but the increased difficulty of constructing two expanders in each stage outweighs the added benefit.

Each stage has a separate recuperative heat exchanger that, with the exception of the precooling flow from the first stage to the second stage, does not interact with any other stage.

In the first stage, helium that is exhausted from the expander is passed through a heat exchanger in contact with the liquid oxygen heat load to provide cooling. Before reaching the liquid oxygen load, a portion of the helium is bled off to the second stage recuperative heat exchanger. In the second stage, expanded helium is passed through a heat exchanger to cool the liquid hydrogen heat load. The cryocooler is designed to provide 100 Watts of cooling at 100 K to the liquid oxygen and 25 Watts of cooling at 20 K to the liquid hydrogen.

1.3 The floating piston expander

The expander utilizes a novel floating piston design, shown by the sample diagram of a single stage in Figure 1.4. A feature of this design is that there are no mechanical linkages to the

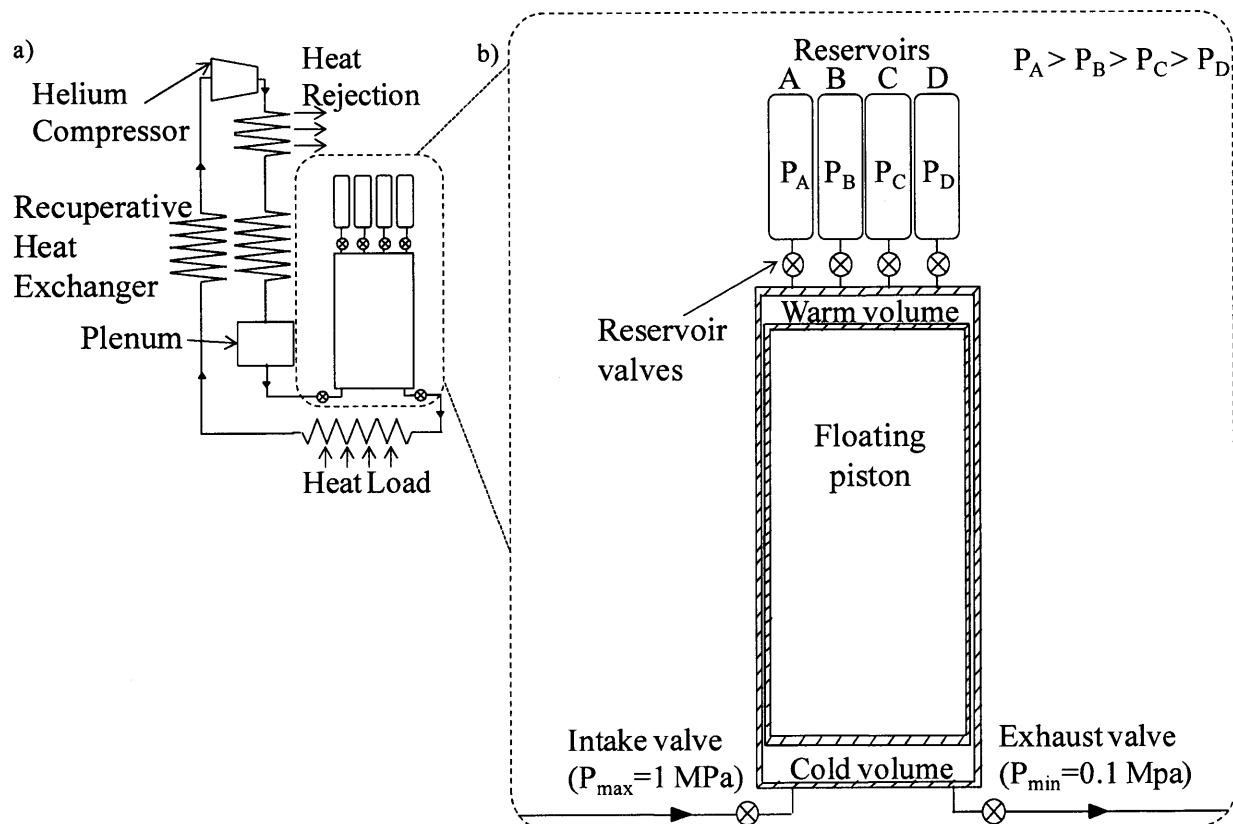


Figure 1.4 Expander schematic with pressure reservoirs. a) A single stage of the modified Collins design. b)

A schematic of the floating piston design for the expander.

piston. The piston resides inside a cylinder attached to four pressure reservoir valves, a high pressure intake valve and a low pressure exhaust valve.

From the discharge port of the compressor and after the heat exchanger used for heat rejection to the environment, high pressure helium is cooled in the recuperative heat exchanger (shown in Figure 1.3 and Figure 1.4). The cooled, high pressure helium then fills a plenum which is connected to the cylinder's cold volume. The plenum ensures a constant supply of high pressure gas in the steady state. In the operation of the expander, the motion of the piston is controlled during the expansion and recompression of the working fluid by selectively and cyclically connecting the piston-cylinder's warm volume to four pressure reservoirs (shown in Figure 1.4) while the opening and closing of the intake and exhaust valves also control the piston motion during the intake and exhaust processes, respectively. These valves allow for computer control of the expander. In the steady state, the pressures in the pressure reservoirs are distributed between the discharge pressure (1 MPa) and suction pressure (0.1 MPa) of the compressor. A more thorough description of the expander cycle can be found in Chapter 2.

A feature of the floating piston design is that there is no sliding seal between and piston and cylinder. This is an intentional feature because a contact seal in this gap would require maintenance that is unacceptable in a space flight application. Unfortunately, this feature comes at a cost as there can be a net flow of helium around the piston during the operation of the cryocooler. This flow can disrupt or modify the pressure distribution in the pressure reservoirs. As a consequence, the control of the piston can be compromised to the point where the expander is rendered inoperable.

1.4 Previous Work

Earlier work on the floating piston expander includes Jones and Smith [4] who demonstrated the feasibility of the floating piston concept. Traum et al. [5] developed electromagnetic smart valves that operate at cryogenic temperatures. The significance of this work was that these cryogenic valves eliminated the need for mechanical actuation in the cold volume of the expander. Additionally this allowed for computer control of the valve actuation and valve timing adjustments during expander operation. Hannon et al. [6] demonstrated single stage operation of the modified Collins machine and floating piston expander. This was a smaller scale prototype designed to achieve 1 Watt of cooling at 10 K. The prototype demonstrated cooling to 60 K with the single stage as well as cooling to 20 K with a precooling flow to simulate the first stage expander. In their initial measurements, Hannon et al. found that there was leakage past the piston between the warm and cold volumes (blow-by), and, as a consequence, the pressures in the reservoirs would slowly decrease to a point where the piston could not be moved in the necessary way. Their solution was to add a small bleed flow into the high-pressure reservoir from the discharge port of the cycle's compressor and a similar bleed from the low-pressure reservoir to the suction port of the cycle's compressor (shown in Figure 1.5).

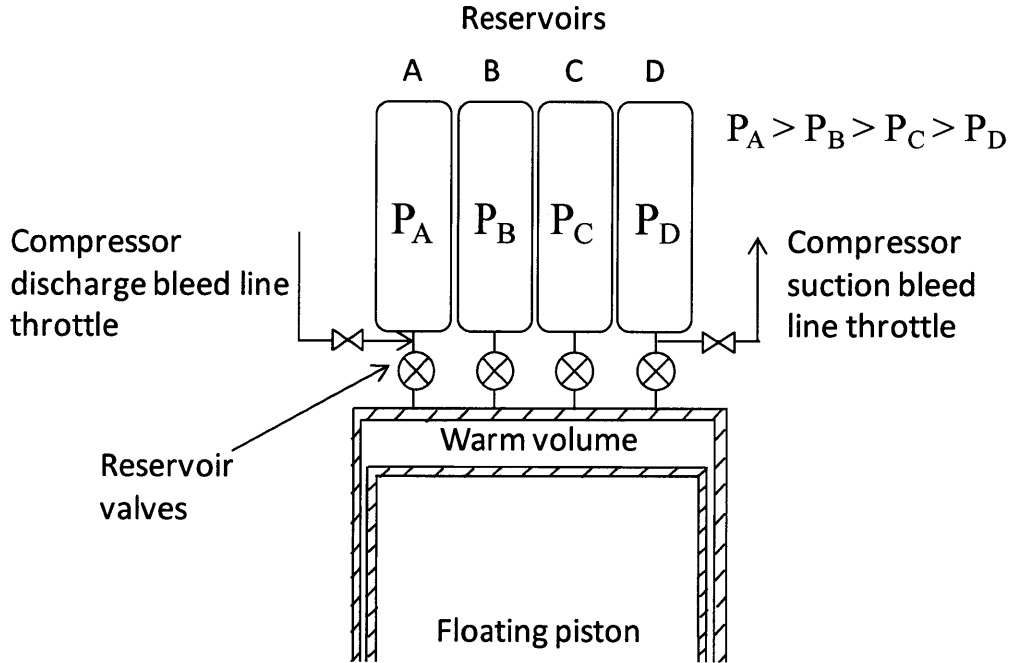


Figure 1.5 Expander used by Hannon et al with bleed line throttles

1.5 Motivation

The bleed lines implemented by Hannon et al. improved expander operation by stabilizing the reservoir pressures at levels that would allow the expander to operate. Unfortunately, the bleed lines did not eliminate the problem of blow-by from the warm volume to the cold volume past the piston. The introduction of a bleed flow into the reservoirs can augment the flow between the warm end and cold end of the piston and, as a consequence, increase the heat load to the cold volume of the expander. In addition, the flow through the two bleed valves is a parasitic flow from the discharge port to the suction port of the compressor which does not provide any additional refrigeration effect. An improved design of this expander then, is to eliminate the need for a bleed flow through the implementation of a better expander control algorithm that maintains a net zero mass flow past the piston in the steady state.

1.6 About this thesis

To this end, this thesis describes work on a model designed to understand the effects of a control algorithm on the long-term pressure distribution of the pressure reservoirs in the cryocooler. An initial model is developed to determine the dependence of expander operation on various control parameters. The model is then extended by using the piston inertia to predict the helium flow through the gap. The piston control scheme uses the new piston-inertia based model to accurately predict helium blow-by and maintain a net zero flow in the steady state.

Chapter 2: Expander Modeling

A thermodynamic model for the expander is developed here to explore the effect of various control parameters on the performance of the expander. This model allows a direct investigation of valve timings on the mass flows between and the pressure distributions of the pressure reservoirs. From this model a performance map can be created for controlling the motion of the floating piston.

2.1 Expander Cycle Description

The targeted (ideal) cycle for the expander is shown in Figure 2.1 as a non-dimensional indicator diagram. The abscissa of this plot is the cold volume, normalized by the maximum volume; whereas, the ordinate is the cold volume pressure normalized to the compressor suction pressure. The steady state pressures of the reservoirs are also indicated as dashed lines.

The cycle begins in state 1 where the cold volume pressure is equal to the pressure in reservoir A and the cold volume is at a minimum. In state 1, the intake valve, exhaust valve, and all reservoir valves are closed.

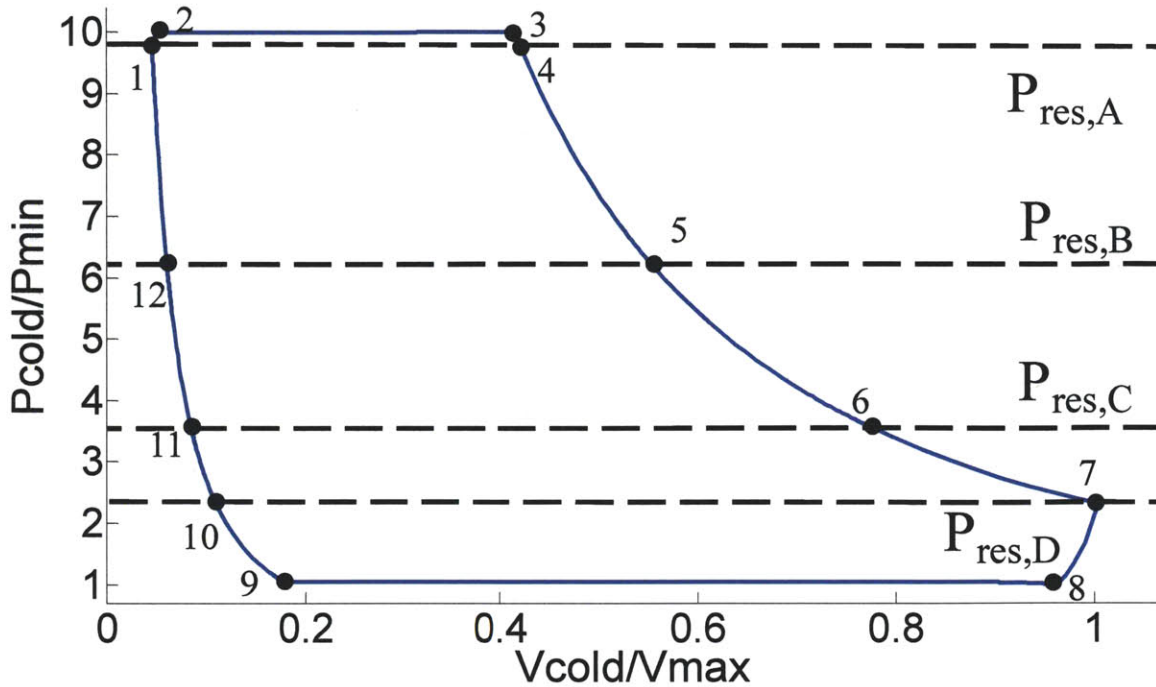


Figure 2.1 Expander cycle dimensionless indicator diagram. The normalized pressure versus the normalized volume is plotted for each state. The horizontal dotted lines represent the steady state pressures of each reservoir ($P_{\min} = 100$ kPa, $V_{\max} = 0.1$ liters).

As part of the blow-in process, the intake valve opens and high pressure helium flows through the intake valve into the cold volume. The pressure in the cold volume rises and forces the piston up toward the warm volume until the cylinder pressure is equalized with the intake pressure at state 2.

At state 2 the intake process begins, the intake valve remains open and the reservoir A valve opens. Due to the pressure difference across the reservoir A valve, helium from the warm volume begins to fill reservoir A and the piston continues to advance into the warm volume. As the piston advances, more high pressure helium is drawn into the cold volume through the intake valve until the piston reaches the predetermined cutoff volume (V_{co}) and the intake valve closes (state 3).

The expansion process begins with the closing of the intake valve. Gas continues to flow into reservoir A and the helium in the cold volume expands until the pressure in the warm volume matches the pressure in reservoir A (state 4) when the reservoir A valve closes. This is immediately followed with the opening of the reservoir B valve so that the expansion process is continued. The gas in the cold volume continues to expand as the helium from the warm volume flows into reservoir B until the pressure in the warm volume matches the pressure in reservoir B (state 5). At this point the reservoir B valve closes and the reservoir C valve opens. The cold volume helium expansion continues as the gas from the warm volume flows into reservoir C until the pressure in the warm volume matches the pressure in the reservoir (state 6). At this point the reservoir C valve closes and the reservoir D valve opens. The cold volume gas continues to expand as the helium from the warm volume flows into reservoir D until the pressure in the warm volume matches the pressure in the reservoir or until the maximum cold volume is reached (state 7). At this point the reservoir D valve closes.

All valves are closed at state 7. The exhaust valve opens beginning the blow-out process where the helium from the cold volume flows out of the cylinder through the exhaust valve. The gas in the warm volume expands as the piston moves toward the cold volume. The pressure in the cold volume continues to decrease until the cold volume pressure matches the exhaust pressure of the expander (state 8), ideally the compressor suction pressure.

In the exhaust process, from state 8 to state 9, the exhaust valve remains open and the reservoir D valve opens. Since the pressure in reservoir D is greater than the expander exhaust pressure, helium from reservoir D fills the warm volume and the piston advances into the cold volume. As the piston advances, more low pressure helium is forced out of the cold volume

through the exhaust valve until the piston reaches the predetermined recompression volume (V_{rec}) and the exhaust valve closes (state 9).

The closing of the exhaust valve at state 9 initiates the recompression process. The helium in reservoir D continues to fill the warm volume, compressing the helium in the cold volume until the pressure in the warm volume matches the pressure in reservoir D (state 10) when the reservoir D valve closes and the reservoir C valve opens. Gas from reservoir C fills the warm volume compressing the helium in the cold volume as the piston moves into the cold volume. When the pressure in the warm volume matches the pressure in reservoir C (state 11), the reservoir C valve closes and the reservoir B valve opens. Gas from reservoir B now fills the warm volume continuing the cold volume gas compression as the piston moves into the cold end of the cylinder. When the pressure in the warm volume matches the pressure in reservoir B (state 12), the reservoir B valve closes and the reservoir A valve opens. Gas from reservoir A fills the warm volume compressing the helium in the cold volume until the pressure in the warm volume matches the pressure in reservoir A (state 1), when the reservoir A valve closes and the cycle is complete.

2.2 Development of an ideal model for each process

The cycle was modeled to understand expander behavior as a function of the cutoff and recompression volumes. In this model the cylinder and piston are assumed to be adiabatic while the gas in the reservoirs is assumed to remain at constant temperature. Mass flow through the piston-cylinder gap is assumed to be zero in this model. As a consequence, the total mass in the reservoirs and the warm volume remains fixed in this model. This total mass is set by setting each reservoir volume, pressure, and temperature to fixed values (5 liters, 500 kPa, and 300 K,

respectively) at the beginning of the simulation. Additional assumptions made in this model are tabulated in Appendix C.

The reservoir, intake, and exhaust valves were each modeled with fixed flow resistances so that the mass flow rate through each valve was the product of its flow resistance and the pressure drop across the valve. The piston mass in this model is set to zero so that the pressures in the cold and warm volumes are always equal and the entire cylinder is at uniform pressure. In each process the work done by the gas in one volume on the floating piston is assumed to be equal to the work done on the gas by the floating piston in the other volume. Helium is modeled as an ideal gas.

In the blow-in process (states 1 to 2), the initial pressure (state 1) in the cold volume (P_{cold}) is the high pressure reservoir pressure (P_A). The intake valve opens and the mass flow through the valve is determined as the product of the valves flow resistance and the pressure difference across the valve,

$$\dot{m}_{\text{valve}} = K_{\text{valve}}(\Delta P_{\text{valve}}) \quad (2.1)$$

where K_{valve} is the flow resistance of the valve and ΔP_{valve} is the pressure difference across the valve. The process is then modeled using the First Law for an open system with a control volume enclosing all of the gas in cylinder. Due to the zero piston mass assumption the pressure is equal on either side of the piston and all helium within the cylinder can be modeled at a uniform pressure.

The First Law for an open system:

$$\frac{dE_{\text{CV}}}{dt} = \dot{Q} - \dot{W} + (\dot{m}h)_{\text{in}} - (\dot{m}h)_{\text{out}} \quad (2.2)$$

where E_{cv} is the energy state of the gas in the control volume and h is the enthalpy of the gas carried across the control volume boundary. In this case there is no mass flow (\dot{m}) out of the control volume and the cylinder is assumed adiabatic therefore the heat transfer into the control volume (\dot{Q}) is zero. There is also no work (\dot{W}) because the cylinder volume is fixed. Assuming perfect mixing in the cold volume, the First Law for the cold volume is re-written as

$$\frac{d(mc_v T)_{cold}}{dt} = (K_{intake}(P_{intake} - P_c)c_p T_{intake})_{in} \quad (2.3)$$

where K_{intake} is the intake valve flow resistance, P_{intake} is the compressor discharge pressure, P_c is the pressure in the cold volume, T_{intake} is the temperature of the intake gas, c_v is the specific heat of helium at constant volume and c_p is the specific heat of helium at constant pressure. Since the temperature is not uniform in the cylinder (temperatures differ between the warm and cold volume), the ideal gas assumption is used to manipulate the left hand side of equation 2.3 for the uniform pressure in the cylinder (due to the zero mass piston assumption). The result is

$$\frac{1}{\gamma - 1} \frac{d(P_c V_{tot})}{dt} = (K_{intake}(P_{intake} - P_c)c_p T_{intake})_{in} \quad (2.4)$$

where V_{tot} is the volume of the cylinder and γ is the ratio of the specific heat at constant pressure and the specific heat at constant volume (1.66 for helium). Since the total volume of the cylinder is fixed it can be pulled out of the differential. Separating the differential and integrating with a fixed time step results in the next pressure state of the cylinder.

Separating the differential equation 2.4:

$$\frac{V_{tot}}{\gamma - 1} (dP_c) = (K_{intake}(P_{intake} - P_c)c_p T_{intake})_{in} dt \quad (2.5)$$

Descritizing for the fixed time step during integration:

$$\Delta P_c = \frac{\gamma - 1}{V_{tot}} (K_{intake}(P_{intake} - P_c)c_p T_{intake})_{in} t_{step} \quad (2.6)$$

Solving for the new pressure state:

$$P_{c,2} = P_{c,1} + \frac{\gamma - 1}{V_{\text{tot}}} (K_{\text{intake}} (P_{\text{intake}} - P_c) c_p T_{\text{intake}})_{\text{in}} t_{\text{step}} \quad (2.7)$$

where t_{step} is the fixed time step used to numerically integrate each process throughout the cycle. Since the piston is assumed massless, this new pressure is the pressure in both the warm and cold volumes. The displacement of the piston is then determined by assuming that the gas in the warm volume undergoes an isentropic compression.

Applying the Second Law to the warm volume,

$$dS = c_v \ln \left(\frac{P_{w,2}}{P_{w,1}} \right) + c_p \ln \left(\frac{V_{w,2}}{V_{w,1}} \right) = 0 \quad (2.8)$$

and simplifying, the volume can be related to the new pressure as

$$\left(\frac{V_{w,2}}{V_{w,1}} \right) = \left(\frac{P_{w,2}}{P_{w,1}} \right)^{-c_v/c_p} = \left(\frac{P_{w,1}}{P_{w,2}} \right)^{\frac{1}{\gamma}} \quad (2.9)$$

$V_{w,1}$ and $P_{w,1}$ refer to the initial state of the gas in the warm volume while $V_{w,2}$ and $P_{w,2}$ refer to the state of the gas in the warm volume after the time step. The new volume of gas in the cold volume is $V_{c,2} = V_{\text{tot}} - V_{w,2}$ and the new helium temperature is found using the ideal gas assumption.

The intake process (process 2-3) is modeled using the same control volume as the blow-in process (process 1-2). In this case, however, there is now helium flowing from the warm volume into reservoir A. Writing the First Law for the cylinder

$$\frac{dE_{\text{cv}}}{dt} = (\dot{m}h)_{\text{in}} - (\dot{m}h)_{\text{out}} \quad (2.10)$$

where the enthalpy flow rate through the cold valve, $(\dot{m}h)_{\text{in}}$, is

$$(\dot{m}h)_{\text{in}} = K_{\text{intake}} (P_{\text{intake}} - P_c) c_p T_{\text{intake}} \quad (2.11)$$

and the enthalpy flow rate from the warm volume into reservoir A, $(\dot{m}h)_{\text{out}}$, is

$$(\dot{m}h)_{\text{out}} = K_{\text{res,A}}(P_w - P_{\text{res,A}})c_p T_w \quad (2.12)$$

where $K_{\text{res,A}}$ is the flow resistance through the valve connecting the warm volume to reservoir A, $P_{\text{res,A}}$ is the helium pressure in reservoir A. The temperature of the helium remaining in the warm volume, T_w , is assumed to be constant. This comes from modeling the mass remaining in the warm volume with no entropy generation

$$dS = c_p \ln\left(\frac{T_{w,3}}{T_{w,2}}\right) - R \ln\left(\frac{P_{w,3}}{P_{w,2}}\right) = 0 \quad (2.13)$$

where R is the ideal gas constant. During intake (process 2-3), the pressure is constant at the intake pressure, therefore the temperature of the gas in the warm volume must remain constant to satisfy equation 2.13. The new piston position is determined using the First Law for each volume. The First Law for the cold volume is

$$\frac{dE_{\text{CV}}}{dt} = -\dot{W}_c + (\dot{m}h)_{\text{in}} \quad (2.14)$$

where \dot{W}_c is the work done by the gas in the cold volume. This work is determined by setting the work done by the gas in the cold volume equal to the work done on the gas, by the piston, in the warm volume. The First Law for the warm volume is

$$\frac{dE_{\text{CV}}}{dt} = -\dot{W}_w - (\dot{m}h)_{\text{out}} \quad (2.15)$$

where \dot{W}_w is the work done on the gas in the warm volume. Simplifying the left hand side (recall T_w is fixed during intake) and solving for the work gives

$$-\dot{W}_w = (\dot{m}h)_{\text{out}} + c_v T_w \frac{dm_w}{dt}. \quad (2.16)$$

Substituting equation 2.16 into equation 2.14 and using the ideal gas law on the left hand side of equation 2.14 gives

$$\frac{1}{\gamma - 1} \frac{d(P_c V_c)}{dt} = -c_v T_w \frac{dm_w}{dt} + (\dot{m}h)_{in} - (\dot{m}h)_{out}. \quad (2.17)$$

When equation 2.17 is integrating for the fixed time step, the equation is solved for the new cold volume

$$V_{c,3} = \frac{1}{P_{c,3}} [P_{c,2} V_{c,2} + (\gamma - 1)(-c_v T_w (m_{3,w} - m_{2,w}) + (\dot{m}h)_{in} t_{step} - (\dot{m}h)_{out} t_{step})]. \quad (2.18)$$

Each expansion process (process 3-4, process 4-5, process 5-6, and process 6-7) is modeled in a manner similar to blow-in. The difference between the blow-in and expansion processes is that helium is only flowing out of the warm volume into each reservoir and there is no flow into the cold volume. The fixed mass in the cold volume is modeled with no entropy generation. The First Law for the entire cylinder volume with no work (zero displacement) and no heat transfer (adiabatic) is

$$\frac{dE_{cv}}{dt} = -(\dot{m}h)_{out} \quad (2.19)$$

where

$$(\dot{m}h)_{out} = K_{res} (P_{w,3} - P_{res}) c_p T_{w,3} \quad (2.20)$$

and K_{res} is the flow resistance of the open reservoir valve, $P_{w,3}$ is the initial pressure in the warm volume, P_{res} is the pressure in the reservoir, and $T_{w,3}$ is the initial temperature of the warm volume. The First Law result is similar to that of the blow-in and the new warm volume pressure is defined as

$$P_{w,4} = P_{w,3} - \frac{\gamma - 1}{V_{tot}} (K_{res} (P_{w,3} - P_{res}) c_p T_{w,3}) t_{step}. \quad (2.21)$$

Since the pressure is equal across the piston and the gas in the cold volume is assumed to expand with no entropy generation, the Second Law gives the new piston position with

$$\left(\frac{V_{c,4}}{V_{c,3}}\right) = \left(\frac{P_{c,4}}{P_{c,3}}\right)^{-c_v/c_p} = \left(\frac{P_{c,3}}{P_{c,4}}\right)^{\frac{1}{\gamma}} \quad (2.22)$$

where $V_{c,3}$ and $P_{c,3}$ refer to the initial volume and pressure of the gas in the cold volume while $V_{c,4}$ and $P_{c,4}$ refer to the state of the gas in the cold volume following the time step.

The blow-out process (process 7-8) is modeled in a manner very similar to the blow-in process with the only difference being the flow direction. During blow-out the cool, low pressure helium flows out of the cold volume through the exhaust valve. The warm volume is modeled as an isentropic expansion.

The exhaust process (process 8-9) is similar to the intake process. The differences are that helium flows out of the cold volume (cold volume helium temperature is modeled as constant with no entropy generation assumed for the gas remaining in the cold volume) and that helium flows into the warm volume from reservoir D. The work done by the gas in the warm volume on the piston is reflected as the work done by the piston on the gas in the cold volume as well.

Each recompression process (process 9-10, process 10-11, process 11-12, and process 12-1) is modeled as a reversible compression in the cold volume and an open system for the entire cylinder with helium flow out of each reservoir into the warm volume. A complete list of the model for all processes in the expander cycle can be found in Appendix A.

2.3 Cutoff and Recompression volume study

In the expander control model the cutoff volume V_{co} , which corresponds to the state 3 volume in Figure 2.1, and the recompression volume V_{rec} , which corresponds to the state 9

volume in Figure 2.1, are chosen fixed points in the cycle. They mark the end of the intake process and the end of the exhaust process, respectively. Increasing the intake stroke (increased V_{co}) will increase the total helium mass in the cold volume. The larger volume of gas in the cold volume raises the likelihood that during expansion, with less distance for the piston to travel to reach the top of the cylinder and more gas for expansion, the piston will touch down on the top of the cylinder. When the piston dwells on the top or the bottom of the cylinder, mass flow through the piston cylinder gap increases due to the increased pressure difference across the piston. Hence, when the piston dwells at the top of the cylinder, gas from the cold volume will flow up into the warm volume to add mass to the reservoirs in the case that the total mass in the reservoirs is too low. Similarly, a longer exhaust stroke (reduced V_{rec}) will reduce the total mass in the cold volume. A smaller volume of gas in the cold volume raises the likelihood that during recompression, with less distance for the piston to travel to reach the bottom of the cylinder and less gas for recompression, the piston will touch down on the bottom of the cylinder. With the piston dwelling on the bottom of the cylinder, the pressure difference across the piston will increase blow-by from the warm volume to the cold volume to remove mass from the reservoirs in the case that the total mass in the reservoirs is too high. The model discussed in the previous section was run with varying cutoff and recompression volumes to see what the impact was on the shape of a steady state cycle. A sampling of stable cycles with a large P-V span as determined by the simulation is shown in Figure 2.2. A good (or ideal) cycle is defined as those that close with a large swept volume (roughly 90% of V_{max} or greater).

These plots suggest that the ranges of acceptable cutoff and recompression volumes are limited. The suggested values for the normalized cutoff volume can vary only from 0.33 to 0.5 whereas the values for the normalized recompression volumes

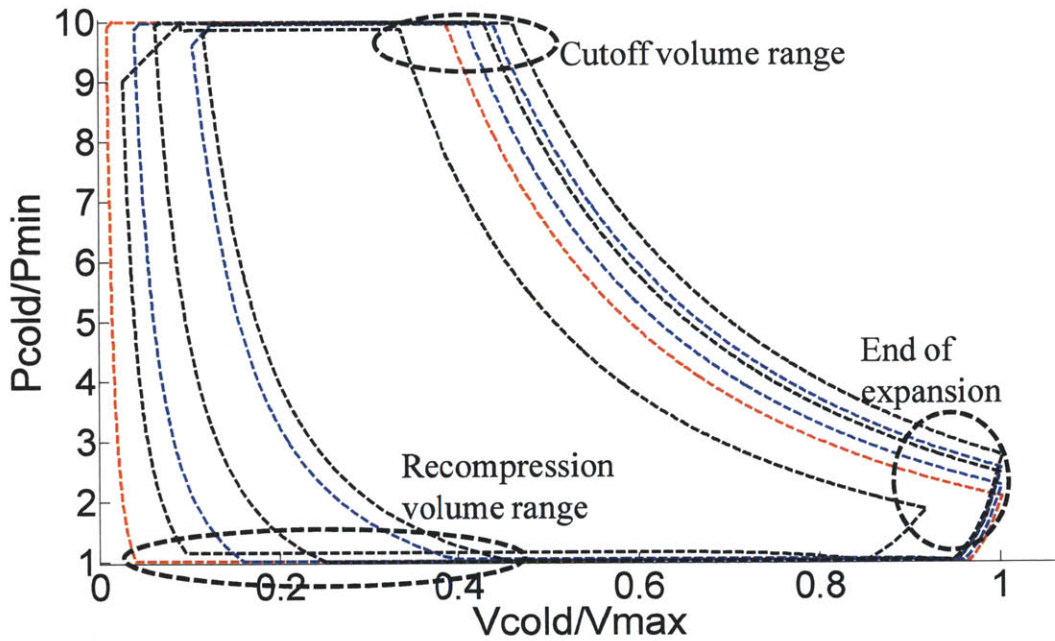


Figure 2.2 Ideal Expander Cycle Samples. The normalized pressure versus normalized volume diagrams for various cutoff and recompression volumes are plotted for the cold volume gas ($P_{\min} = 100$ kPa, $V_{\max} = 0.1$ liters).

can vary from 0 to 0.5. If the simulation is run with values outside of this range, the cycles degenerate into cycles that do not span the entire range of available volumes or pressures. Figure 2.3 is a sample of indicator diagrams for cycles in which the recompression volumes are chosen to be too large. In this case, the large recompression volume ends the exhaust stroke so early that a large portion of the gas that was cooled during expansion is recompressed instead of being exhausted, thus reducing the cooling power of the expander. As a result, the piston resides primarily in the warm volume throughout the cycle. Figure 2.4 is a sample of indicator diagrams for cycles in which the cutoff volumes are too low. The shortened intake stroke reduces the mass in the cold volume and consequently the gas is expanded without taking full advantage of the maximum volume in the cylinder. This results in a piston that resides primarily in the cold end of the expander throughout the cycle, thereby reducing the total cooling.

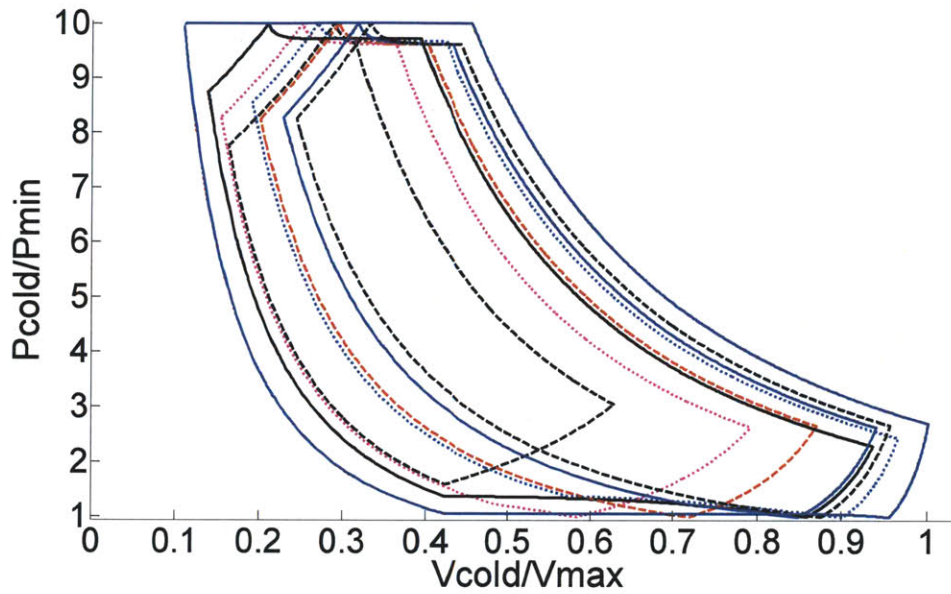


Figure 2.3 High V_{rec} expander cycle samples. The normalized pressure versus the normalized volume diagrams for various cutoff and recompression volumes are plotted for the cold volume gas. In this sample all of the recompression volumes are too large and the maximum swept volume of the expander is not achieved ($P_{min}=100$ kPa, $V_{max}=0.1$ liters).

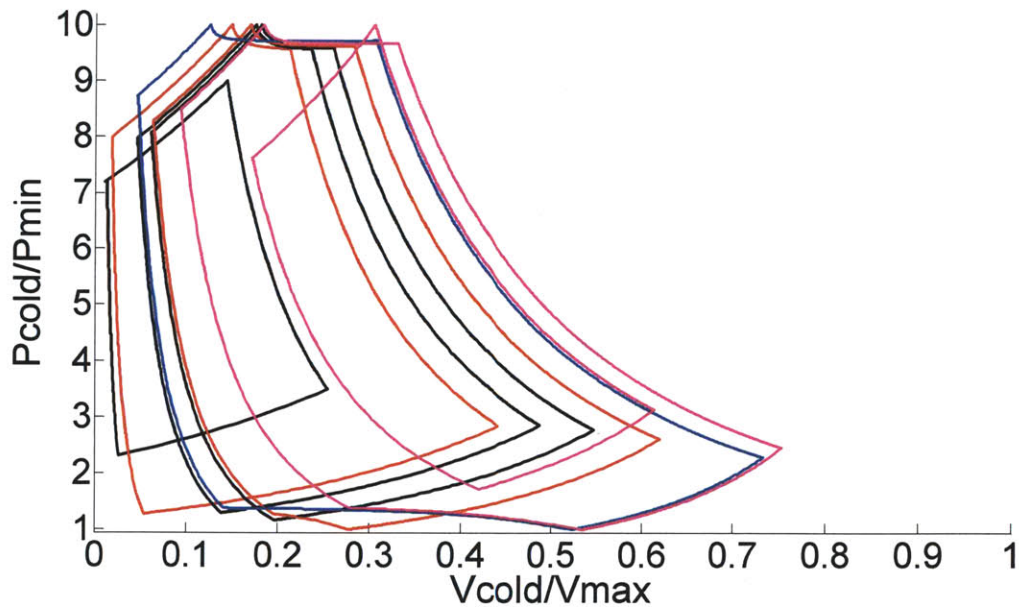


Figure 2.4 Low V_{co} expander cycle samples. The normalized pressure versus the normalized volume diagrams for various cutoff and recompression volumes are plotted for the cold volume gas. In this sample all of the cutoff volumes are too small and the maximum swept volume of the expander is not achieved ($P_{min}=100$ kPa, $V_{max}=0.1$ liters).

The steady state pressures that are attained by each of the reservoirs as a function of recompression and cutoff volumes are shown in Figures 2.5 and 2.6. More specifically, Figure 2.5 is a plot of the normalized reservoir pressures as a function of a normalized cutoff volume (V_{co}). Each line in Figure 2.5 corresponds to a specific and fixed recompression volume. Similarly, Figure 2.6 is a plot of the normalized reservoir pressures as a function of the normalized recompression volume (V_{rec}). Each line in Figure 2.6 corresponds to a specific and fixed cutoff volume. Both plots represent a collection of cycles that close and operate smoothly. In both plots, the variations of the pressure in the high and low pressure reservoirs are larger than the variation in the intermediate reservoirs which is consistent with the observed performance of previous prototypes [7]. Therefore, given that the maximum and minimum pressures are 1 MPa and 0.1 MPa respectively, it can be expected that reservoir B and reservoir C will settle to

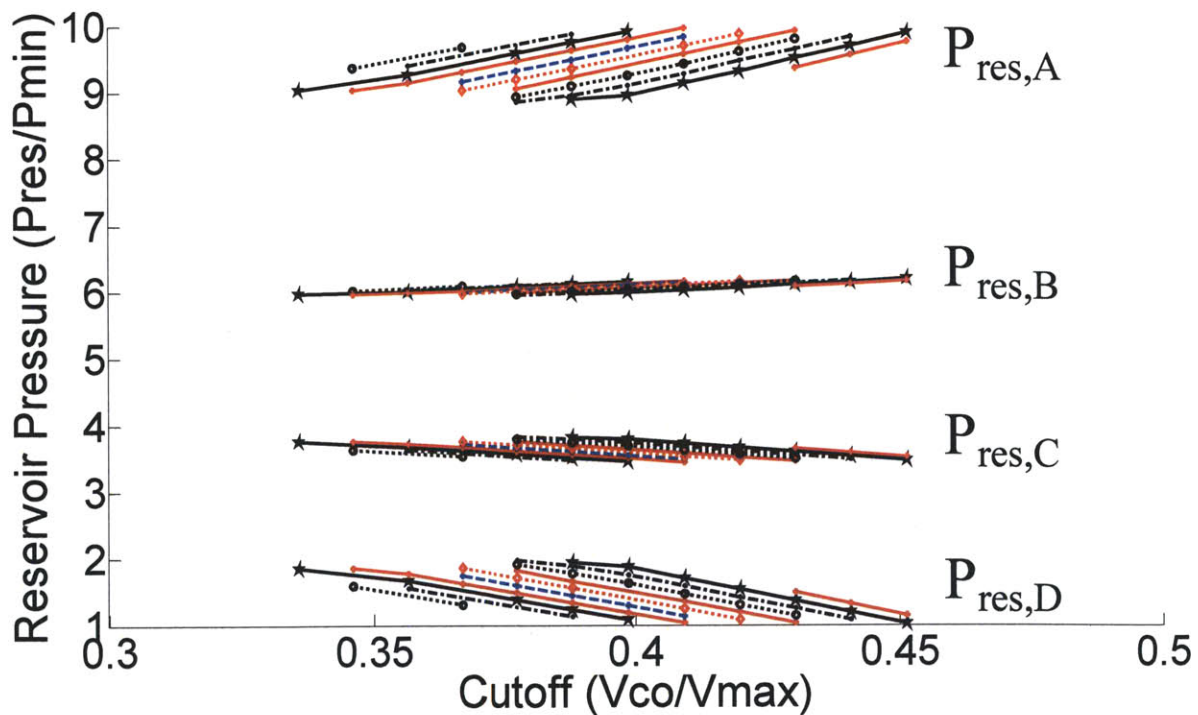


Figure 2.5 Reservoir pressure vs. cutoff volume. The normalized reservoir pressures for a fixed recompression volume are displayed as a function of the normalized cutoff volume ($P_{min} = 100$ kPa, $V_{max} = 0.1$ liters).

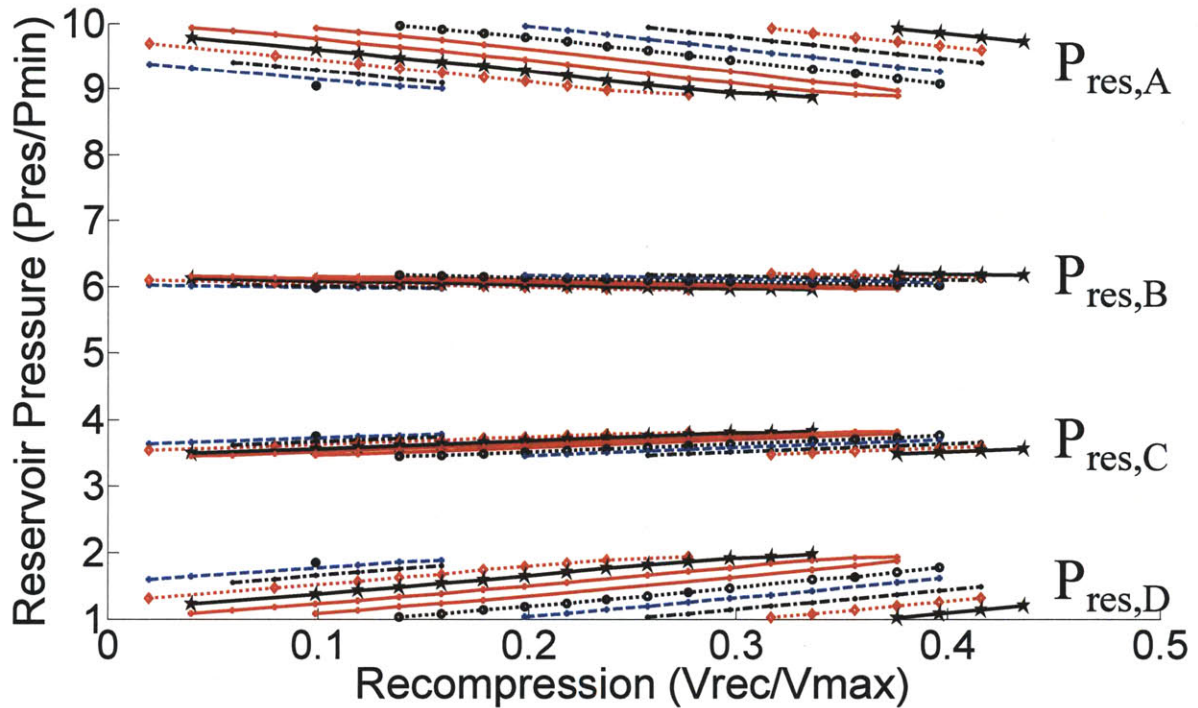


Figure 2.6 Reservoir pressure vs. recompression volume. The normalized reservoir pressures for a fixed cutoff volume are displayed as a function of the normalized recompression volume ($P_{\min} = 100$ kPa, $V_{\max} = 0.1$ liters).

approximate pressures of 600 kPa and 350 kPa regardless of the cutoff and recompression volumes selected. The numerical results shown in Figure 2.5 and Figure 2.6 are tabulated in Appendix B. The cutoff and recompression volumes for the indicator diagrams shown in Figure 2.2 are also tabulated in Appendix B.

The sensitivity of the low pressure reservoir (D) to the recompression volume can be understood by considering the specifics of the intake and discharge processes to that reservoir. In steady state the mass flow into reservoir D occurs during process 6-7 in Figure 2.1; whereas the mass flow out of reservoir D occurs during processes 8-9-10. If the recompression volume is increased slightly (state 9 is moved to the right in Figure 2.1) the mass flow out of reservoir D is reduced. As a consequence, mass begins to accrue in reservoir D and the pressure in reservoir D slowly increases over many cycles. As the pressure rises in reservoir D the volume of state 10

decreases which, in turn, increases the net mass flow out of reservoir D. The increased pressure in reservoir D also reduces the net mass flow into reservoir D during process 6-7. These changes in the net mass flow act as a negative feedback to drive the reservoir pressure to a new equilibrium where the mass flow into reservoir D during expansion is equal to the mass flow out of reservoir D during exhaust and the first recompression.

Analogously, the sensitivity of the high pressure reservoir (A) to the cutoff volume can be understood by considering the specifics of the intake and discharge processes to that reservoir. In steady state the mass flow into reservoir A occurs during processes 2-3-4 in Figure 2.1; whereas the mass flow out of reservoir A occurs during process 12-1. If the cutoff volume is decreased slightly (state 3 is moved to the left in Figure 2.1) the mass flow into reservoir A is reduced. As a consequence, the mass in reservoir A and hence the pressure in reservoir A slowly decreases over many cycles. As the pressure decreases in reservoir A the volume of state 4 increases which, in turn, increases the net mass flow into of reservoir A. The reduced pressure in reservoir A also results in a reduced mass flow out of reservoir A during process 12-1. These changes in the net mass flow act as a negative feedback to drive the reservoir A pressure to a new equilibrium where the net mass flow into and out of the reservoir is equal.

The intermediate pressure reservoirs (reservoirs B and C) are less sensitive to changes in the cutoff and recompression volumes because the mass flow in and out of these reservoirs are not directly tied to the length of the intake and exhaust strokes. No mass flow into or out of the reservoirs takes places at constant pressure as observed with reservoirs A and D. Any change in the mass flow into the reservoir during expansion is reflected as a change in mass flow out of the reservoir during recompression. This reflection stabilizes the pressure in both of the intermediate

reservoirs. As a result, only the volumes at which the reservoir B and reservoir C valves open and close change with new cutoff and recompression volumes but the pressures do not.

2.4 Total warm helium mass study

The analysis above fixed the mass in reservoirs such that the average pressure ratio ($P_{\text{average}}/P_{\text{min}}$ where $P_{\text{min}}=100$ kPa) of the reservoirs was 5.0. The impact of the average pressure ratio on the steady state reservoir pressures for the expander was modeled by running simulations with different average reservoir pressures. Figure 2.7 shows the steady state reservoir pressures as a function of the average reservoir pressure ratio ranging from 1.5 to 8.0 for three different cutoff and recompression volumes. The steady state pressure in reservoir A monotonically

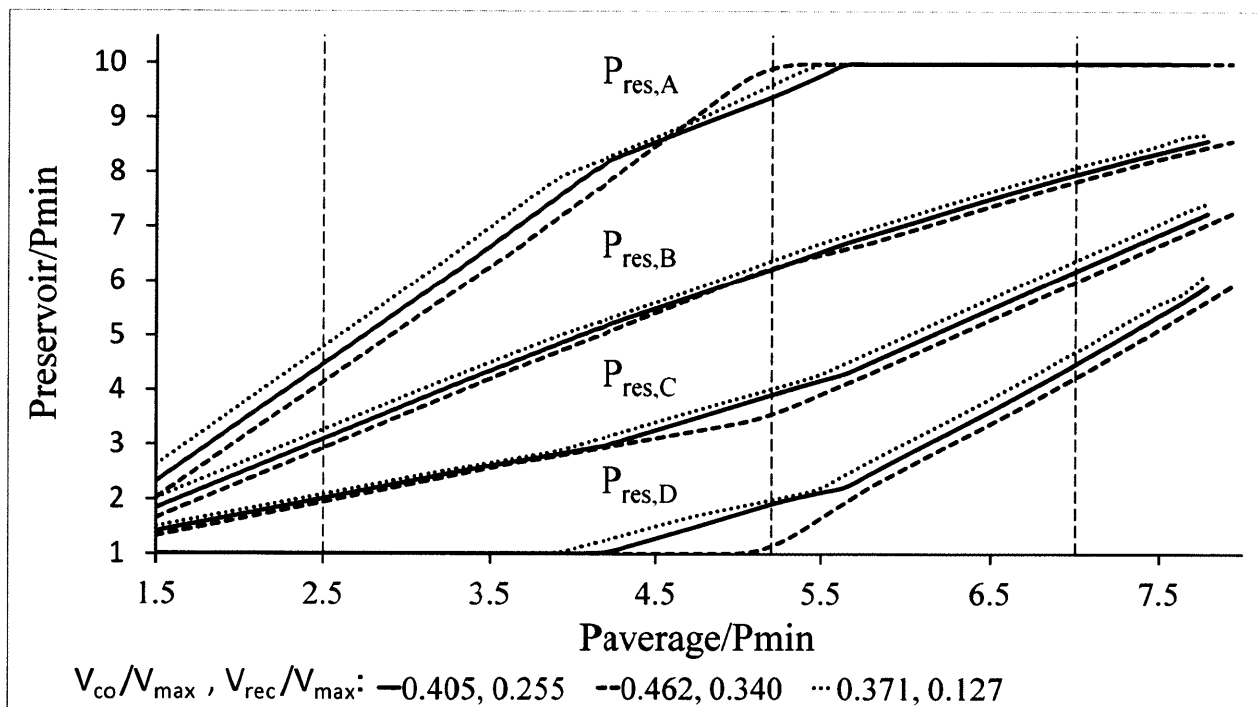


Figure 2.7 Average reservoir pressure vs. steady state reservoir pressure. The normalized reservoir pressures versus the normalized average reservoir pressures are plotted for three cutoff and recompression volumes ($P_{\text{min}} = 100$ kPa, $V_{\text{max}}=0.1$ liters).

increases with the average pressure and then saturates at the compressor discharge pressure for average reservoir pressures above 5.5. Similarly the reservoir D pressure is fixed at the compressor suction pressure up to an average reservoir pressure of roughly 4. The reservoir D pressure then monotonically increases with average pressure above 4. The pressures for the intermediate reservoirs show no such saturation behavior for the ranges shown in Figure 2.7. The simulations show that for good control of the piston motion, the distribution of pressures in the pressure reservoirs would, ideally, be distributed evenly between the compressor discharge and suction pressures in the machine. In Figure 2.7 this distribution occurs when the average pressure ratio for the reservoirs is between 4.5 and 5.5.

Figure 2.7 shows reservoir pressure distributions for cycles that closed. Some of these cycles, however, did not sweep the entire available volume or pressure ranges. For example, the three cycles shown in Figure 2.8 correspond to normalized average pressures of 2.5, 5.2, and 7 (the normalized cutoff and recompression volumes for the cycles shown in Figure 2.8 are 0.405 and 0.255, respectively). In the case when the normalized average pressure is 2.5, due to the lower reservoir pressures, the piston is forced to reside in the warm end of the cylinder throughout the cycle. In the case when the normalized average pressure is 7, due to the higher reservoir pressures, the piston is forced to reside in the cold end of the cylinder throughout the cycle. In the case when the normalized average pressure is 5.2, the cycle spans the entire P-V space maximizing the work per cycle and hence the cooling power per cycle. This cycle is in the ideal range suggested earlier. The three dotted vertical lines in Figure 2.7 correspond to the three cycles shown in Figure 2.8. In retrospect these results are not surprising when the extreme limits are considered. In the case of an infinite initial pressure in the reservoirs, the high pressures in the reservoirs drive and hold the piston to the cold end of the cylinder throughout the cycle. In

the zero initial pressure limit, the piston is forced to the top of the cylinder by both the compressor discharge and suction pressures in the cold volume throughout the cycle. In either of these extreme cases the piston is immobile.

Although the model assumes there is no leakage past the piston, the results of Figure 2.7 and Figure 2.8 can be used to determine the expected behavior of the floating piston expander with a small leak across the piston. A net average flow of helium from the warm volume to the cold volume will decrease the mass (and pressure) in the reservoirs. The average pressure in the reservoirs will decrease and the pressure distribution of the reservoirs will begin to concentrate towards the minimum pressure in the expander (as shown in Figure 2.7 for values of $P_{\text{average}}/P_{\text{min}} < 4.0$). The cycle the expander executes will be restricted only to larger cold volumes

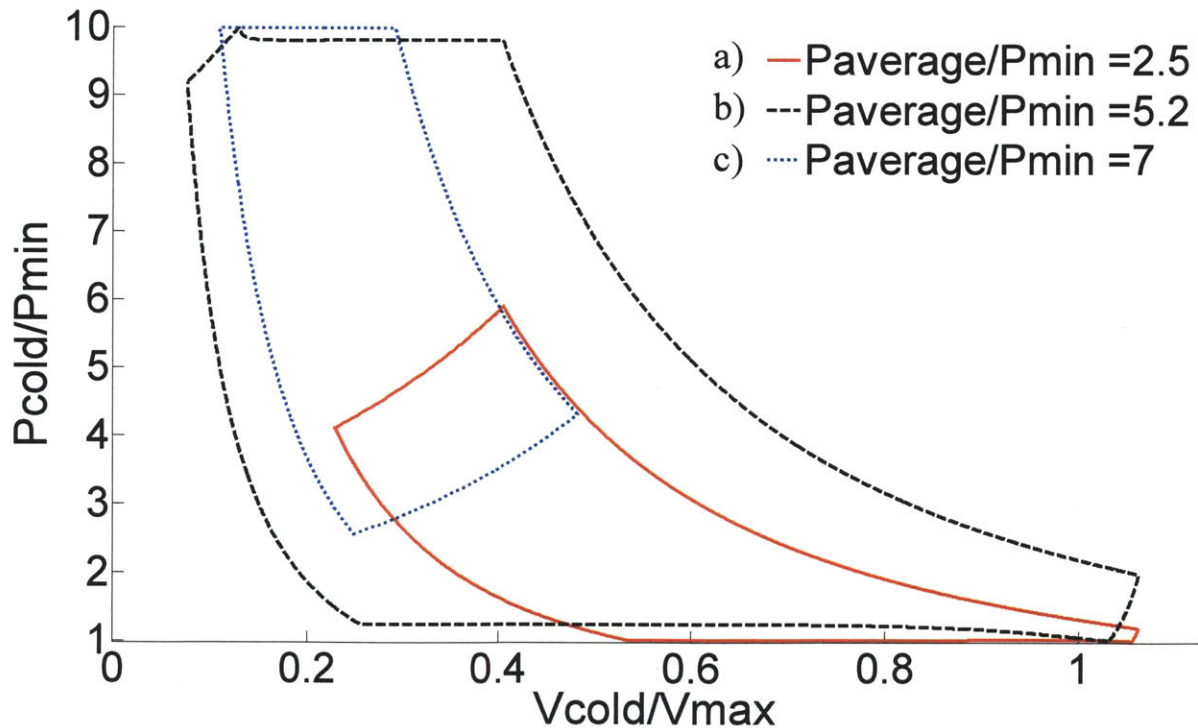


Figure 2.8 Average pressure indicator diagrams. The resultant normalized indicator diagrams for the varying average pressure ($P_{\text{min}} = 100 \text{ kPa}$, $V_{\text{max}} = 0.1 \text{ liters}$). a) A cycle with an average reservoir pressure that is too small. b) A cycle with an average reservoir pressure that allows the full cycle to occur (ideal range). c) A cycle with an average reservoir pressure that is too large.

and lower pressure as shown by the red ($P_{\text{average}}/P_{\text{min}} = 2.5$) cycle in Figure 2.8. A net average flow of helium from the cold volume to the warm volume would increase the mass (and pressure) in the reservoirs. The average pressure in the reservoirs will increase and the pressure distribution of the reservoirs will begin to concentrate towards the maximum pressure in the expander (as shown in Figure 2.7 for values of $P_{\text{average}}/P_{\text{min}} > 5.5$). The cycle the expander executes will be restricted only to smaller cold volumes and higher pressures as shown by the blue ($P_{\text{average}}/P_{\text{min}} = 7$) cycle in Figure 2.8.

The model used up to this point depicts the performance of an idealized expander. For integrating these results into a physical prototype, some of these idealizations must be reconsidered. However, the conclusions of this study remain valuable for predicting expander behavior. In what follows here and in Chapter 3, the model is augmented to include more accurate flow characteristics for the intake, exhaust, and reservoir valves. Additionally, the sizes of the reservoirs used up to this point are quite large (5 liters per reservoir). In fact, the study here shows that significantly smaller reservoirs can be used.

2.5 Valve Flow

The K values used for the impedances of the valves in the study above were arbitrarily assigned and adjusted to make the operating frequency of the expander 1 Hz. These valves can be better approximated to the actual values by considering the simplified drawing of the valve design shown in Figure 2.9. The intake valve is mounted on the cold cylinder head inside a pressurized plenum. In Figure 1.3 the plenum sits between the intake valve and the high pressure side of the recuperative heat exchanger. In the physical cryocooler the intake valve is mounted directly in the plenum and the intake flow passes through the entire valve assembly as shown in Figure 2.9. The plenum acts as a pressure stabilizer for the flow to the intake port. The exhaust

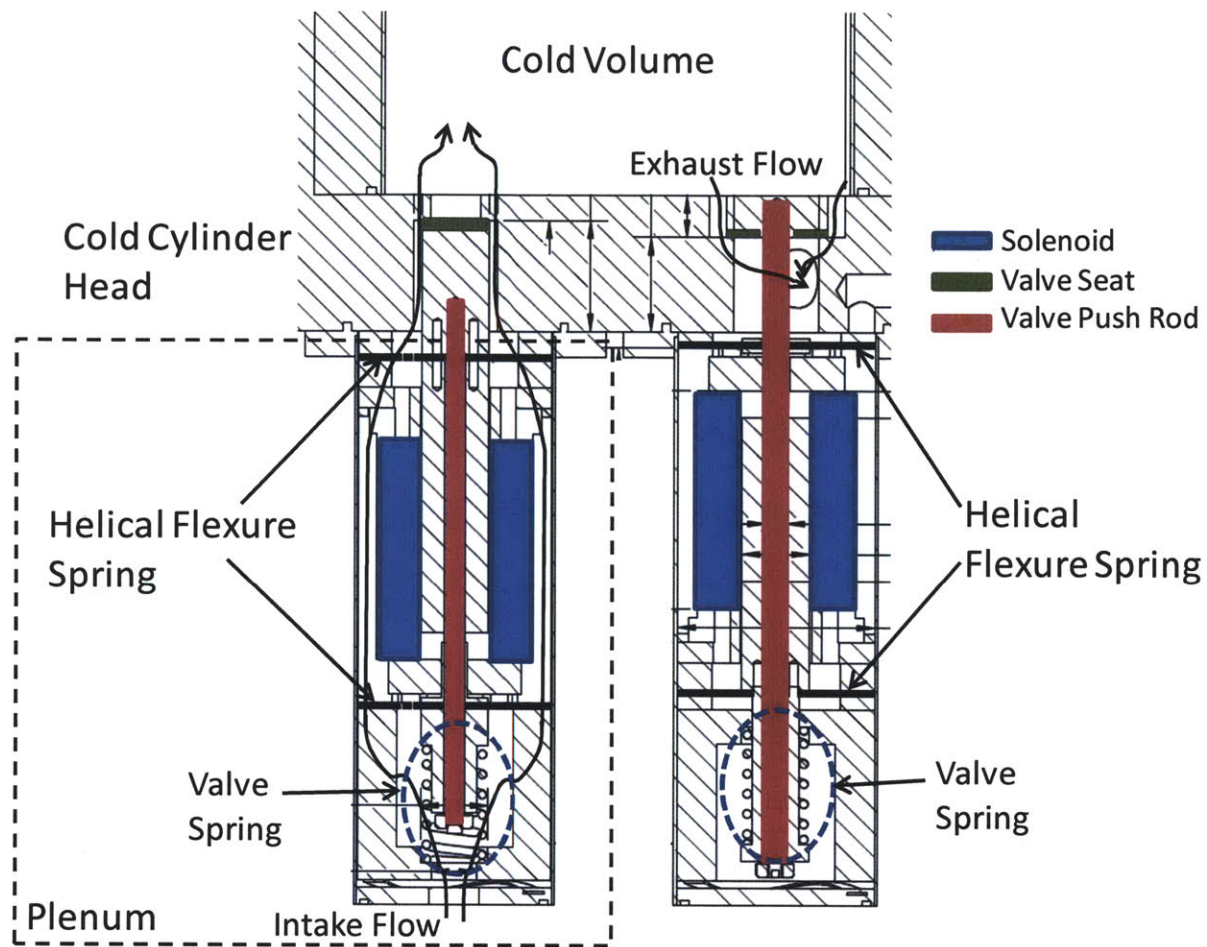


Figure 2.9 Cold Valve Schematics. When activated, the high pressure intake valve (left) pulls down from the seat and the low pressure exhaust valve (right) pushes up into the cold volume.

valve is mounted directly to the exhaust port of the cold cylinder head. The exhaust gas flows out through a port just below the valve seat. In both valves, current is supplied to the solenoid, pushing the valve rod against the spring force (the force that normally holds the valve closed).

To get a better prediction of the helium flow through the intake and exhaust valves. The valves were modeled by assuming that the helium was incompressible through the duct for the small, fixed time step. Minor losses were taken into account as well. The state of the gas downstream of the valve is adjusted for every time step. In the case that the pressure ratio across

the valve exceeds that of the critical pressure ratio, then the mass rate flow through the valve is determined based on the critical pressure ratio. White [8] defines the critical pressure ratio as

$$P^*_{\text{critical}} = \left(\frac{2}{\gamma + 1} \right)^{\gamma/\gamma-1} \quad (2.23)$$

where γ is the specific heat ratio for helium (1.66). The critical pressure ratio for helium is 0.488. Consequently, the helium mass flow rate through the valve is never greater than the mass flow rate achieved by this critical pressure ratio. With the correct pressure ratio, the helium flow through the intake and exhaust valves, is

$$\frac{P_1}{\rho g} + \frac{V_1^2}{2g} = \frac{P_2}{\rho g} + \frac{V_2^2}{2g} + h_f + \sum h_m \quad (2.24)$$

where P_1 and P_2 are the upstream and downstream pressures, respectively. V_1 and V_2 are the upstream helium velocity (assumed to be zero) and the downstream helium velocity, respectively. The variable g is the gravitational constant, ρ is the instantaneous helium density, h_f is the head loss due to friction and $\sum h_m$ is sum of the minor losses in the valve. Additionally,

$$h_f + \sum h_m = \frac{V_2^2}{2g} \left(\frac{fL}{D_h} + \sum K \right) \quad (2.25)$$

where f is the friction factor through the valve opening, L is the length of the valve opening, D_h is the hydraulic diameter of the pipe and $\sum K$ is the sum of the loss coefficients for each valve. With $f \ll 1$ and $L/D_h < 1$ in each valve, $f L/D_h$ is assumed to be negligible. Therefore, substituting equation 2.25 into equation 2.24, the resulting flow equation is

$$V_2 = \sqrt{\frac{2(P_1 - P_2)}{\rho} \left(\frac{1}{1 + \sum K} \right)} \quad (2.26)$$

The valves that will connect between the warm volume and each reservoir are purchased off the shelf and have a rated flow coefficient (C_v) of 0.210. The flow through these valves is determined using the formulas provided by Gems Sensors and Controls [9]. If $P_2 > 0.5P_1$,

$$C_v = \frac{V}{16.05 \sqrt{\frac{(P_1^2 - P_2^2)}{(SG) T}}} \quad (2.27)$$

or if $P_2 \leq 0.5P_1$,

$$C_v = \frac{V}{13.61 P_1 \sqrt{\frac{1}{(SG) T}}} \quad (2.28)$$

Where V is the gas velocity through the valve, P_1 is the upstream gas pressure, P_2 is the downstream gas pressure, SG is the specific gravity of the gas (compared to air density at STP), and T is the gas temperature.

Equations 2.26, 2.27, and 2.28 are added to the expander model described in section 2.2. Instead of using an equivalent flow resistance for each valve, the total helium flow through each valve over the fixed time period is determined. The resulting impedance of the real valves is much smaller than that of the valves from the previous study. However, because each reservoir valve has the ability to be throttled, the flow through the valve can be adjusted to slow down the expander operating frequency. With the each reservoir valve throttle down to roughly 35% of its fully open flow rate, the expander again operates in the 1 Hz to 2 Hz range with behavior similar to the previous study. This updated valve flow model is then incorporated into the First and Second Law equations for each process. It is important to use the accurate model for the valve flow because, when blow-by is considered, the valve flow will impact the dynamics of the piston

motion. The piston motion produces a pressure difference across the piston that drives the blow-by flow.

2.6 Reservoir Volume Size

In the model described above the volume of each reservoir was assumed to be five liters; a value that is far too large to be practical in the real device. The question becomes then, how small can the volumes of the reservoirs be made and still achieve the desirable performance found in that model?

One of the simplifications that the large reservoir assumption affords is that the surface area of the reservoir is large and hence the heat transfer to the environment is large. Any dissipation that occurs in these reservoirs is immediately dissipated to the environment, keeping the temperature of the gas in the reservoir constant and near the assumed environmental temperature of 300 K. As the reservoir volume is reduced, the work dissipated in the gas in the reservoir is (roughly) the same as that of the large reservoir. Since the heat transfer rate is proportional to the surface area and the temperature of the reservoir, it is expected that the average temperature of the gas in the reservoir will increase as the surface area (volume) of the reservoir is reduced. More explicitly, the heat transfer is

$$Q = h_{\text{eff}}A_{\text{surf}}(T_{\text{reservoir}} - T_{\text{ambient}}) \quad (2.29)$$

where h_{eff} is the effective heat transfer coefficient, A_{surf} is the surface area of each reservoir, $T_{\text{reservoir}}$ is the average gas reservoir temperature and T_{ambient} is ambient temperature; solving for $T_{\text{reservoir}}$ gives shows an estimated 20 K temperature difference.

$$T_{\text{reservoir}} = \frac{Q}{h_{\text{eff}}A_{\text{surf}}} + T_{\text{ambient}} \quad (2.30)$$

To approximate the reservoir temperature, h_{eff} is assumed to be 20 W/m²-K due to natural convection and radiation, A_{surf} is estimated from a 1 liter cube, and T_{ambient} is set to 300 K. The

total energy dissipated in the reservoirs is roughly equal to the cooling power (100 W) of the cryocooler. Presuming that this dissipated energy is evenly distributed across all four reservoirs, Q is set to 25 Watts for each reservoir. Substituting these values into equation 2.30, the temperature of the reservoir is approximately 320 K, or 20 K above ambient temperature. Every reservoir temperature was therefore set at 320 K and treated as isothermal for this updated expander model used to determine the reservoir sizes. Each reservoir was set to the same volume and the expander model was cycled with a fixed cutoff and recompression volume selected from the results shown in Figure 2.5 and Figure 2.6. The reservoir volume size was reduced until the P-V span in the steady state began to diminish. In Figure 2.10 the reservoir size

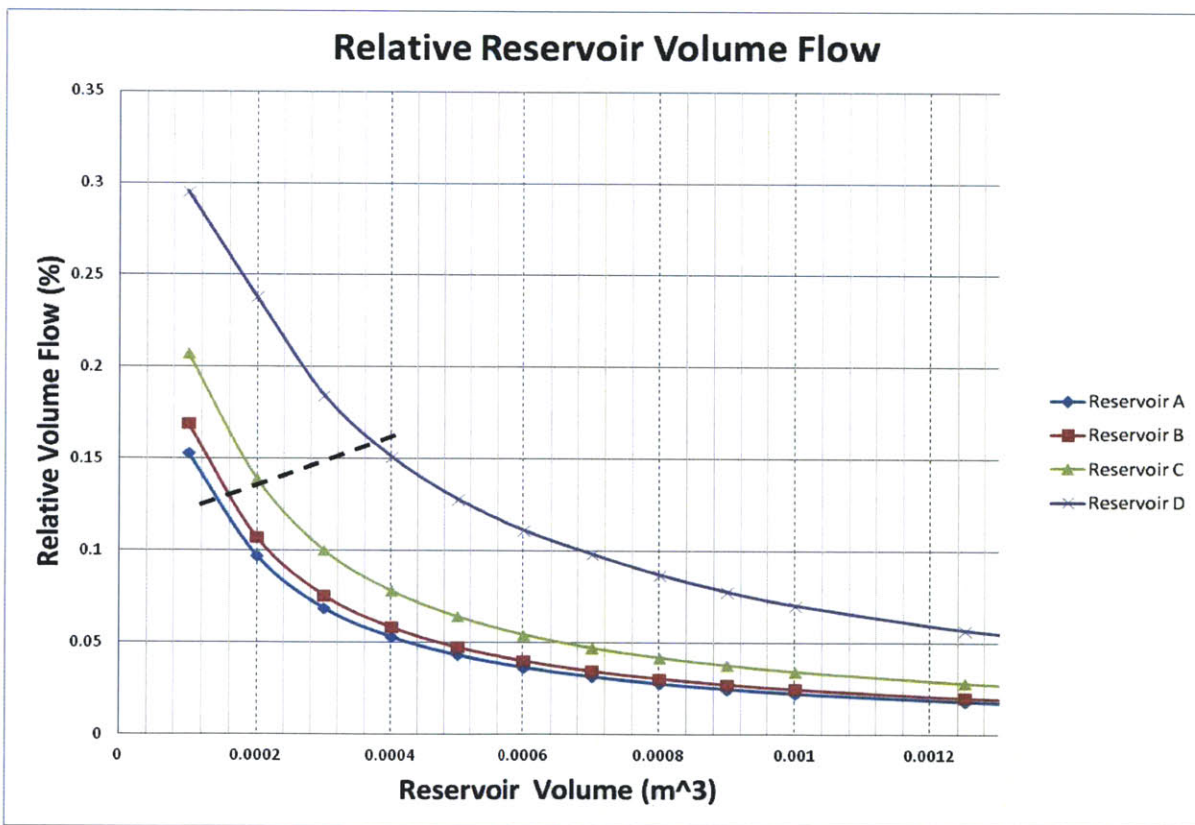


Figure 2.10 Reservoir Volume Flow. The x-axis represents the volume of each pressure reservoir and the y-axis represents the helium volume flow in each reservoir as a percentage of the total helium volume in each reservoir. The data points at 0.0001 m³ are cases that resulted in a diminished P-V span. The dotted line represents the smallest combination of reservoir volumes.

is compared to the relative volume flow of helium in each reservoir.

Figure 2.10 shows the plots of the amplitude of the periodic volume flow into and out of each reservoir normalized by the total volume of the individual reservoir (the relative volume flow) as a function of individual reservoir volume. The total volume that is displaced into the reservoir volumes by the expander is 0.0001 m^3 . Not surprisingly then, the relative volume displaced into the four reservoirs increases dramatically when the reservoir volumes approach this value. In turn, these increases adversely affect the expander because the cycle does not span the available PV space and hence reduces the net cooling power. The volume flow in reservoir D, the low pressure reservoir, is the largest because the largest displacement occurs during exhaust process when reservoir D is open. Therefore, as the reservoir volumes decrease, the relative volume flow in reservoir D will increase more rapidly than the higher pressure reservoirs because the displacement during exhaust remains relatively unchanged.

The simulations used to generate Figure 2.10 show that the PV diagrams begin to degenerate for individual reservoir volumes of 0.0001 m^3 , setting a lower bound for the reservoir volumes. Other adverse effects also appear in the simulations. The pressure begins to fluctuate significantly in the reservoirs which, in turn, can lead to significant temperature fluctuations in the reservoirs due to adiabatic compression, casting some doubt on the constant temperature assumption of the simulations. As a result, a maximum relative volumetric flow rate into reservoir D was limited to 20%. Further simulations of the reservoirs showed that the volumes of each could be individually reduced further and still achieve stable operation. The smallest combination of reservoir volumes (0.14, 0.16, 0.21, and 0.38 liters for reservoirs A, B, C, and D, respectively) is indicated by the intersections of the dotted line and the corresponding reservoir traces in Figure 2.10.

Since these reduced volumes are likely to have inadequate surface area for dissipating to the environment the energy dissipated within them, the operating temperatures of the reservoirs became a concern and so the heat transfer rates were considered for each reservoir. In previous designs, there was no cooling for the reservoirs so natural convection and radiation were considered the only modes of heat transfer for the reservoirs. Due to the low effective thermal resistance of conduction in the reservoir walls, the wall temperature of each reservoir was taken to be the average gas temperature of the reservoir throughout the cycle. The temperature of the gas in the reservoir will cycle more rapidly than the walls and therefore the wall temperature should only increase with the average gas temperature in the steady state.

In what follows, the reservoirs were assigned a diameter of 5.08 cm (2 inches) so that the assumption of a bulk mean temperature could reasonably be used to model the reservoir (the thermal penetration depth for helium at a frequency of 1 Hz is 0.0127 m).

The convective heat transfer coefficient on the outside of the reservoir is defined as

$$h_{cv} = \frac{Nu k_{air}}{L_{res}} \quad (2.31)$$

where Nu is the Nusselt number for the flow over the reservoir, k_{air} is the thermal conductivity of the air (roughly 26 W/m-K at ambient temperature), and L_{res} is the length of the reservoir cylinder. Because the majority of the surface area in each reservoir will be on the vertical cylinder walls, heat transfer from the top and bottom of each reservoir is neglected. The Nusselt number, approximated from the vertical wall correlation in Incropera et. al. [10] is

$$Nu = \left\{ 0.825 + \frac{0.387 Ra_L^{1/4}}{[1 + (0.492/Pr_{air})^{9/16}]^{8/27}} \right\}^2 \quad (2.32)$$

where the Prandtl number for air (Pr_{air}) is 0.707 and the Rayleigh number (Ra_L) is defined as

$$Ra_L = \frac{g\beta(T_{wall} - T_{amb})L_{res}^3}{\nu\alpha} \quad (2.33)$$

where β is defined as the inverse of the average of the wall temperature, T_{wall} , and ambient temperature $\beta = (1/(0.5(T_{wall} + T_{amb})))$, ν is the kinematic viscosity of the air, and α is the thermal diffusivity of the air. The correlation for the radiation heat transfer coefficient is defined in Incropera et. al. [10] as

$$h_{rad} = \varepsilon\sigma(T_{wall} + T_{amb})(T_{wall}^2 + T_{amb}^2) \quad (2.34)$$

where ε is the emissivity of the reservoir material which is assumed to be stainless steel ($\varepsilon = 0.3$) and σ is the Stefan-Boltzmann constant ($5.67 \times 10^{-8} \text{ W/m}^2\text{-K}^4$).

The isothermal assumption of the reservoirs is then dropped from the model. The heat transfer is applied in the First Law equation for each reservoir to determine the helium state in the reservoir. The wall temperature (mean reservoir temperature) is then reset at the end of expansion and the end of recompression for each cycle. The model is run until a steady state is reached. For the study, three sets of reservoir volumes were modeled and the average temperatures and cooling rates for the volumes that achieved a steady state are shown in Table 2.1.

Table 2.1 Reservoir Temperature Results. The average steady state temperature of each reservoir is shown for two sets of reservoir volumes. The half liter reservoir results shown use an assumed forced convection heat transfer coefficient of $25 \text{ W/m}^2\text{-K}$ because steady state operation could not be reached with natural convection and radiation.

Reservoir Volumes (Liters) from High to Low Pressure	Average Reservoir Temperature (K)	Mean Reservoir Temperature (K)
1, 1, 1, 1	338, 327, 315, 302	320
0.5, 0.5, 0.5, 0.5	329, 319, 310, 302	315.25*

The mean reservoir temperature of the one liter reservoirs is 320 K, as previously predicted. The 0.5 liter reservoirs could not reach steady state with only natural convection and radiation so forced convection was considered. An average heat transfer coefficient for natural convection is 2-25 W/m²-K where, with a fan, the heat transfer coefficient (forced convection) could increase an order of magnitude or more (25-250 W/m²-K)[10]. Hence, the 0.5 liter reservoirs were modeled with an assumed forced convection heat transfer coefficient of 25 W/m²-K and a steady state was reached as shown in Table 2.1. The smallest combination of reservoir volumes (see Figure 2.10) does not reach a steady state solution with natural convection, forced convection or radiation. If reservoir volumes of this size are selected, then it will be necessary to increase the surface area of the reservoirs so that the energy can be dissipated effectively. It is also important to note that this study assumes that all dissipation occurs in the reservoirs. It is reasonable to assume that some of the dissipation will occur in the valves and plumbing between the warm volume and each reservoir. In that case the results shown in Table 2.1 would be slight underestimates of the heat dissipation. However the largest dissipation will occur in the reservoirs due to the large surface area for heat transfer.

2.7 Chapter 2 summary

In this chapter a model for the floating piston expander was developed to study the effects of the control points on expander operation. The model assumed that the piston was perfectly sealed and had no mass. The results of the study showed that there is specific region in which the cutoff volume and recompression volume must be set in order to achieve greater expander operation (largest PV span). Additionally, the study showed that the intermediate pressure reservoirs (reservoirs B and C) are less sensitive to the cutoff and recompression volumes than the high and low pressure reservoirs (reservoirs A and D). The impact of the

average reservoir pressure on expander performance was also studied. When the average pressure of the reservoirs is roughly equal to half of the difference between the compressor discharge and compressor suction pressures, the expander shows the best operation (largest PV span). Another result of this study showed that the intermediate pressure reservoirs (B and C) are more sensitive to changes in the average reservoir pressure than the high and low pressure reservoirs. These results give an indication for how the expander should be controlled to maintain steady operation but, blow-by must be introduced into the model to improve the accuracy of predicting the expander behavior.

The size of the reservoirs was also studied to show how small the reservoirs could be sized and still achieve high performance in the expander. The study also showed that natural convection and radiation alone may not provide enough dissipation of the work done on the helium in the expander. Therefore, some forced convection may be required to meet the cooling needs of the prototype.

Chapter 3: Floating Piston Expander Control Algorithm

The model discussed in Chapter 2 establishes the normal operating range of cutoff and recompression volumes for an expander that has no leakage (blow-by) across the floating piston between the cold and warm volumes. In reality, there is always some leakage across the piston that leads to a mass flow from the warm end of the expander to the cold end, or vice versa. If the flow is from the warm end to the cold end, the loss of the gas in the warm end eventually drives the reservoir pressures below that required for the steady operation of the expander.

The goal here is to incorporate blow-by into the model discussed in Chapter 2 so that an appropriate expander control algorithm can be developed to compensate for these blow-by losses in the expander.

3.1 Expander model with helium blow-by

In the blow-by model the piston-cylinder gap is allowed to leak. Contrary to the idealized models described in Chapter 2 the piston is assumed to have mass. As a result of the inertia of the piston, the pressures at the cold and warm ends of the piston will differ, driving flow through the piston cylinder gap.

An estimate for this flow can be made assuming a Poiseuille flow through the gap. The gap thickness is roughly 0.002 to 0.004 inches (5.08×10^{-5} to 10.16×10^{-5} m on the radius) at the cold end of the piston while a tighter clearance (0.0005 inches or 1.27×10^{-5} m on the radius for

one inch of the piston length) was designed for the warm end of the piston. The gap is smaller on the warm end to create a better seal between the cold and warm volume. The warm end was chosen for the tighter clearance because, at any given point in the expander cycle, the smaller helium densities (due to higher temperatures in the warm volume) will result in a reduced mass flow rate through the gap. The flow is assumed to be pressure driven and incompressible for simplicity. The Navier-Stokes equation for the flow is simplified by considering that the gap height is much smaller than the piston circumference so that a flat plate assumption can be made. The model is further simplified because the gap thickness (0.0005 inches or 1.27×10^{-5} m) is much smaller than the gap length (1 inch or 0.0254 m) which means that the pressure gradient along the gap length can be assumed linear (lubrication theory). Assuming laminar, fully developed flow, the resulting velocity distribution for the fluid flow between two plates is [11]

$$v = -\frac{dP}{dx} \frac{\delta^2}{2\mu} \left(\frac{y}{\delta} - \frac{y^2}{\delta^2} \right) \quad (3.1)$$

where $\frac{dP}{dx}$ is the pressure gradient in the flow direction, δ is the gap thickness, μ is the fluid viscosity, and y is the position between the plates as shown in Figure 3.1.

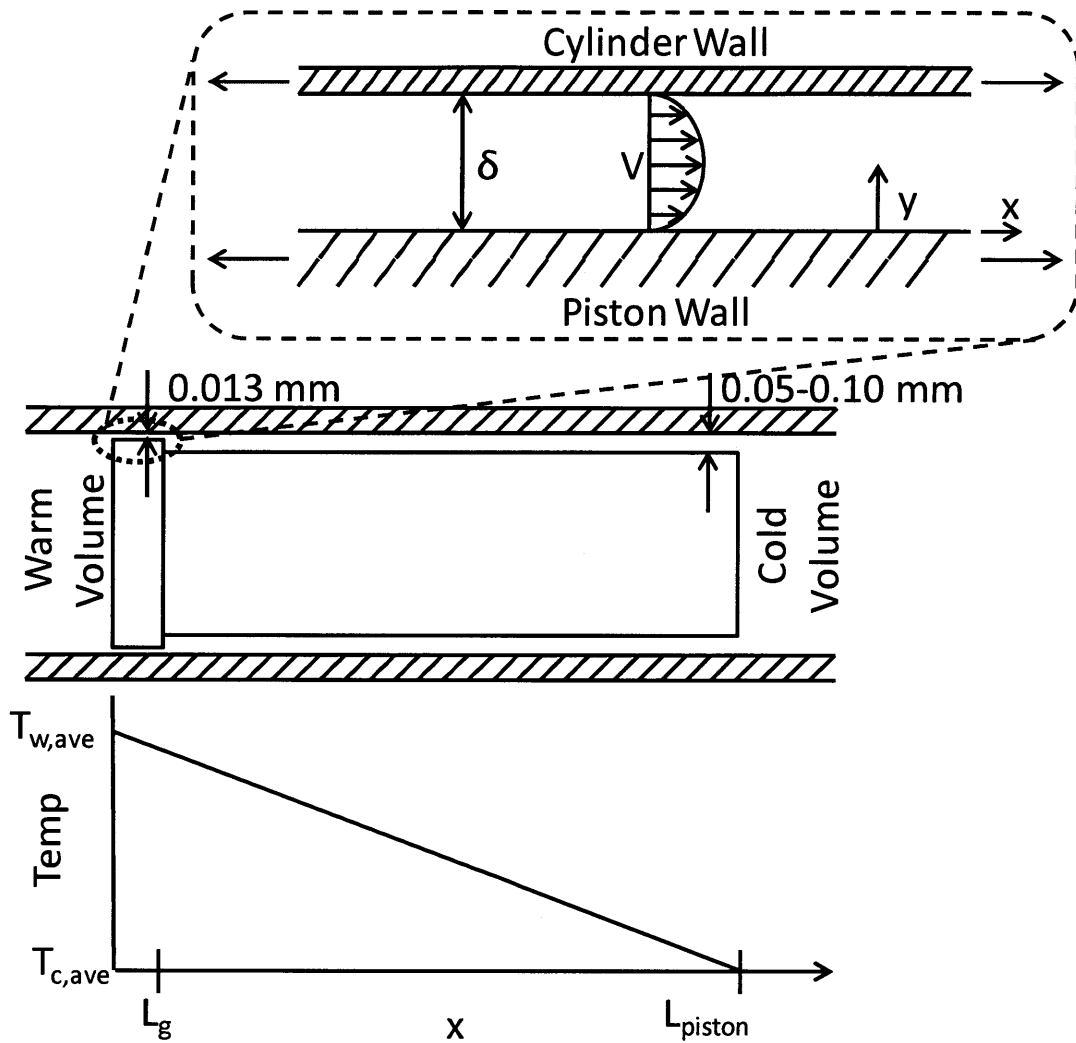


Figure 3.1 Gap flow model. A velocity profile for the flow through the gap is shown with a plot of the assumed temperature profile along the length of the piston.

Integrating equation 3.1 for the entire gap and multiplying by the piston circumference gives the volume flow rate of helium during blow-by

$$\dot{V} = -\pi D_p \frac{\Delta P}{L_g} \frac{\delta^3}{12\mu} \quad (3.2)$$

where D_p is the piston diameter, L_g is the gap length, and ΔP is the pressure drop across the piston. When the helium is flowing out of the warm volume, the mass flow rate is determined using the warm volume density. For flow into the warm volume, the density of the gas just

below the one inch gap is estimated by assuming the pressure to be equal to the cold volume pressure and assuming that the temperature profile of the gas along the length of the piston is linear (as shown in Figure 3.1). It is assumed that, due to the regeneration effects that take place in the helium leakage flow through the piston cylinder gap between the cold and warm volumes, the temperature of the gas at the top of the piston is roughly equal to the average temperature of the warm volume throughout the cycle. It is expected that the heat transfer between the gas in the gap and the walls will, over time, drive the temperature of the walls to the average gas temperature in the warm volume (at the top of the cylinder). Similarly, blow-by flow into the cold volume is presumed to enter at the average temperature of the cold volume throughout the cycle due to regeneration effects in the piston-cylinder gap. The average temperatures ($T_{w,ave}$ and $T_{c,ave}$) are initialized at 400 K and 100 K and re-calculated at the end of each cycle. The temperature used to determine the helium density of the gas one inch (0.0254 m) below the top of the piston is estimated using

$$T_{\text{gap,entrance}} = \frac{T_{c,ave} - T_{w,ave}}{L_{\text{piston}}} L_g + T_{w,ave} \quad (3.3)$$

where L_{piston} is the piston length. A function to determine the amount of helium blow-by that occurs for a fixed time step is created in MATLAB. The function uses the pressure difference across the piston and the state of the helium upstream of the gap entrance (upstream is determined by the pressure gradient) at the beginning of each time step to determine the blow-by mass flow rate.

The Poiseuille flow solution assumes fully developed flow. However, there is a time constant associated with reaching the fully developed flow. The shortest processes in the expander cycle are blow-in and blow-out (each lasting roughly 0.005 seconds) and are therefore

the most likely to fall below this time constant. An estimate of the time constant for blow-in and blow-out can be made using the time dependent Bernoulli equation [11]. The time constant for the developing flow is

$$\tau = \frac{2L_g}{\sqrt{\frac{2\Delta P}{\rho}}} = 0.0001 \text{ seconds} \quad (3.4)$$

for blow-in and blow-out, where ρ is density of the flow into the gap. From this, it is expected that the flow will be fully developed in all processes throughout the cycle. The viscous effects of the moving piston on the flow of helium through the gap (plane Couette flow) are also neglected in this model.

Using equation 3.2, the blow-by that is caused by the weight of the piston can be estimated. Because the blow-by induced by this force will be constant, the mass in the warm end of the cylinder will increase during steady state operation without the piston contacting the surface of the cylinder (piston touchdown). For example, the piston mass in the first stage is roughly 0.4 kg and if the pressure difference across the piston is equated to the gravitational force on the piston and the surface area of the piston face, the blow-by mass flow rate (estimating the density at 300 K and 0.5 MPa) is 5.2×10^{-8} kg/s. For a 1 Hz machine, this represents a negligible amount of helium added to the warm volume per cycle. However, without controlling this flow, roughly ten minutes of operation (550 cycles) would result in a one percent increase of the average reservoir pressure (when operating in the ideal reservoir pressure range with one liter reservoirs).

For the motion of the piston, a function is created in MATLAB to determine the new piston position, velocity, and acceleration using Newton's Second Law of Motion with inputs of the previous position, velocity, and the pressure difference across the piston. Once the new

piston position, acceleration, and the helium mass lost due to blow-by are known, the new helium state can be determined in each volume. This is determined using the First Law of Thermodynamics for both the cold volume and the warm volume.

During blow-in, there is only helium flow into the cylinder through the intake valve. At the start of the model, the cylinder is initialized with the piston stationary at the bottom of the cylinder in the cold volume. The pressure drop across the piston is initialized to zero and the initial pressure in the warm volume is set to be equal to the high pressure reservoir pressure. The First Law for the cold volume is

$$\frac{dE_{cv}}{dt} = \dot{Q} - \dot{W}_{cold} + (\dot{m}h)_{in} - (\dot{m}h)_{out} \quad (3.4)$$

where \dot{Q} is zero (adiabatic), \dot{W}_{cold} is the work done by the gas in the cold volume, $(\dot{m}h)_{in}$ is the helium flow into the cylinder through the intake valve, and $(\dot{m}h)_{out}$ is the helium flow due to blow-by. Assuming perfect mixing, equation 3.4 can be modified to

$$\frac{d(mc_v T)_{cv}}{dt} = -\dot{W}_{cold} + (\dot{m}_{intake} c_p T_{intake})_{in} - (\dot{m}_{blo} c_p T_{c,1})_{out} \quad (3.5)$$

where T_{intake} is the temperature of the intake gas and $T_{c,1}$ is the initial helium temperature in the cold volume. The intake mass flow rate, \dot{m}_{intake} , and the blow-by mass flow rate, \dot{m}_{blo} , are determined using the previously discussed equations. The rate of work done by the cold volume gas is

$$\dot{W}_{cold} = P_c \frac{dV_c}{dt} \quad (3.6)$$

Substituting equation 3.6 into equation 3.5, using the ideal gas assumption to manipulate the left hand side and integrating over the time step gives

$$\frac{(P_{c,2}V_{c,2} - P_{c,1}V_{c,1})}{\gamma - 1} = -P_{c,1}(V_{c,2} - V_{c,1}) + (m_{\text{intake}}c_p T_{\text{intake}})_{\text{in}} - (m_{\text{blo}}c_p T_{c,1})_{\text{out}} \quad (3.7)$$

where $V_{c,1}$ is the initial cold volume, $V_{c,2}$ is the final cold volume, $P_{c,1}$ is the initial cold volume pressure, m_{intake} is the net mass flow through the intake valve, m_{blo} is the net mass flow due to blow-by, and the final pressure in the cold volume, $P_{c,2}$, is the only unknown. Solving for $P_{c,2}$ gives

$$P_{c,2} = \frac{1}{V_{c,2}} \left[P_{c,1}V_{c,1} + (\gamma - 1) \left(-P_{c,1}(V_{c,2} - V_{c,1}) + (m_{\text{intake}}c_p T_{\text{intake}}) - (m_{\text{blo}}c_p T_{c,1}) \right) \right] \quad (3.8)$$

The pressure in the warm volume can be determined using the First Law for a control volume enclosing all of the gas in the warm volume. During blow-in, the only flow into the warm volume is due to blow-by. Therefore, using the same First Law approach as that used for the cold volume, the final pressure in the warm volume for the fixed time step, $P_{w,2}$, is

$$P_{w,2} = \frac{1}{V_{w,2}} \left[P_{w,1}V_{w,1} + (\gamma - 1) \left(-P_{w,1}(V_{w,2} - V_{w,1}) + (m_{\text{blo}}c_p T_{w,\text{ave}})_{\text{in}} \right) \right] \quad (3.9)$$

where $V_{w,2}$ is the final warm volume, $V_{w,1}$ is the initial warm volume, $P_{w,1}$ is the initial warm volume pressure, and $T_{w,\text{ave}}$ is the mean temperature of the warm volume throughout the cycle, as described earlier. The helium mass in each volume is found by using mass conservation for the fixed time step. The temperature in each volume is found using the ideal gas law.

The intake process is modeled in a manner similar to blow-in. The control volumes are the same for both processes but, since the high pressure reservoir valve is open, there is an additional flow across the control volume boundary out of the warm volume. The pressure

difference across the piston is again used to determine the new position, velocity, and acceleration of the piston. The mass flow through the intake valve and the high pressure reservoir valve are determined from the pressure drop across the valve as well. From this, a First Law analysis of each volume is needed to determine the state. The resulting equation for the pressure in the cold volume is the same as equation 3.8 while the pressure in the warm volume becomes

$$P_{w,2} = \frac{1}{V_{w,2}} \left[P_{w,1} V_{w,1} + (\gamma - 1) \left(-P_{w,1} (V_{w,2} - V_{w,1}) + (m_{blo} c_p T_{w,ave})_{in} - (m_{res} c_p T_{w,1})_{out} \right) \right] \quad (3.10)$$

where m_{res} is the net helium mass flow into the high pressure reservoir and $T_{w,1}$ is the initial temperature in the warm volume. Again, mass conservation is used to determine the new helium mass in each volume and the ideal gas law is used to determine the new temperature in each volume.

The expansion process uses the same method as the blow-in and intake processes. However, the intake valve is closed during expansion so the only flow in to or out of the cold volume is the result of blow-by. Again, Newton's Second Law is used to determine the new piston position, acceleration and velocity. The mass flow through the pressure reservoir valves is determined from the pressure drop across each valve as well. A First Law analysis of the warm volume shows that the pressure can be determined using equation 3.10. The resulting pressure in the cold volume is

$$P_{c,2} = \frac{1}{V_{c,2}} \left[P_{c,1} V_{c,1} + (\gamma - 1) \left(-P_{c,1} (V_{c,2} - V_{c,1}) - (m_{blo} c_p T_{c,1})_{out} \right) \right]. \quad (3.11)$$

The model for the blow-out, exhaust, and recompression processes is analogous to the model for the blow-in, intake, and expansion processes, respectively. The difference for blow-out is that

helium flows out of the cold volume through the open exhaust valve. For exhaust, the difference is that helium flows out of the cold volume and into the warm volume from the low pressure reservoir. For the recompression process, the difference is that helium flows into the warm volume from the pressure reservoirs. Additionally, because the warm volume is now pushing on the cold volume for these processes, the pressure will typically be greater in the warm volume resulting in blow-by down the piston, toward the cold volume. The MATLAB code for this modeled can be found in Appendix D.

As a result of the clearance seal design feature, this expander is expected to have low frictional drag on the piston due to the lack of direct contact with the walls of the cylinder. Previous free-piston expander designs used an o-ring seal at the warm end of the piston that put an estimated 9.3 N drag force on a 2.54 cm diameter piston [7]. If this o-ring design were adopted for the 10 cm diameter piston discussed here the scaled drag force would be 35 N.

Clearly 35 N is expected to be an upper bound as a contact friction force on the piston for the current design. The mass flow rate past the piston will depend on the frictional drag on the piston. Figure 3.2 is a plot of the mass flow rate past the piston in the clearance seal design as a function of the assumed frictional drag on the piston for forces from 0.35 to 35 N. The net mass flow rate past the piston dramatically increases for drag forces above 3.5 N. Below 3.5 N, the mass flow rate saturates to a value of 4.6×10^{-8} kg/s, comparable to the flow induced by gravitational effects. In this analysis, the frictional drag forces on the piston are, rather arbitrarily, assumed to be 0.7 N (within the saturated region of friction forces). Variations of the actual value of the frictional forces are not expected to have a large effect on the mass flow rates past the piston provided they remain below 3.5 N.

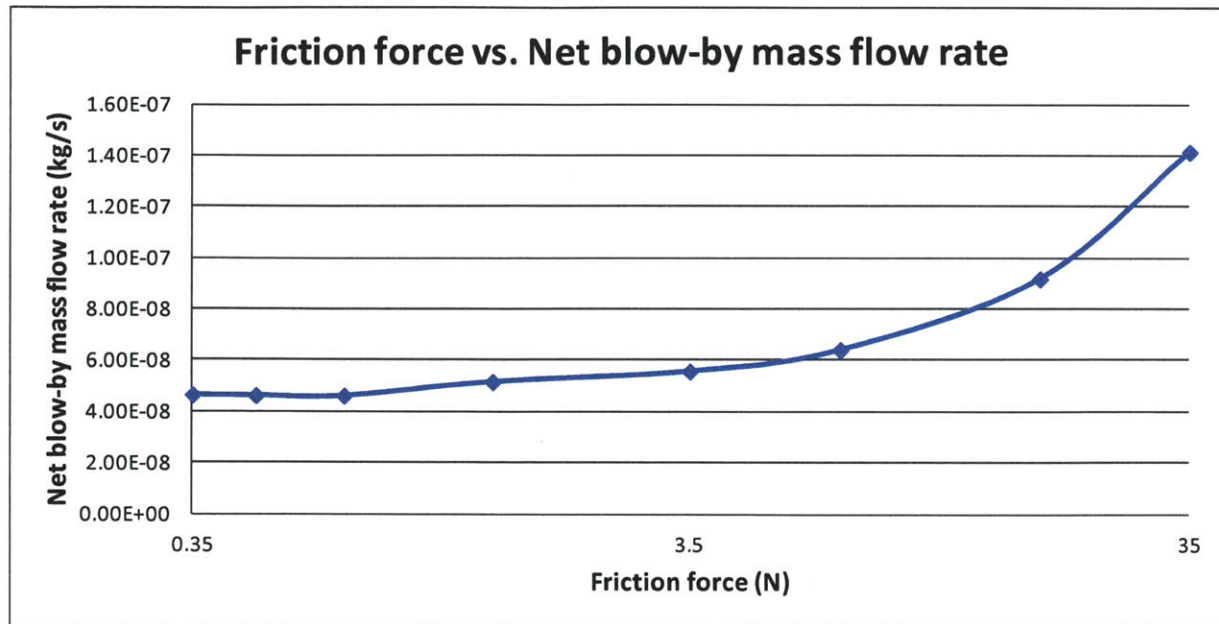


Figure 3.2 Effect of friction force coefficient on net blow-by mass flow rate. The resulting net mass flow rate of helium due to blow-by is plotted as a function of the friction drag force.

To initialize the model, the pressures in the pressure reservoirs are set and distributed between the maximum and minimum cycle pressure such that the average pressure of the reservoirs reflects the ideal range discussed in Chapter 2 (see Figure 2.7). The piston is assumed to be initially at rest at the bottom of the cold end of the cylinder. The warm and cold volume pressures are initialized to the pressure in the high pressure reservoir and the model is cycled multiple times to observe steady operation. An example of the expander model results for the first stage is shown in Figure 3.3. The figure shows the pressure on both sides of the piston plotted against the cold helium volume. The pressure in the warm volume tends to be slightly less than the pressure in the cold volume during intake and expansion, when the piston is moving toward the warm end of the cylinder. Analogously, the pressure in the warm volume is usually slightly larger than the pressure in the cold volume during exhaust and recompression, when the piston is moving toward the cold end of the cylinder.

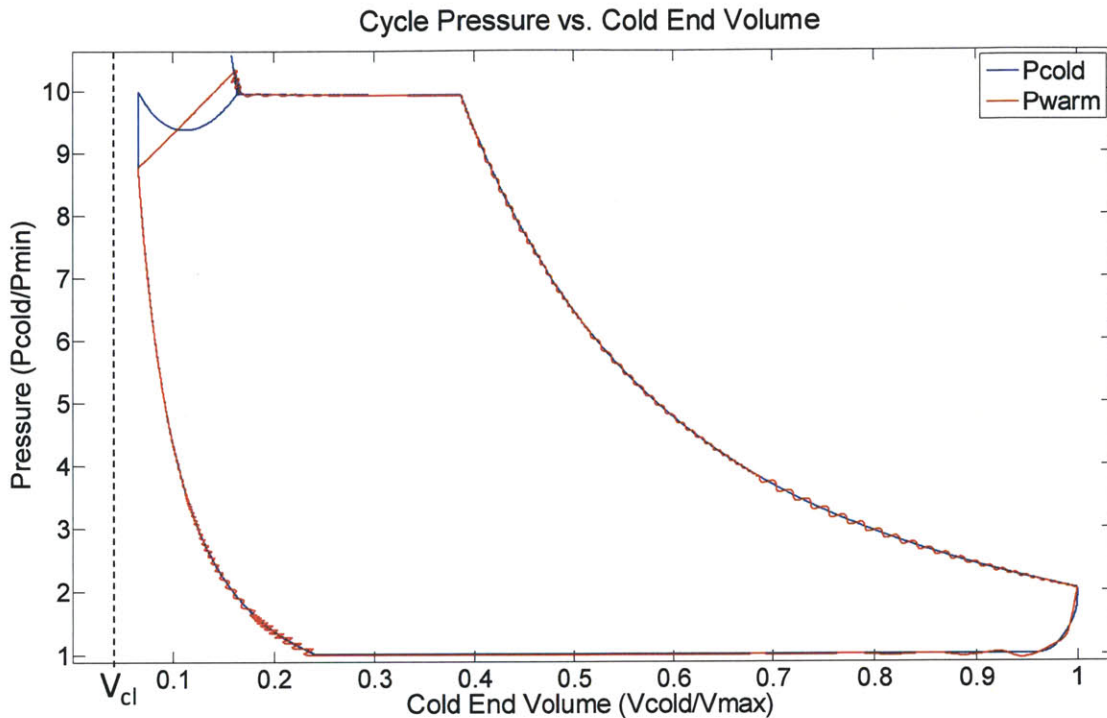


Figure 3.3 Sample first stage expander model with piston inertia. The pressure in the cold volume and the pressure in the warm volume are plotted against the volume of gas in the cold end of the cylinder for the first stage expander.

The spike that occurs during the intake process of the cycle is large because, due to the acceleration of the piston, the gas in the warm volume is compressed beyond the maximum pressure. This, in turn, causes the warm volume gas to expand and push the piston back down toward the cold volume which compresses gas in the cold volume. The piston briefly oscillates at this point until the pressures begin to equalize. The frequency of this oscillation occurs at roughly the natural frequency of the expander. The acceleration and (amplified) velocity of the piston are plotted in Figure 3.4 for the duration of the blow-in and intake processes. The oscillation circled in the figure occurs in the first 0.01 seconds and has a frequency of roughly 400 Hz.

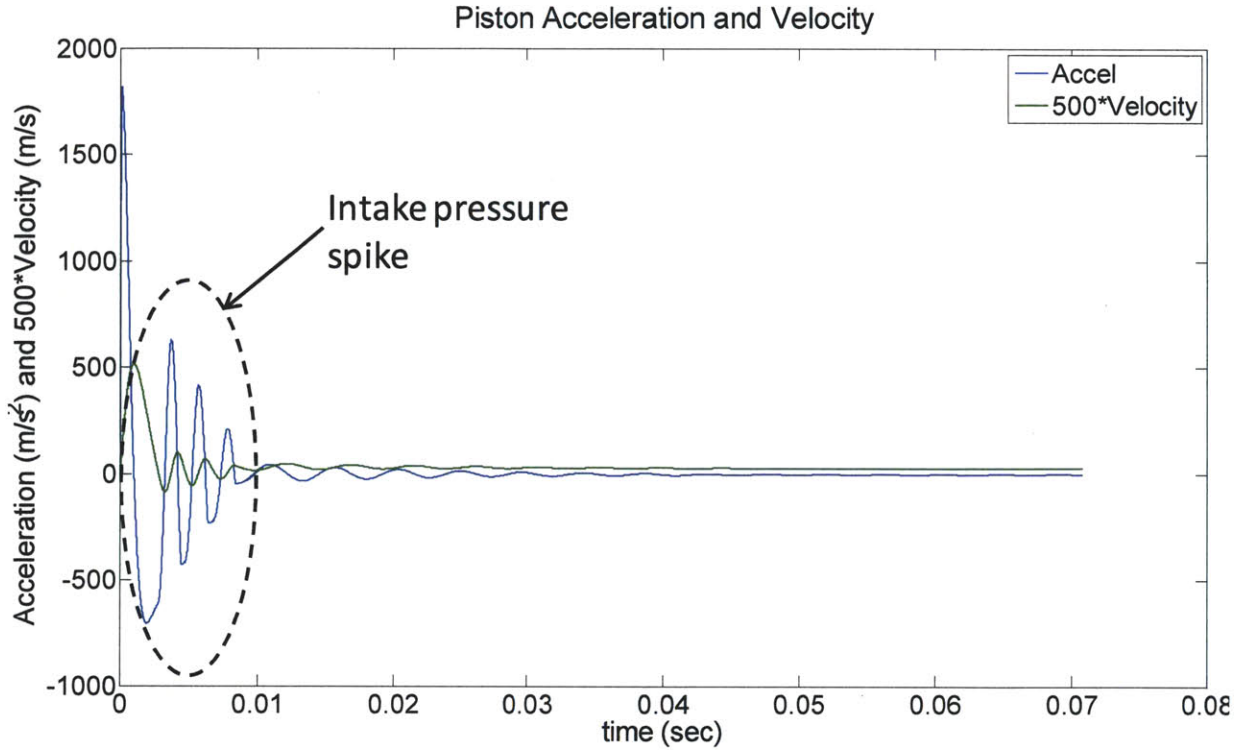


Figure 3.4 First stage acceleration and velocity during intake. The acceleration of the piston and the velocity of the piston (amplified 500 times) are plotted over the duration of the intake processes.

The natural frequency of the expander is estimated by approximating the spring constant on either side of the piston using the equation

$$f = \frac{1}{2\pi} \sqrt{\frac{K_{c+w}}{m_{piston}}} \quad (3.12)$$

where the spring constant for the cold and warm volumes, K_{c+w} , is taken as the mean spring constant throughout the expander cycle. The spring constants are estimated at various points throughout the expander operation using the equation

$$K = \gamma A_p^2 \frac{P}{V} \quad (3.13)$$

where A_p is the area of the piston face, P is the helium pressure in the volume being considered, and V is the volume of helium. Equation 3.13 is derived from the Hooke's Law ($F=-K\Delta x$) and

the isentropic assumption ($PV^\gamma = \text{Constant}$) for the helium remaining in the cylinder. Using equations 3.13 and 3.12 the natural frequency of the expander is estimated to be between 330 Hz and 500 Hz which covers the 400 Hz oscillation observed in Figure 3.4. This trend is not observed in any other part of the expander cycle because the frequency everywhere else does not fall within this natural frequency range.

An example of the expander cycle for the second stage is shown in Figure 3.5. The expander in the second stage is longer (0.653 m versus 0.434 m) and heavier (0.591 kg versus 0.394 kg). As a result, the piston acceleration and velocity are not as large at the beginning of the intake. Additionally, the spike in pressure during intake is not as pronounced in stage 2 because the resulting piston oscillation does not fall within the natural frequency of the stage.

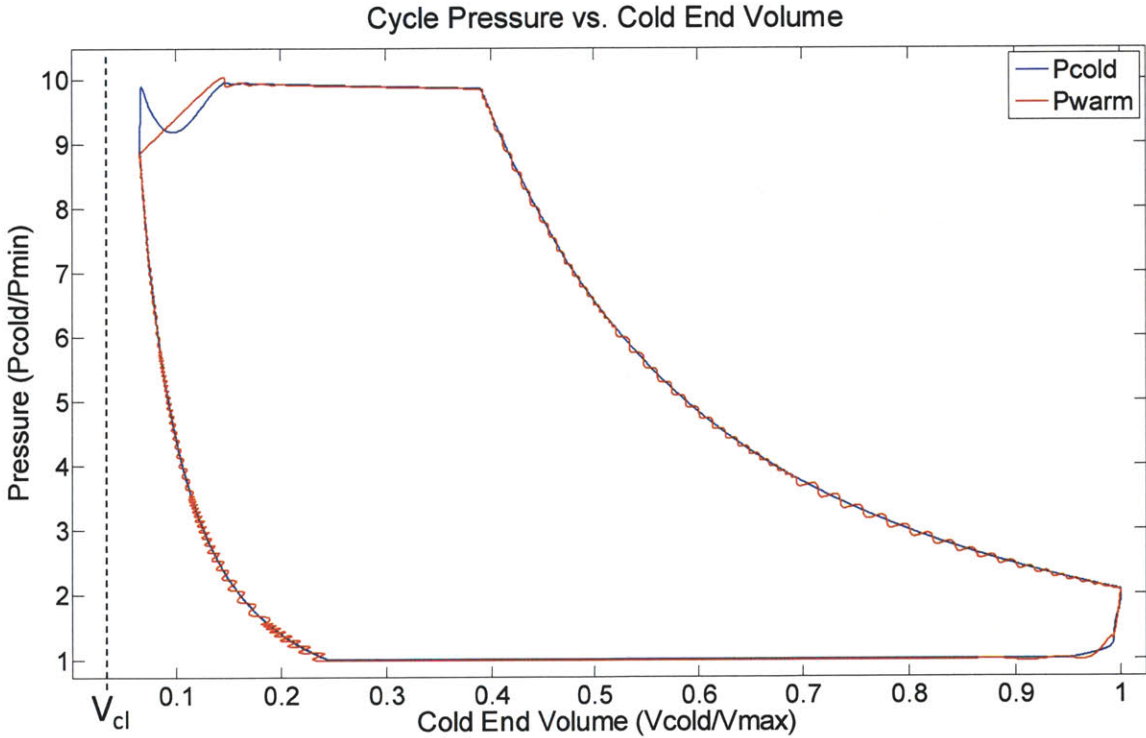


Figure 3.5 Sample second stage expander model with piston inertia. In the second stage the piston is longer and heavier than in the first stage.

3.2 Steady State operation of the expander

The previous prototype showed that there was a continuous drop in the pressure of the pressure reservoirs throughout the expander operation. It is believed that this is due to flow past the piston, flow from the warm volume to the cold volume, that was driven by the piston frequently contacting the bottom of the cylinder at the cold end of the expander. This contact increases the pressure difference across the piston, and hence the blow-by flow. In steady state operation, the piston should not contact the top or the bottom of the cylinder. Hence, each expander stage is modeled without the piston surface contact to determine the impact of the blow-by flow in the steady state.

For this model of the expanders, the pressures in the pressure reservoirs were initially distributed such that the mean reservoir pressure was in the ideal range discussed in Chapter 2 of 5.0. Additionally, the cutoff and recompression volumes were set in the ranges observed in Figure 2.3 and Figure 2.4 (40% of V_{max} and 25% of V_{max} , respectively). For the expander models that follow, the control algorithm shown in Table 3.1 was used where $P_{cycle, mean}$ is half the mean of the intake pressure and the exhaust pressure, and $P_{res, mean}$ is the mean pressure in all four reservoirs. Table 3.2 shows the conditions required for switching between reservoirs during

Table 3.1 Simple control scheme for expander model. When the average reservoir pressure is above or below the cycle mean pressure (plus a tolerance of 5kPa) the cutoff and recompression volumes are adjust to get the expander back to this operating point. ($P_{cycle, mean} = 0.5$ MPa)

Control Condition	V_{co}/V_{max}	V_{rec}/V_{max}
If $P_{cycle, mean} - 5 \text{ kPa} < P_{res, mean} < P_{cycle, mean} + 5 \text{ kPa}$	0.40	0.25
If $P_{res, mean} < P_{cycle, mean} - 5 \text{ kPa}$	0.50	0.25
If $P_{res, mean} > P_{cycle, mean} + 5 \text{ kPa}$	0.375	0.1 (1 st stage) 0.05 (2 nd stage)

Table 3.2 Reservoir switch conditions for expansion and recompression. The pressures in the warm volume at which the reservoir valves open and close during expansion and recompression are shown as fractions of the reservoir pressure.

Process	Reservoir A	Reservoir B	Reservoir C	Reservoir D
Expansion	1.01	1.01	1.01	1.01
Recompression	0.98	0.98	0.98	0.98

expansion and recompression for the expander models that follow in this and subsequent sections. The table shows that each reservoir valve will open and close when the pressure in the warm volume is equal to specified coefficient of the reservoir pressure.

The indicator diagram in Figure 3.6 shows the first stage operation after 100 cycles of the expander model. The expander has achieved a “steady state” but there is a steady blow-by flow,

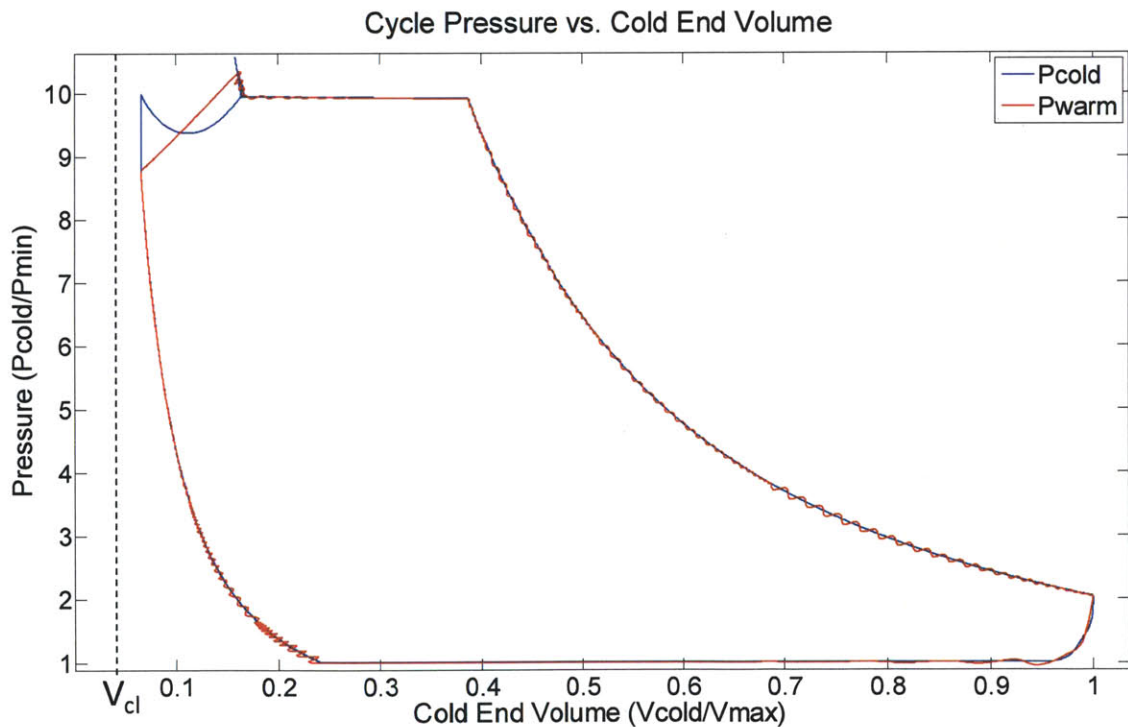


Figure 3.6 First stage expander model with no touchdown after 100 cycles. The pressure in both cold and warm volumes is plotted against the volume of gas in the cold end of the cylinder for the first stage expander.

due to the weight of the piston, creating a net average mass flow past the piston towards the warm volume. This flow is consistently adding mass to the warm volume which, in turn, increases the average pressure of the pressure reservoirs over long periods of time. After 100 cycles, the total mass in the warm end of the first stage has increased by roughly 0.1% and the mean reservoir pressure has increased by 0.13% as a result. Note that, during the first cycle, some of the mass that was initially in the warm volume is distributed into the reservoirs creating an additional increase in the mean reservoir pressure.

Similar trends can be found in the second stage expander. Figure 3.7 shows the second stage indicator diagram after 100 cycles. In the second stage, the total mass in the warm end has increased by roughly 0.16% and the mean reservoir pressure has increased by 0.18% as a result. Figures 3.6 and 3.7 indicate steady cycle behavior; however, blow-by flow will still impact

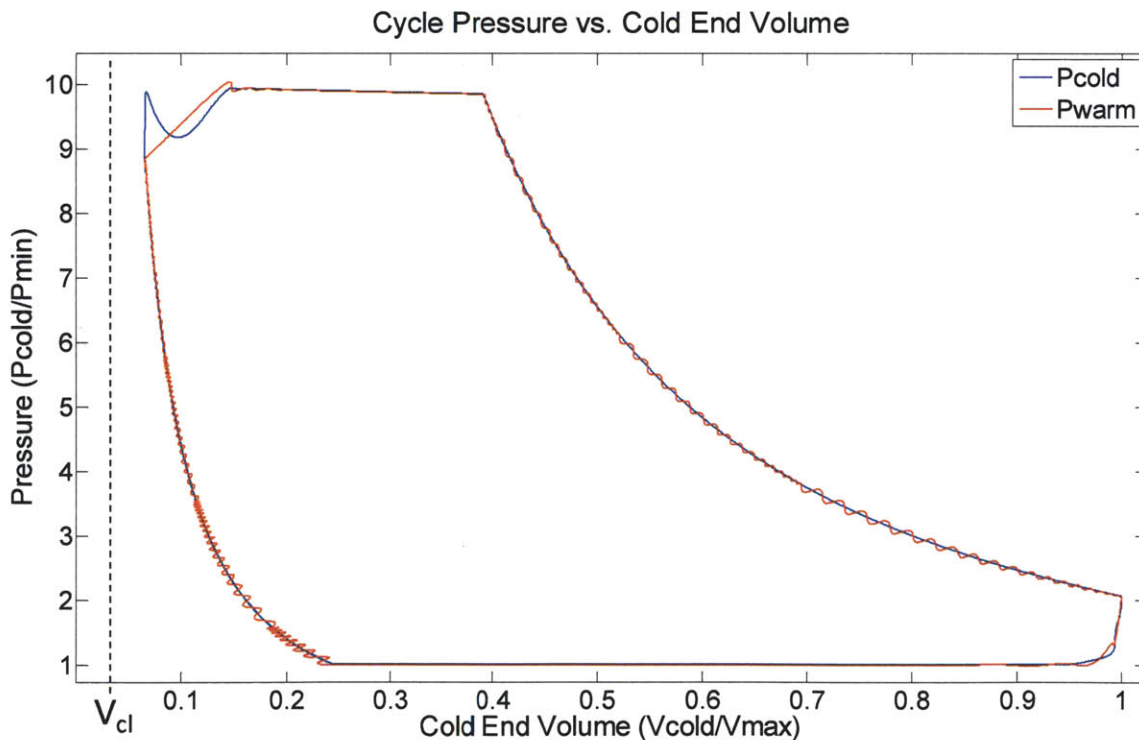


Figure 3.7 Second stage expander after 100 iterations. The pressure in both cold and warm volumes is plotted against the volume of gas in the cold end of the cylinder for the first stage expander.

“steady state” performance over time if it is not accounted for. Therefore, steady state operation controls of the expander will require that this additional mass be monitored on a cycle by cycle basis.

3.3 Adding mass to the warm volume

The previous section has shown that there is a net mass flow across the piston from the cold volume to the warm volume when the expander is operated in a stable cycle with no touchdown. The control of the mass flow across the piston can be achieved by allowing the piston to selectively touchdown and reside on one end of the cylinder or the other. In the case that the expander is operating with reservoir pressures that drift below an optimal range, as shown to occur in past prototypes [7], mass should be added to the warm volume to regain good performance. To get mass flow from the cold end of the piston to the warm end, the piston can be set against the top of the cylinder. The pressure difference that appears across the piston when it is hard against the cylinder head drives mass from the cold end of the expander to the warm end.

For adding mass to the reservoirs, several control scenarios were considered before the scenario used here was selected. The best method for adding mass to the reservoirs is to set down the piston during expansion, after the intake valve has closed and before the reservoir D valve closes. This method allows more control over the piston motion such that the contact force is smaller and cooling of the cold volume gas occurs every cycle. Setting down the piston at the end of expansion increases the pressure difference across the piston to the pressure difference between the cold volume and the low pressure reservoir. The helium then flows from the cold volume, through the piston cylinder gap, and into the low pressure reservoir. The piston dwells at this position for 100 milliseconds. This time is fixed so that the mass can be added to the

warm volume and distributed to the reservoirs over multiple cycles. Additionally, the helium mass in the reservoirs may be so low that it is not possible to add enough through blow-by in one cycle before an equilibrium pressure is reached across the piston. This control scenario also maintains the targeted 1 Hz frequency as opposed to the previous scenario.

The results of a simulation for the latter control scenario are shown in Figures 3.8 through 3.17. In this simulation the reservoir pressure ratios (P/P_{\min}) are initially distributed so that the mean reservoir pressure ratio is 4.0, below the ideal value established in Chapter 2 of 5.0. More specifically, the pressure ratio distribution of the reservoirs is 7.5, 4.5, 2.5, and 1.5 for reservoirs A, B, C, and D, respectively. The cutoff and recompression volumes are initially set to their ideal steady state values of 40% and 25% of the maximum volume, respectively. The model runs for 100 cycles under these conditions to allow the pressures in the reservoirs to move to their “steady state” values.

At cycle 100, the control scenario discussed above is initiated. Since the mean reservoir pressure is below the minimum target pressure ratio of 4.95 (Table 3.1 has the specifics of the target values), the cutoff volume is increased from the steady 40% value to 50% of the maximum volume. The piston then reaches and contacts the warm (top) end of the cylinder and is allowed to dwell there for 100 ms while the reservoir D valve is held open. Gas leaks past the piston from the cold volume into the warm volume and into reservoir D.

Figure 3.8 and 3.9 are indicator diagrams for the simulations of the first and second stage expanders after 100 cycles. Since the average pressure in the reservoirs is low, the expander cycle does not span the range of available cylinder volumes. In these first 100 cycles, there is a small mass flow past the piston that changes is the mass of helium in the reservoirs from 2.500 g to 2.503 g in the first stage and 2.513 g in the second stage.

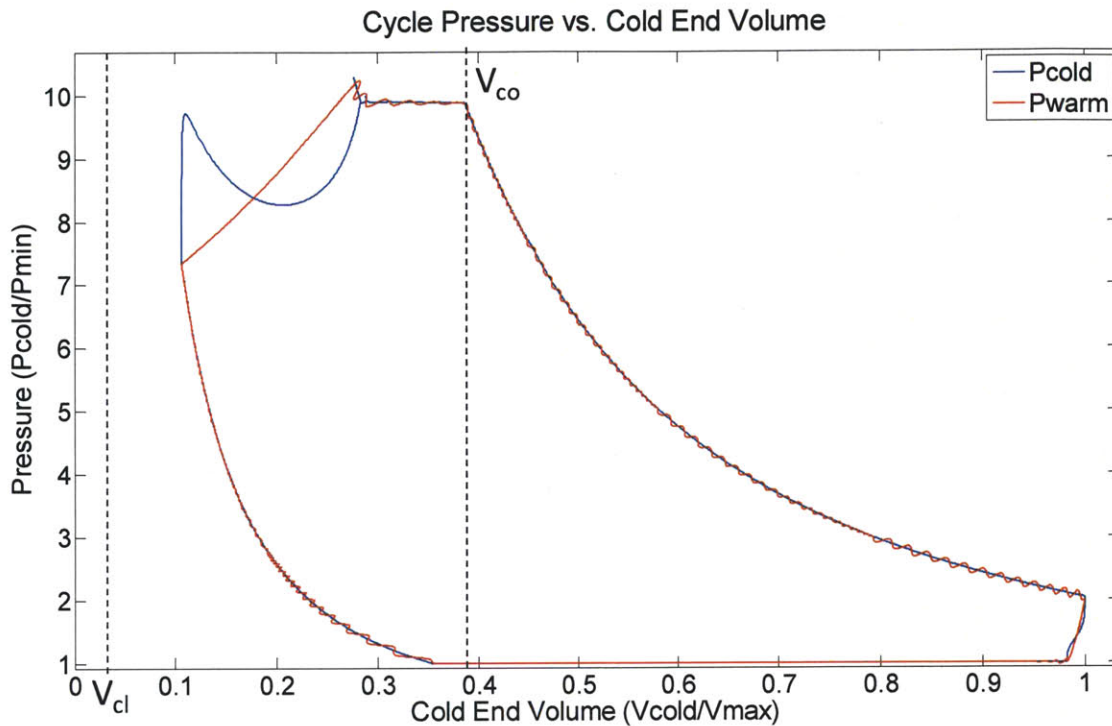


Figure 3.8 First stage indicator diagram for low mean reservoir pressure. The cold volume helium pressure and the warm volume helium pressure are plotted against the volume of helium in the cold end of the expander. The model shows expander operation after 100 cycle iterations. $P_{res}/P_{min}=4.1$ which is different from the pressure ratio quoted in the text of 4.0. The disparity is due to the gas initially in the warm volume that is distributed to the reservoirs after a few cycles. The vertical line, V_{cl} , is the clearance volume in the cold end. The vertical line, V_{co} , is the cutoff volume. The percentage value described in the text is with respect to the maximum swept volume (0.1 liters) where the maximum volume in this diagram ($V_{cold}/V_{max} = 1.0$) also includes the clearance volume, causing the cutoff volumes to look shifted.

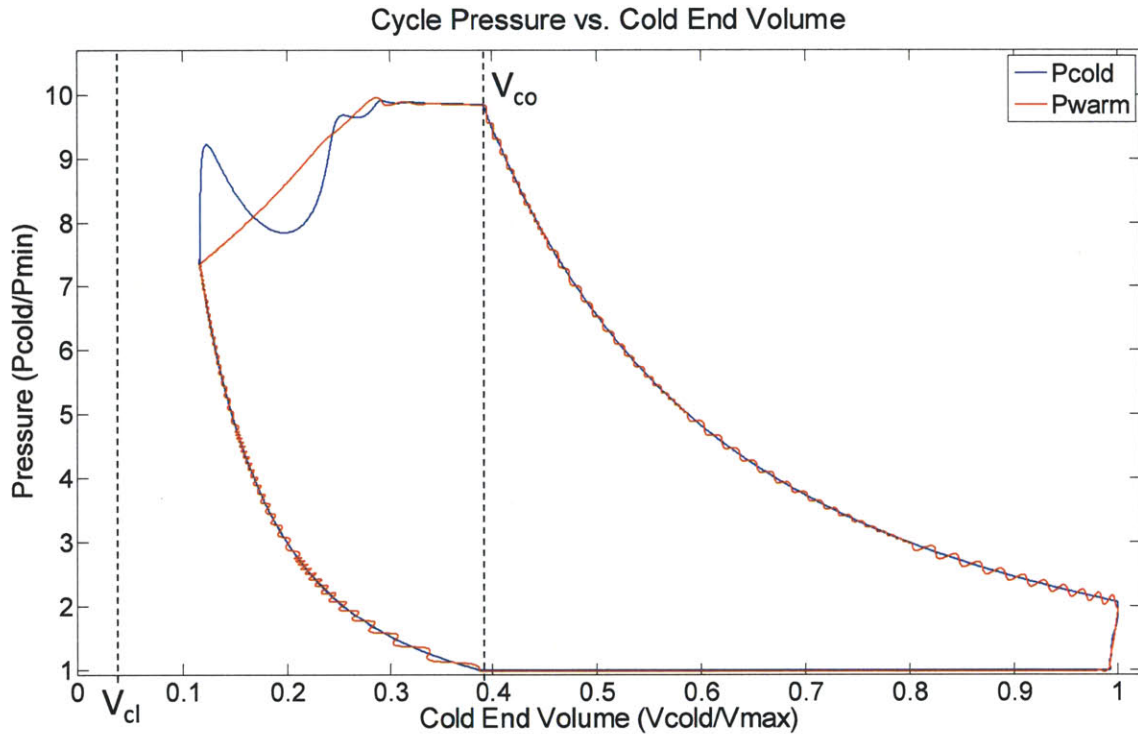


Figure 3.9 Second stage indicator diagram for no addition with low mean pressure. The cold volume helium pressure and the warm volume helium pressure are plotted against the volume of helium in the cold end of the expander. The model shows expander operation after 100 cycle iterations (mean $P_{res}/P_{min}=4.1$, see comment in Figure 3.8).

After the hundredth cycle the cutoff volume is shifted and the piston is allowed to dwell on the top of the cylinder. This process distorts the cycle as shown in Figure 3.10 for the first stage. The pressure at the end of expansion when the piston is contacting the cylinder head is higher ($P/P_{min}=3.0$) than the corresponding pressure in the “steady state” cycle ($P/P_{min}=2.0$ in Figure 3.8). Note that for this model the pressure in the cylinder at the end of expansion is not necessarily equal to the pressure in reservoir D but merely the pressure in the cylinder when the maximum volume was reached. The shape of the indicator diagram in Figure 3.10 differs from the shape in Figure 3.8 because, when the piston is contacting the top of the cylinder, the pressure in the cylinder and the pressure in the low pressure reservoir come to equilibrium at a lower pressure than the end of expansion in the “steady state.” Therefore, with little mass in the

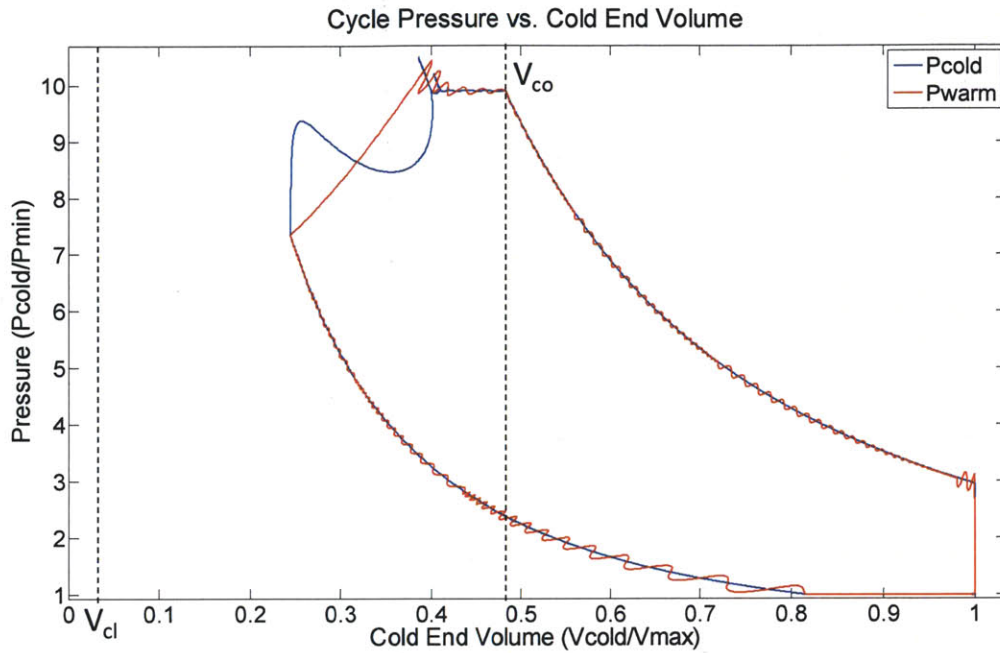


Figure 3.10 First stage indicator diagram for early helium addition. The cutoff volume (V_{co}) is increased; the piston reaches the top of the expander and dwells for 0.1 seconds before the blow-out process begins. (cycle number 114, mean $Pres/Pmin=4.13$).

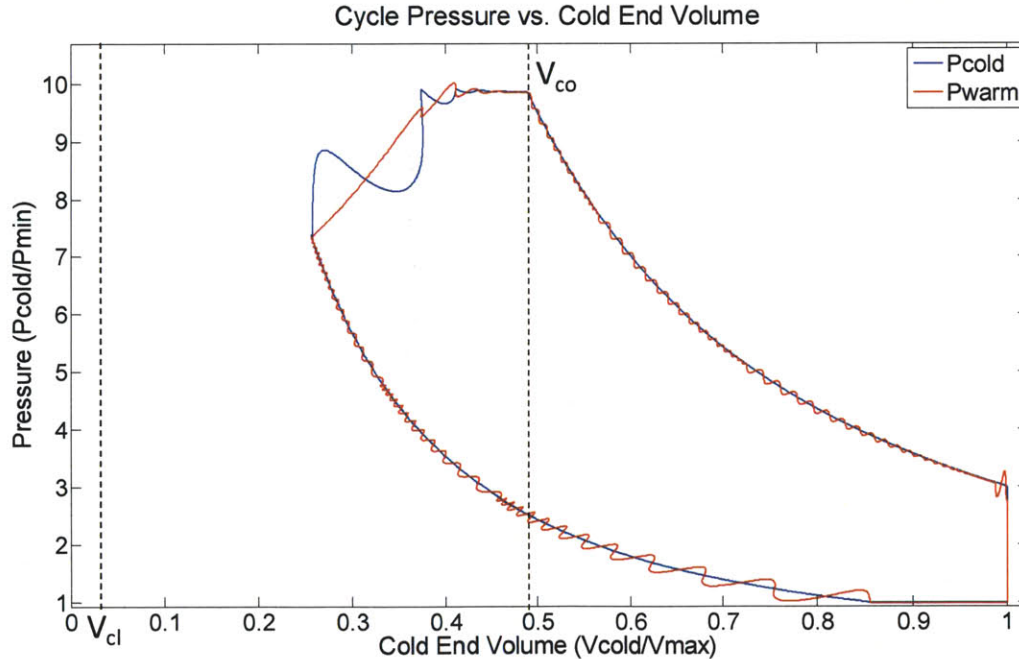


Figure 3.11 Second stage indicator diagram for early helium addition. The cutoff volume (V_{co}) is increased; the piston reaches the top of the expander and dwells for 0.1 seconds with before the blow-out process begins. (cycle number 114, mean $Pres/Pmin= 4.13$).

reservoir and a pressure closer to the minimum pressure, the low pressure reservoir (D) quickly reaches the minimum pressure during exhaust and the piston hangs until a 0.5 second time limit is enforced for the exhaust process, at which point the recompression begins. As a result, the swept volume of the piston is limited. The same argument can be made for the difference in shapes of the second stage indicator diagrams shown in Figure 3.9 and Figure 3.11.

As the mass in the reservoirs begins to approach the target value of 3.0 g, the indicator diagrams improve as shown in Figure 3.12 and Figure 3.13 for the first and second stage, respectively. During the piston dwell time, the mass in reservoir D has increased such that the pressure of the gas in the cylinder and the pressure of the gas in the reservoir reach equilibrium at a higher pressure than in the beginning of the helium addition process, however this pressure is

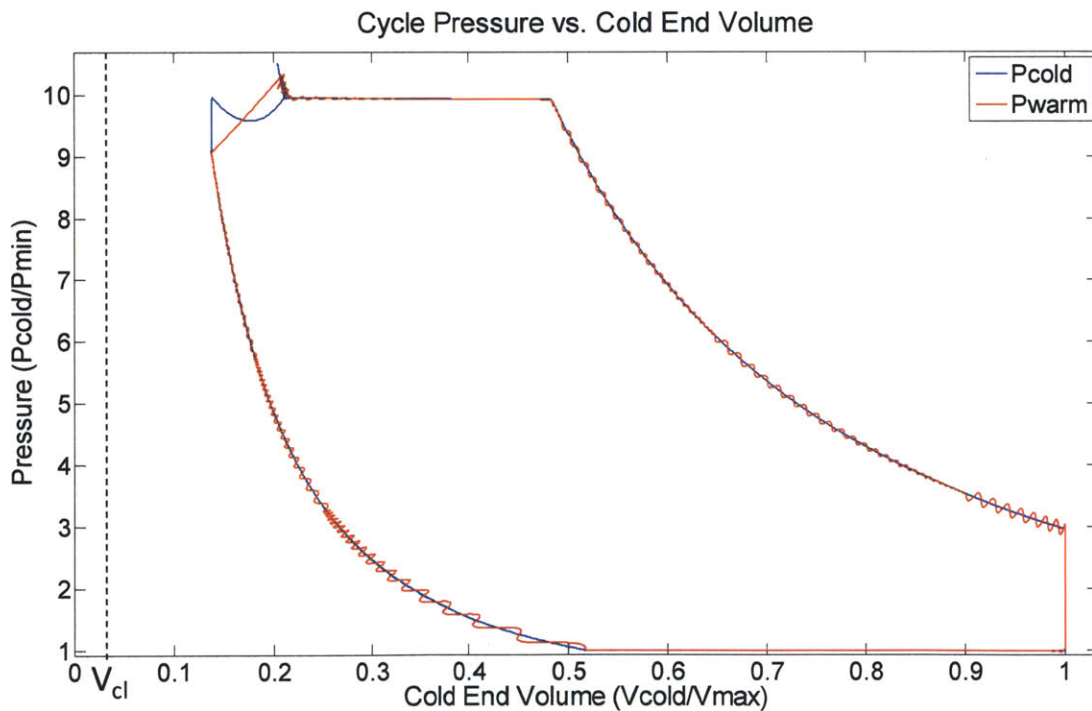


Figure 3.12 First stage indicator diagram for helium addition near target pressure. The expander model just before the minimum average reservoir pressure is reached. The average reservoir pressure ratio in this indicator diagram is 4.94 at the end of the 700th cycle.

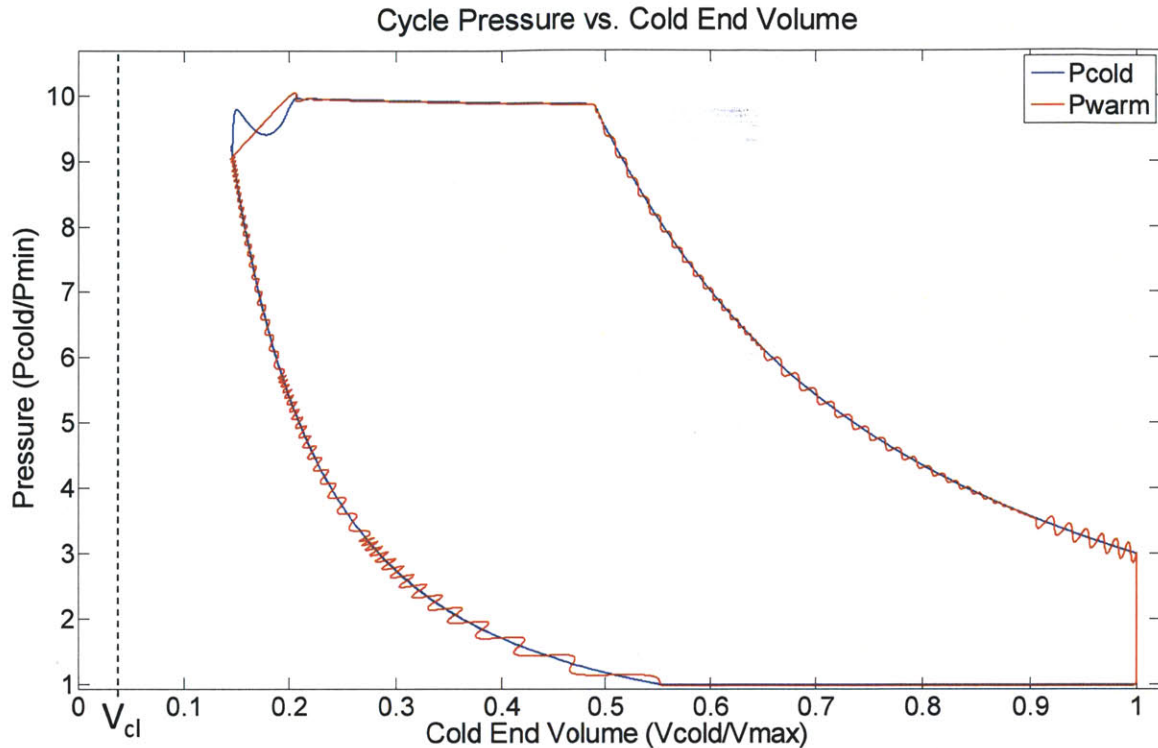


Figure 3.13 Second stage indicator diagram for helium addition near target pressure. The expander model just before the minimum average reservoir pressure is reached. The average reservoir pressure ratio in this indicator diagram is 4.94 at the end of the 669th cycle.

still below the steady state value. As a result the reservoir D pressure reaches the minimum pressure during exhaust at a smaller volume ($V/V_{\max}=0.51$ in Figure 3.12 versus $V/V_{\max}=0.81$ in Figure 3.10) before the time limit initiates the recompression process.

Once the cycle reaches the optimum reservoir pressure range, the control turns off and the cutoff and recompression volumes are returned to the steady state values. The indicator diagrams in Figure 3.14 and Figure 3.15 show the expanders in normal operation after the helium addition has occurred. The reservoirs have returned to the ideal pressure range. The total helium mass in the warm end reservoirs has increased by 20.6% in the first stage and 20.9% in the second stage.

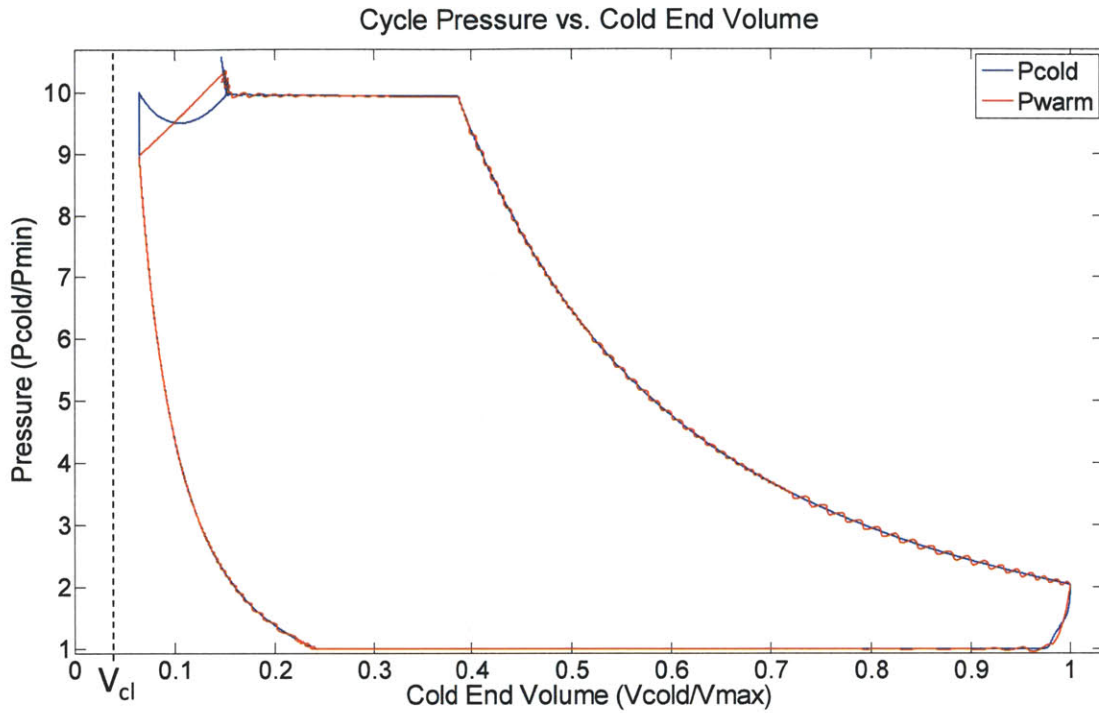


Figure 3.14 First stage indicator diagram after helium addition. The indicator diagram for the warm and cold volumes of the expander shows that, by the 725th cycle, the expander has achieved normal operation.

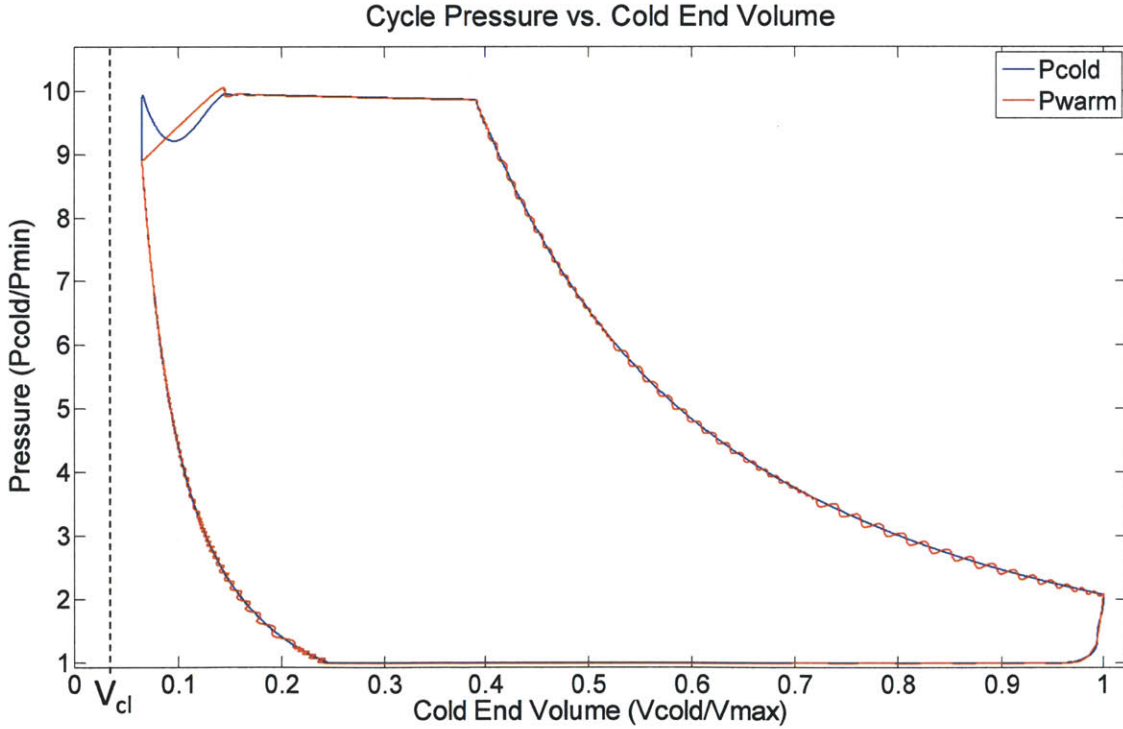


Figure 3.15 Second stage indicator diagram after helium addition. The indicator diagram for the warm and cold volumes of the expander shows that, by the 700th cycle, the expander has achieved normal operation.

Figures 3.16 and 3.17 are tracks of the reservoir pressure changes in each stage as a function of the number of cycles until the target mean reservoir pressure is reached. The figures show a steady increase in the mean reservoir pressure after 100 cycles, when the control is initiated. Once the mean reservoir pressure has reached the target value the control is shutoff (roughly 700 cycles in the first stage and 670 cycles in the second stage) and the individual reservoir pressures begin redistributing as the cycle resumes its “steady state” switch points. The pressures in reservoirs B and C do not change as dramatically as the reservoirs A and D. This is consistent with the results of Chapter 2.

A step increase in the cutoff volume was chosen as opposed to a gradual increase over many cycles because a gradual increase will not guarantee that the piston touches down and increased helium blow-by flow occurs when it is needed. The key benefit of the control method

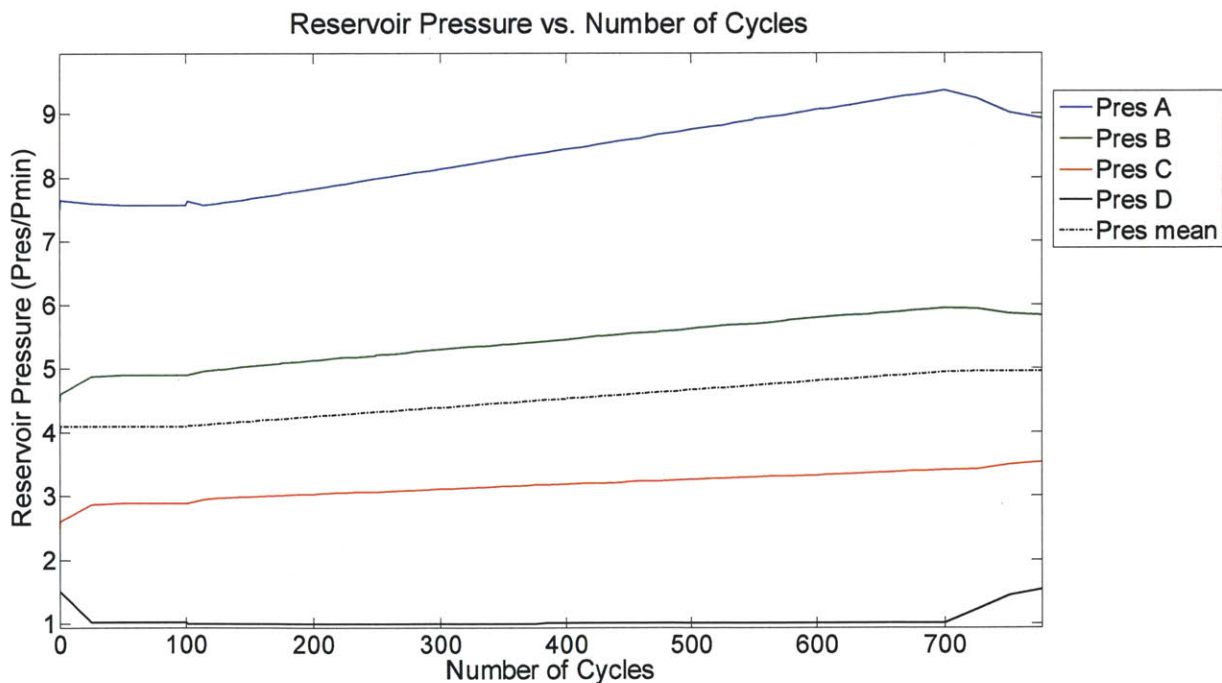


Figure 3.16 First stage reservoir pressures plotted over time. The reservoir pressures and the mean reservoir pressure are plotted as a function of cycle number for the helium addition control algorithm.

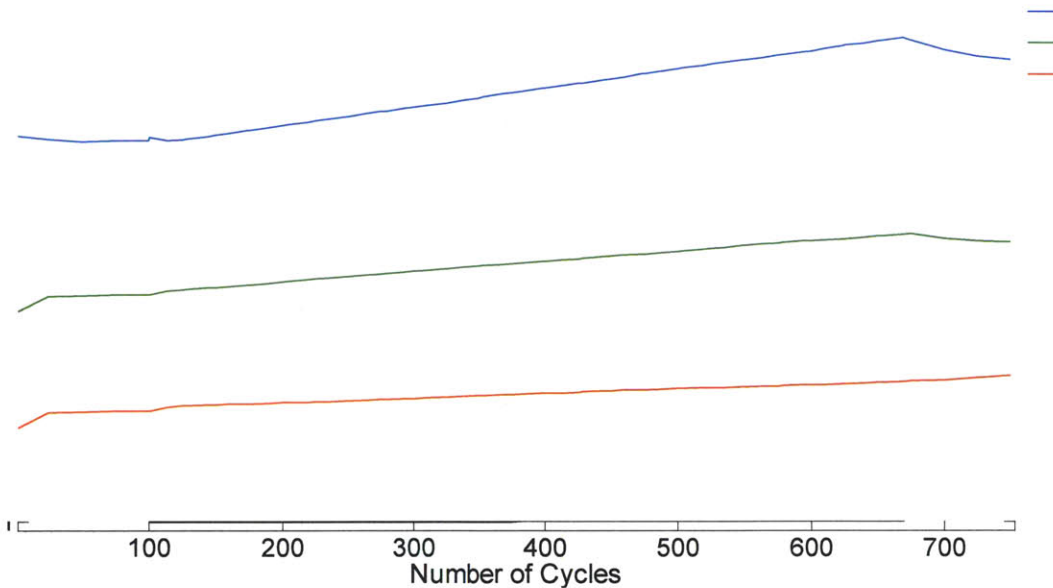


Figure 3.17 Second stage reservoir pressures plotted over time. The reservoir pressures and the mean reservoir pressure are plotted as a function of cycle number for the helium addition control algorithm.

used here is that there is an immediate, steady, linear increase of the mean reservoir pressure when helium is being added to the reservoirs as shown in Figures 3.16 and 3.17.

3.4 Removing mass from the warm volume

For the case when helium mass has accrued in the reservoirs and the reservoir pressures are operating above the ideal range, mass should be removed from the warm volume to return the expander to “steady state” operation. This mass flow can be achieved by setting the piston on the bottom of the cylinder so that the pressure difference across the piston drives additional mass flow from the warm end of the expander to the cold end.

The process proposed here is very similar to that used to move mass from the cold end to the warm end of the expander. To remove mass from the reservoirs, the piston is set down during recompression, after the exhaust valve has closed and before the high pressure reservoir

(A) valve closes. Setting the piston down during recompression increases the pressure difference across the piston to the pressure difference between the open reservoir and the gas remaining in the cold volume. The helium then flows from the reservoir, into the warm volume, through the piston-cylinder gap, and into the clearance volume in the cold end of the cylinder. The piston dwells at this position for 100 milliseconds. Because the blow-by flow is pressurizing the intentionally small clearance volume, it may take multiple cycles to remove the required amount of mass due to the limited space for the mass to fill.

The results of a simulation for this scenario are shown in Figures 3.18 through 3.25. In this simulation the reservoir pressure ratios (P/P_{\min}) are initially distributed so that the mean reservoir pressure ratio is 5.5, above the ideal value established in Chapter 2 of 5.0. More specifically, the pressure ratio distribution of the reservoirs is 9.25, 7.25, 3.5, and 2 for reservoirs A, B, C, and D, respectively. The cutoff and recompression volumes are initialized at the ideal values (40% and 25% of the maximum volume, respectively) and the model runs for 100 cycles under these conditions to allow the pressures in the reservoirs to move to their “steady state” pressures. An indicator diagram for each stage of the expander after 100 cycles is shown in Figure 3.18 and Figure 3.19. The figures show that the piston is not able to reach the full swept volume during operation due to the reservoir pressures that are too large.

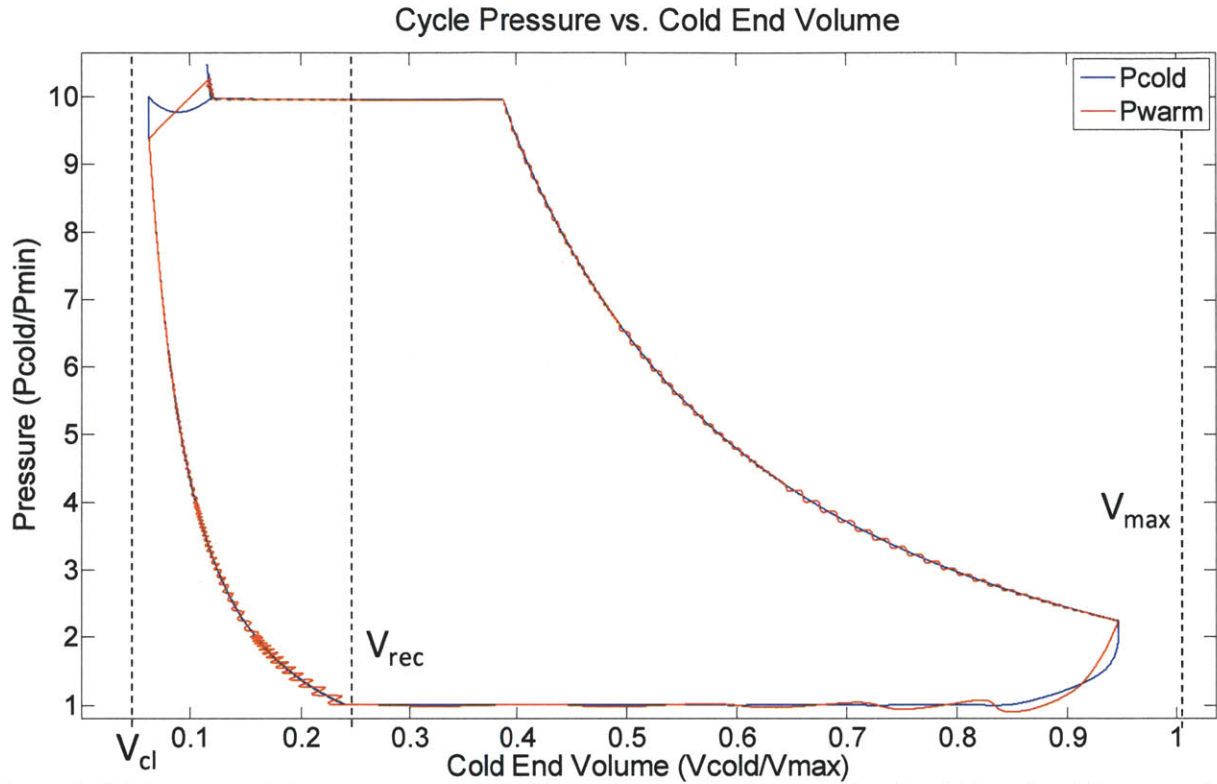


Figure 3.18 First stage high pressure model. Indicator diagram for the expander after 100 cycles. The reservoir pressures are too high and therefore reduce the swept volume of the piston. $P_{res}/P_{min} = 5.62$ which is different from the pressure ratio quoted in the text of 5.5. The disparity is due to the gas initially in the warm volume that is distributed to the reservoirs after a few cycles. The vertical line, V_{cl} , is the clearance volume in the cold end. The vertical line, V_{rec} , is the recompression volume. The percentage of the maximum volume quoted in the text for V_{rec} is based on the maximum swept volume (0.1 liters) whereas the maximum volume in this diagram ($V_{cold}/V_{max} = 1.0$) also includes the clearance volumes, causing the recompression volumes to look shifted.

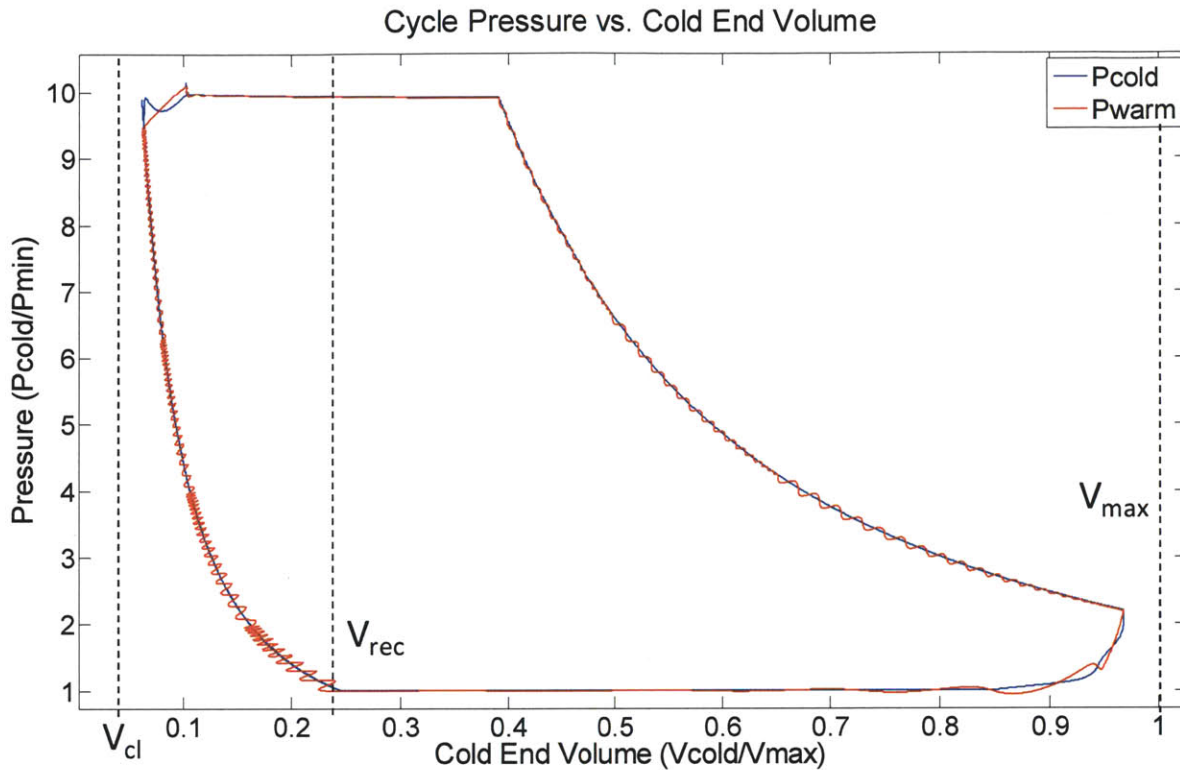


Figure 3.19 Second stage high pressure model. Indicator diagram for the expander after 100 cycles. The reservoir pressures are too high and therefore reduce the swept volume of the piston (mean $P_{res}/P_{min} = 5.62$, see comment in Figure 3.18).

Following the 100th cycle, the control scenario discussed above is initiated. Since the mean reservoir pressure is above the target pressure ratio of 5.05, the recompression volume is reduced from the steady 25% value to 10% (1st stage) or 5% (2nd stage) of the maximum volume. The piston then touches down on the cold (bottom) end of the cylinder and is allowed to dwell there for 100 ms while the reservoir A valve is held open. Gas leaks from reservoir A, through the gap, and into the clearance volume at the cold end of the cylinder.

This process distorts the cycle as shown in Figure 3.20 for the first stage. The reduced recompression volume causes a greater mass flow out of reservoir D. Consequently, the pressure in reservoir D decreases allowing for greater displacement during expansion before the reservoir

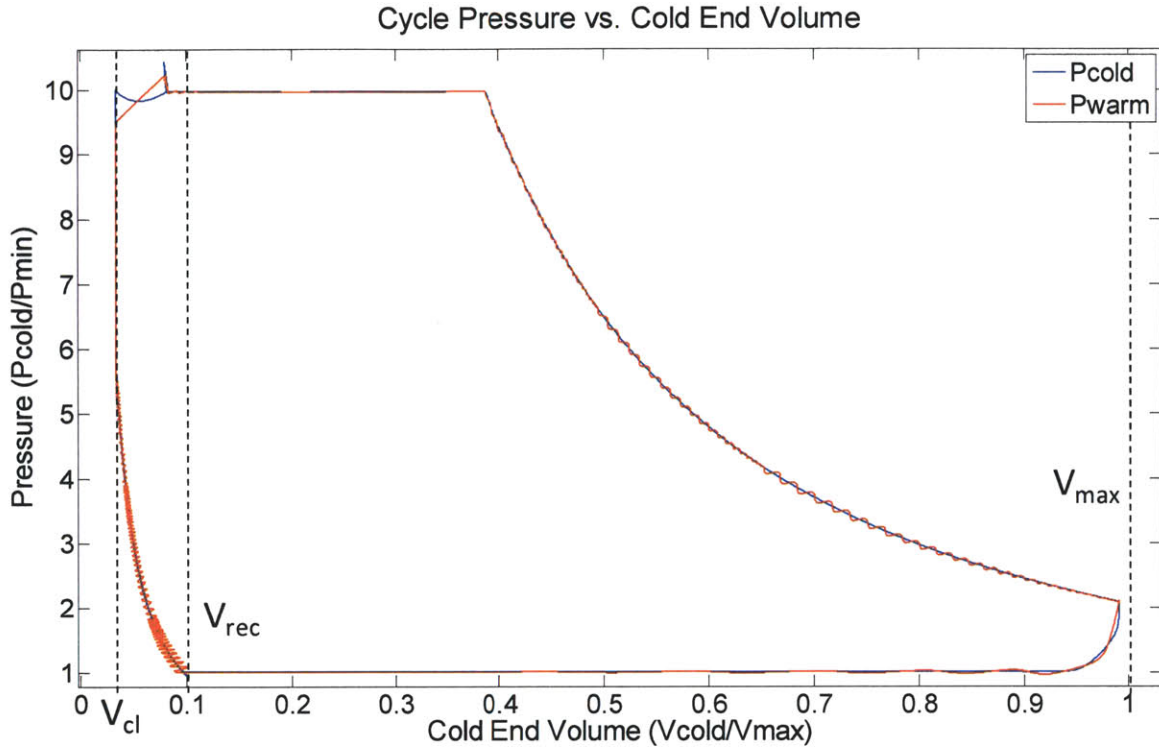


Figure 3.20 First stage helium reduction expander model. The piston reaches the bottom of the cylinder during recompression allowing for increased blow-by to the cold volume (cycle number 125, mean Pres/Pmin=5.57).

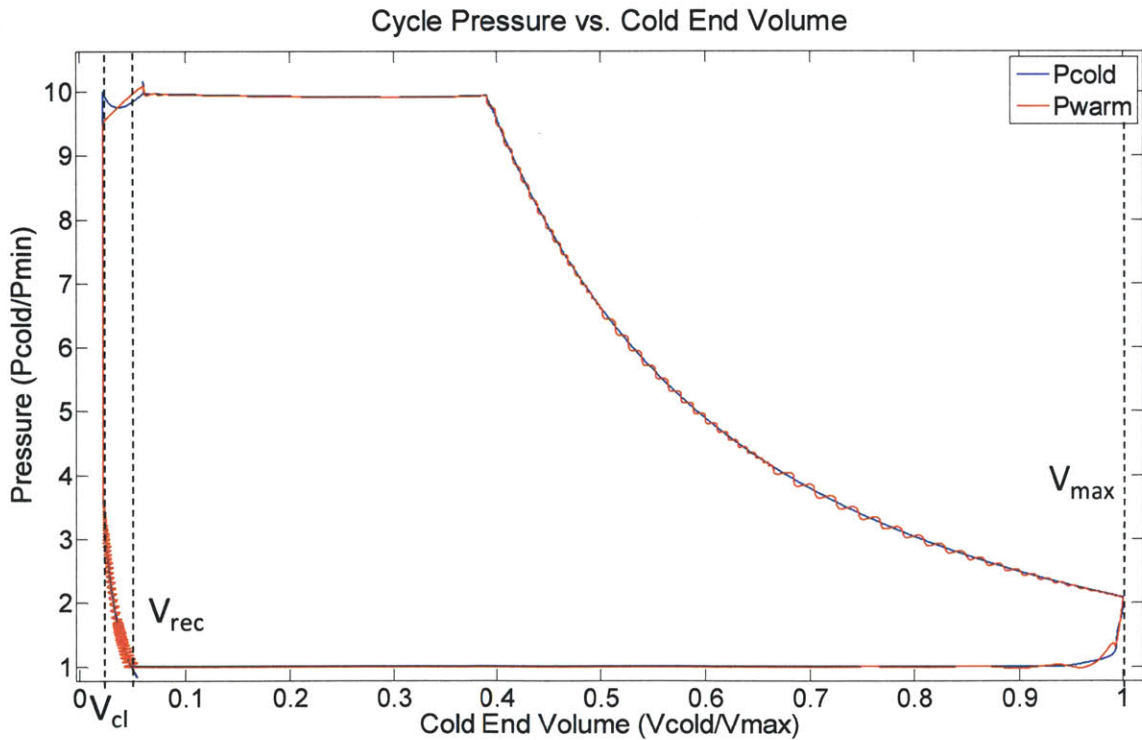


Figure 3.21 Second stage helium reduction expander model. The piston reaches the bottom of the cylinder during recompression allowing for increased blow-by to the cold volume (cycle number 125, mean Pres/P_{min}=5.51).

D valve closes. This same argument can be made for the difference in the shape of the second stage indicator diagrams shown in Figure 3.19 and Figure 3.21.

Each expander stage continues to reduce the helium mass in the reservoirs using the same method until the target value of 3.0 g is reached. Once the total reservoir mass is reduced beyond this point, the expander returns to normal operation. The indicator diagrams in Figure 3.22 and Figure 3.23 show the first stage expander and the second stage expander in steady state operation following the helium reduction in the warm volume. The total helium mass in the warm end has been reduced by 9.6% in the first stage and 8.9% in the second stage.

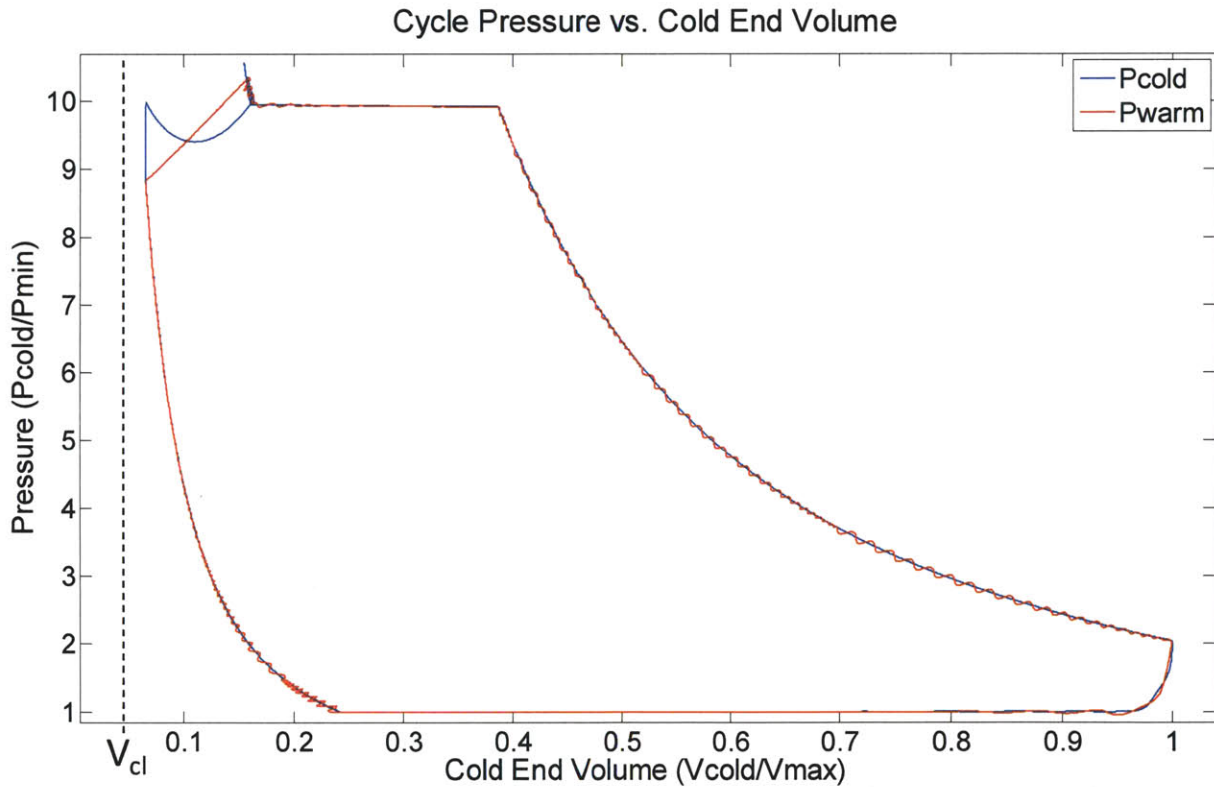


Figure 3.22 First stage helium reduction normal operation. The expander returns normal operation following the reduction of helium from the reservoirs (cycle number 425, mean $P_{res}/P_{min}=5.05$).

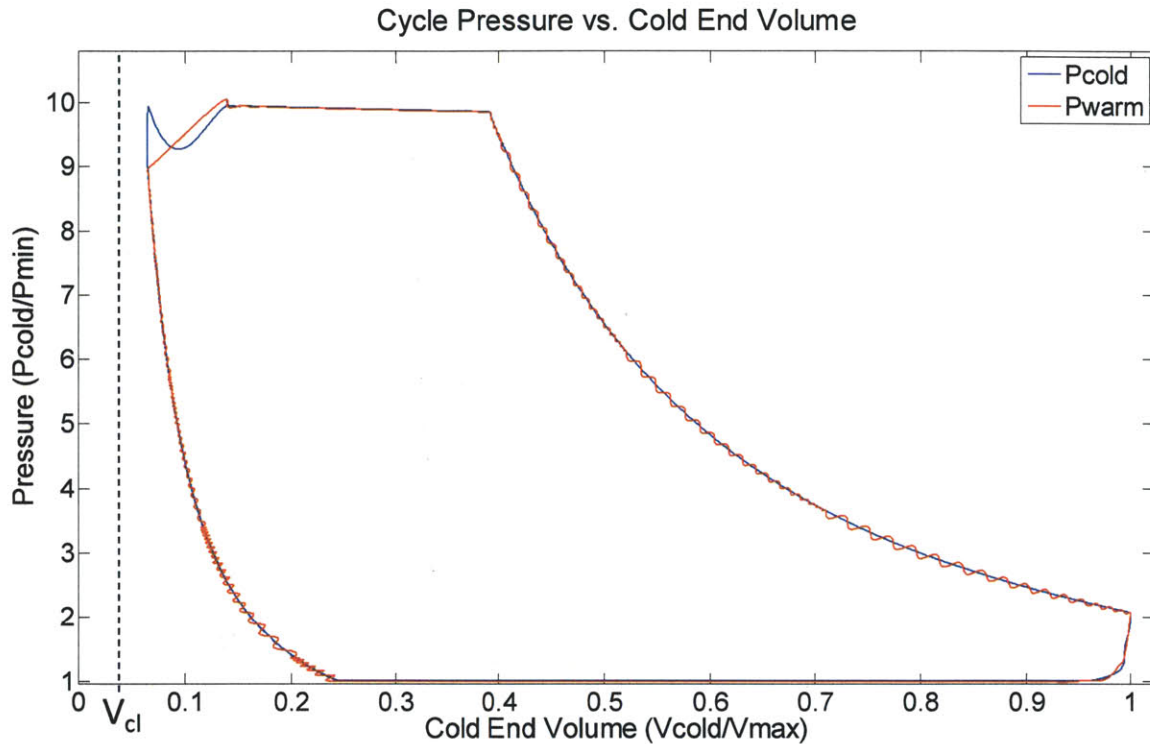


Figure 3.23 Second stage helium reduction normal operation. The expander returns normal operation following the reduction of helium from the reservoirs (cycle number 250, mean $P_{res}/P_{min}=5.05$).

Figure 3.24 and 3.25 are tracks of the reservoir pressure changes in each stage as a function of the number of cycles until the targeted mean reservoir pressure is reached. The figures show a steady decrease in the mean reservoir pressure after 100 cycles, when the control is initiated. Once the mean reservoir pressure has reached the target value, the control is shutoff (roughly 425 cycles in the first stage and 250 cycles in the second stage) and the individual reservoir pressures begin redistributing as the cycle resumes its steady state cutoff and recompression volumes.

Similar to the previous example of adding mass to the reservoirs, a step decrease in the recompression volume was chosen over a gradual decrease over many cycles. This is because a gradual decrease will not guarantee that the piston touches down and that increased helium blow-by flow occurs when it is needed. The control method used here allows for an immediate,

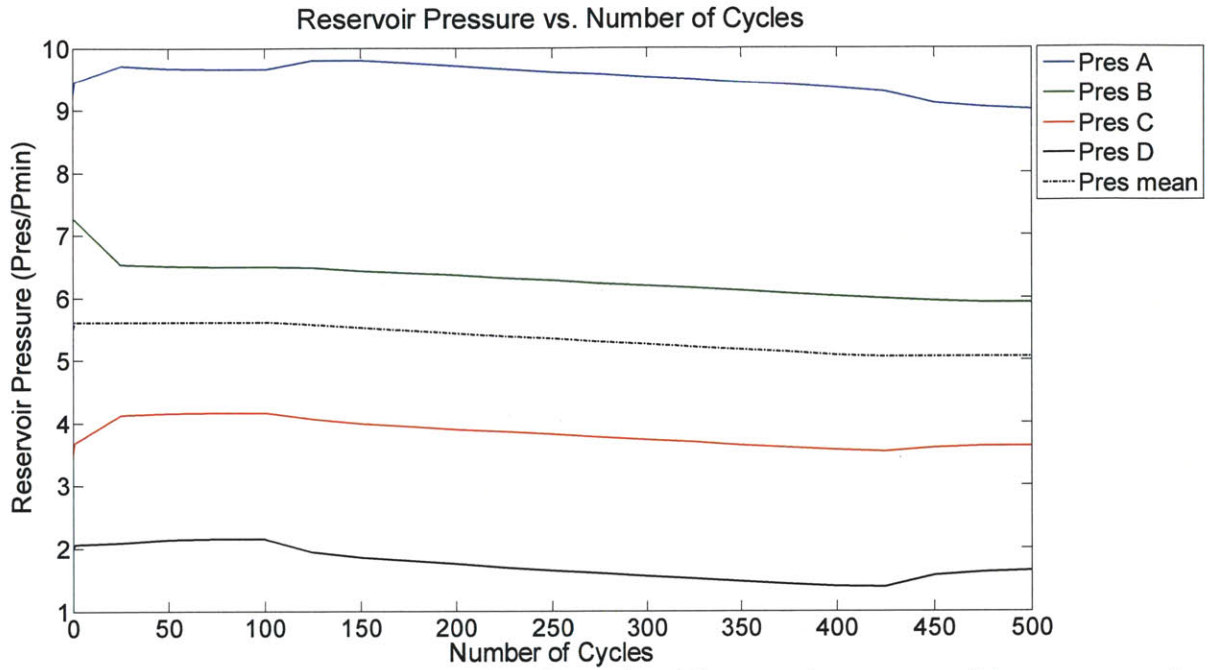


Figure 3.24 First stage reservoir pressures plotted over time. The reservoir pressures and the mean reservoir pressure are plotted as a function of cycle number for the helium reduction control algorithm.

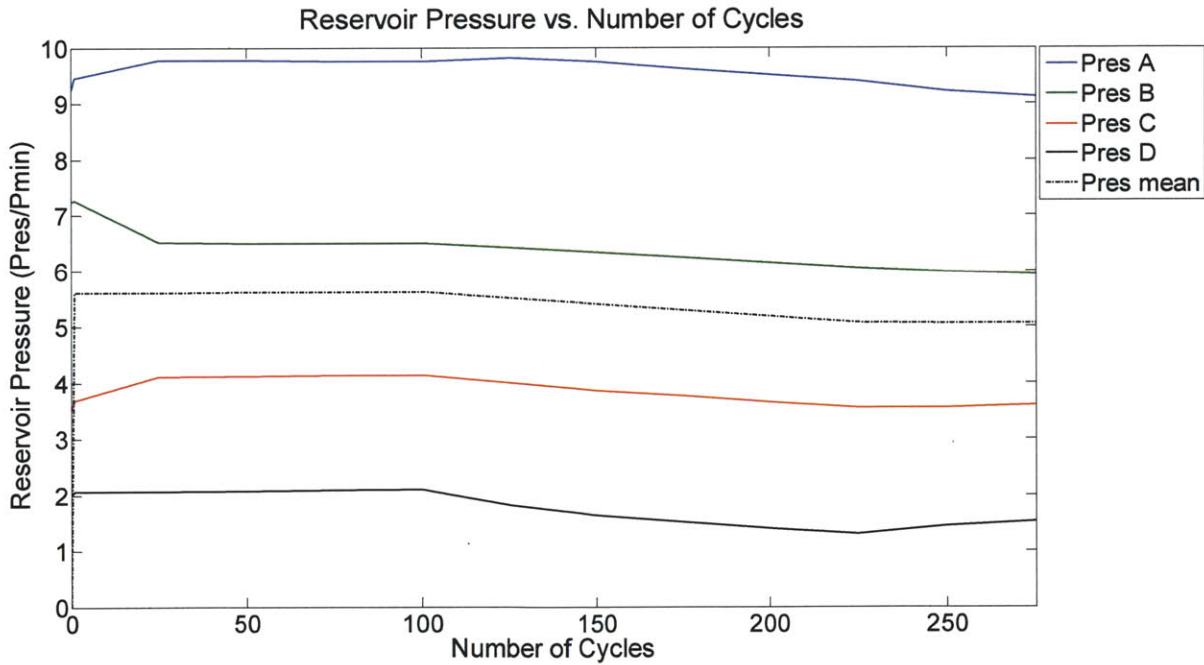


Figure 3.25 Second stage reservoir pressures plotted over time. The reservoir pressures and the mean reservoir pressure are plotted as a function of cycle number for the helium reduction control algorithm.

steady, and linear decrease of the mean reservoir pressure when helium is being removed from the reservoirs as shown in Figures 3.24 and 3.25.

3.5 Controlling steady state expander operation

The idealized piston control has already been discussed in Chapter 2. In that discussion it was assumed that the pressures in the warm volume would equal the pressure in the reservoir to which it was connected before the next reservoir was in turn connected to the warm volume. In practice, the times for complete pressure equalization are quite long and the cycle time for the expander with this control scenario becomes too long to be practical. As a consequence, the switch states for the control of the cycle are displaced from the “equal pressure” condition. A cycle with displaced switching states is shown in Figure 3.26. The switching states of the cycle

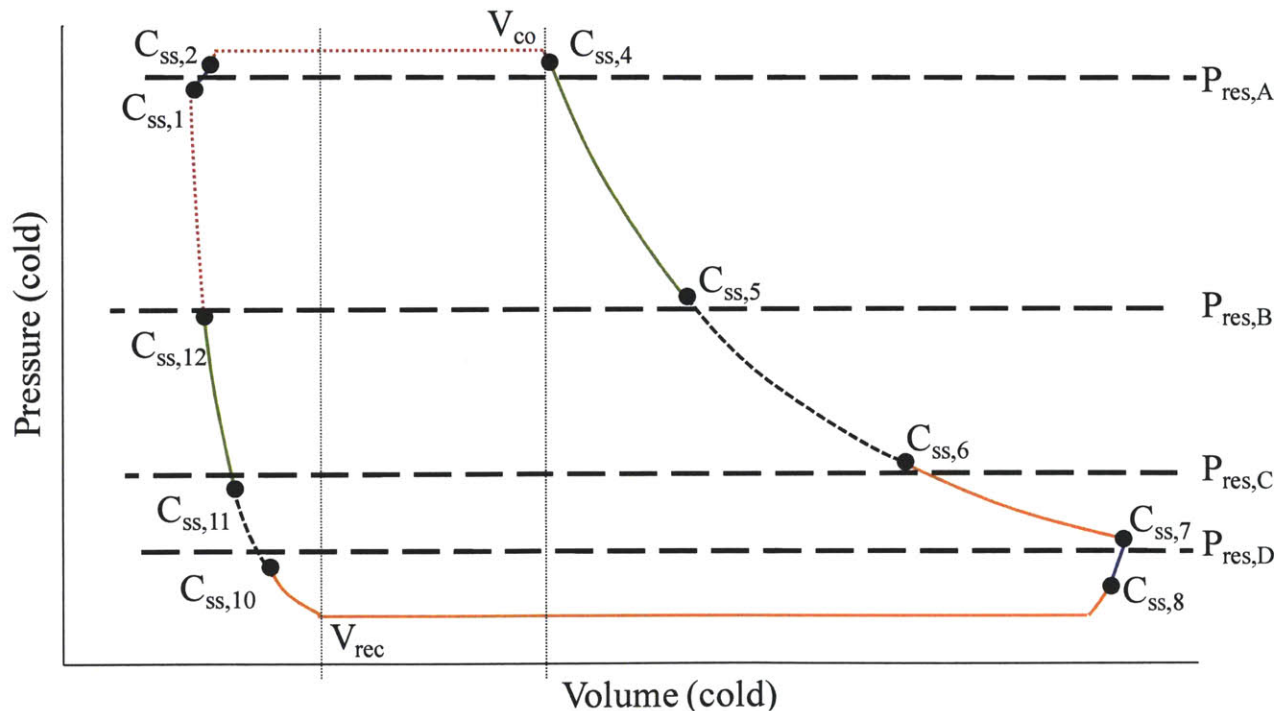


Figure 3.26 Indicator diagram for the switch state constants. The constant for switching between each process in the control algorithm are displayed in the indicator diagram. Each matching color and line style represents when the valve to a reservoir is open with the exception of the processes between $C_{ss,1}$ and $C_{ss,2}$ and between $C_{ss,7}$ and $C_{ss,8}$ when no reservoir valve is open.

are of two varieties. One type is associated with the pressures in the cylinder and the other is associated with the cutoff and recompression volumes. The former type is integrated into the model so that, when the pressure in the warm volume reaches the pressure displaced by the constant (marked by C_{ss} in Figure 3.26), the next process in the cycle is initiated. The only processes that are not ended by a pressure switch state are intake and exhaust. These processes are ended when the volume of gas in the cold end of the cylinder reaches V_{co} (intake) or V_{rec} (exhaust). For the expansion processes, the switch state pressures are displaced above the corresponding reservoir pressure and, for the recompression processes, the switch state pressures will be displaced below the corresponding reservoir pressure. As a result, during the cycle, the magnitude of the pressure in each reservoir oscillates around a mean value.

The switch state constants are numbered according to the corresponding state in the cycle. These constants are the ratio of the switch state pressure in the warm volume to the pressure of the corresponding reservoir (except P_{max} is used for $C_{ss,2}$ and P_{min} is used for $C_{ss,8}$). For example, switch state 4 ($C_{ss,4}$) corresponds to state 4 in the cycle when reservoir A closes and reservoir B opens during expansion. A typical value for this constant is 1.01; the valve closes when the warm volume pressure is 1% greater than the reservoir A pressure. Similarly an example of recompression switch state would be $C_{ss,10}$ in Figure 3.26 where the reservoir D valve closes and the reservoir C valve opens. The switch state is below the reservoir pressure so that a typical value is 0.98. A table of the pressure switch state constants used in this work is shown in Table 3.3.

A benefit of linking the switch states to the pressures in the reservoirs is that the cycle is stable and self correcting if the pressure distribution in the reservoirs substantially deviates from the steady state distribution. For example, if for some reason reservoir B starts with a pressure

that is below the pressure in reservoir C as shown in Figure 3.27, the cycle will transfer gas from reservoir C to reservoir B with this algorithm. Following the expansion process shown in Figure 3.27, at $C_{ss,4}$ the system switches the connection of the warm volume from reservoir A to reservoir B. From $C_{ss,4}$ to $C_{ss,5}$ the piston continues to move towards the warm end and gas is driven into reservoir B until the warm volume pressure matches the pressure at $C_{ss,5}$. The system then closes reservoir B and does not open the valve to reservoir C (as the pressure in the warm volume is below the switch state pressure corresponding to reservoir C) but rather, continues the cycle by opening the valve to reservoir D. The net effect of this expansion process is a net flow into reservoir B with no flow into reservoir C. By contrast the corresponding process in the recompression portion of the cycle can be seen in Figure 3.27. At $C_{ss,10}$ the pressure in the warm volume matches the switch state pressure corresponding to reservoir D at which point the

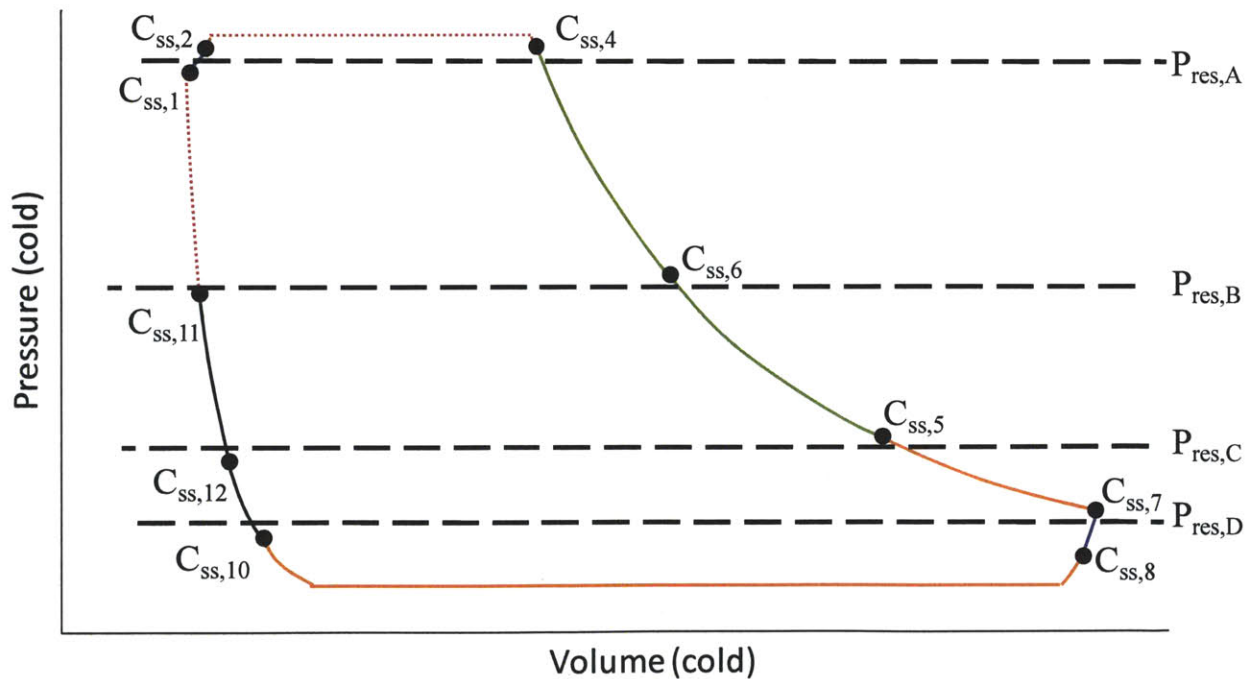


Figure 3.27 Indicator diagram for switch states when two reservoir pressures are switched. This is similar to Figure 3.22 except that, during expansion, the reservoir C valve never opens and, during recompression, the reservoir B valve never opens.

reservoir D valve closes and the reservoir C valve opens. From $C_{ss,10}$ to $C_{ss,11}$ the piston continues to move towards the cold end and gas flows out of reservoir C until the warm volume pressure matches the pressure at $C_{ss,11}$. The system then closes the reservoir C valve and does not open the valve to reservoir B (as the pressure in the warm volume is greater than the switch state pressure corresponding to reservoir B) but rather, continues the cycle by opening the valve to reservoir A. The net effect of this recompression process is a net flow out of reservoir C with no flow out of reservoir B. The execution of one cycle then removes mass from the inappropriately high pressure reservoir C and moves that mass in to the inappropriately low pressure reservoir B. The cycle “heals” the errant pressure distribution of the reservoirs. Figure 3.28 tracks the reservoir pressure changes when the expander is modeled with the inappropriate reservoir pressures. The figure shows that in roughly 30 cycles the expander returns the reservoirs to their normal operating pressures.

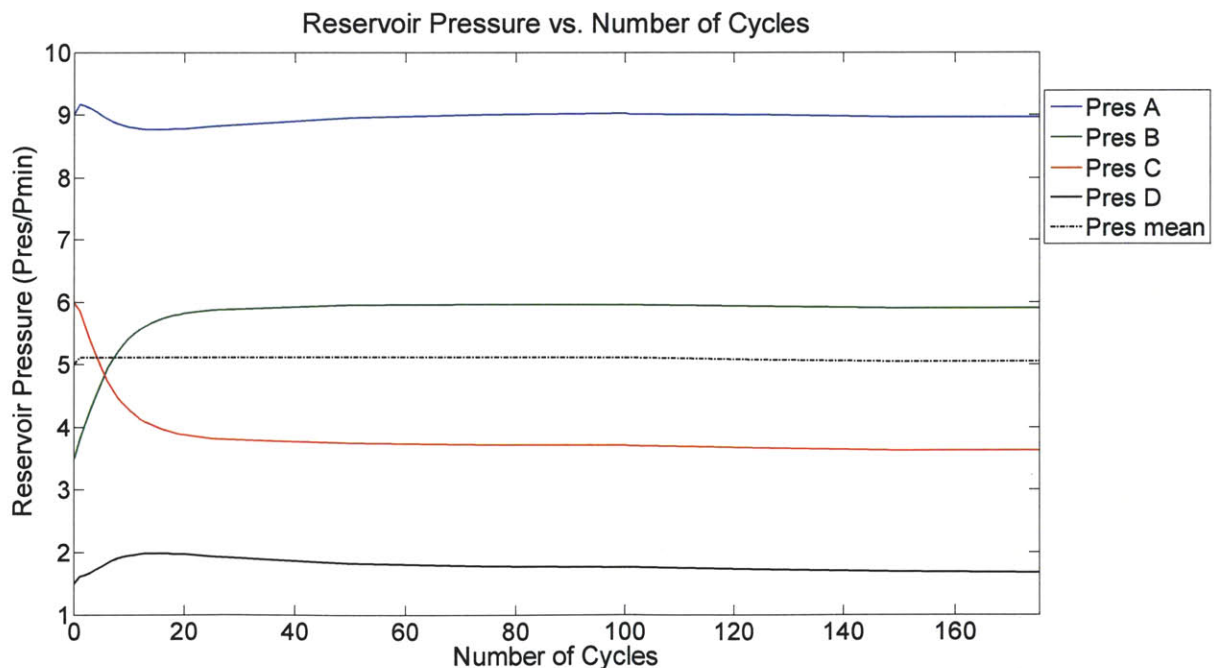


Figure 3.28 The reservoir pressures plotted over time. The reservoir pressures as well as the mean reservoir pressure are plotted for each cycle as the expander approaches steady operation.

The simulations have shown that a control algorithm based only on position and pressure cutoffs can have, under certain conditions, cycles that do not close. In these cycles, the system gets stuck in a particular state and does not progress further. The algorithm was adjusted to have a time limit for each of the eight recompression and expansion processes to ensure that the system did not hang-up in any particular state. The time limit for each of the expansion and recompression processes was set at 0.1 s. The limits for intake and exhaust processes were set at 0.5 s and the limits for the blow-in and blow-out processes were set to 25 ms.

A summary of the controls for the steady state operation of the expander is shown by the diagram in Figure 3.29. The diagram is colored to match the cycle described in Figure 3.26. The cycle should begin with the opening of the intake valve. The valve for reservoir A should be opened at $C_{ss,2} * P_{intake}$ or when the 0.025 second time limit is reached. The intake valve should be closed when the cutoff volume (V_{co}) is reached or when the 0.5 second time limit is reached. The reservoir A valve should close at $C_{ss,4} * P_{res,A}$ or after 0.1 seconds and the reservoir B valve should open. The reservoir B valve should close at $C_{ss,5} * P_{res,B}$ or after 0.1 seconds and the reservoir C valve should open. The reservoir C valve should close at $C_{ss,6} * P_{res,C}$ or after 0.1 seconds and the reservoir D valve should open. The reservoir D valve should close at $C_{ss,7} * P_{res,D}$, V_{max} , or after 0.1 seconds. Then the exhaust valve should be opened. The valve for reservoir D should be opened when the pressure in the warm volume reaches $C_{ss,8} * P_{min}$ or when the 0.025 second time limit is reached. The exhaust valve should be closed when the recompression volume is reached (V_{rec}) or when the 0.5 second time limit is reached. The reservoir D valve should close at $C_{ss,10} * P_{res,D}$ or after 0.1 seconds and the reservoir C valve should open. The reservoir C valve should close at $C_{ss,11} * P_{res,C}$ or after 0.1 seconds and the reservoir B valve should open. The reservoir B valve should close at $C_{ss,12} * P_{res,B}$ or after 0.1 seconds and the

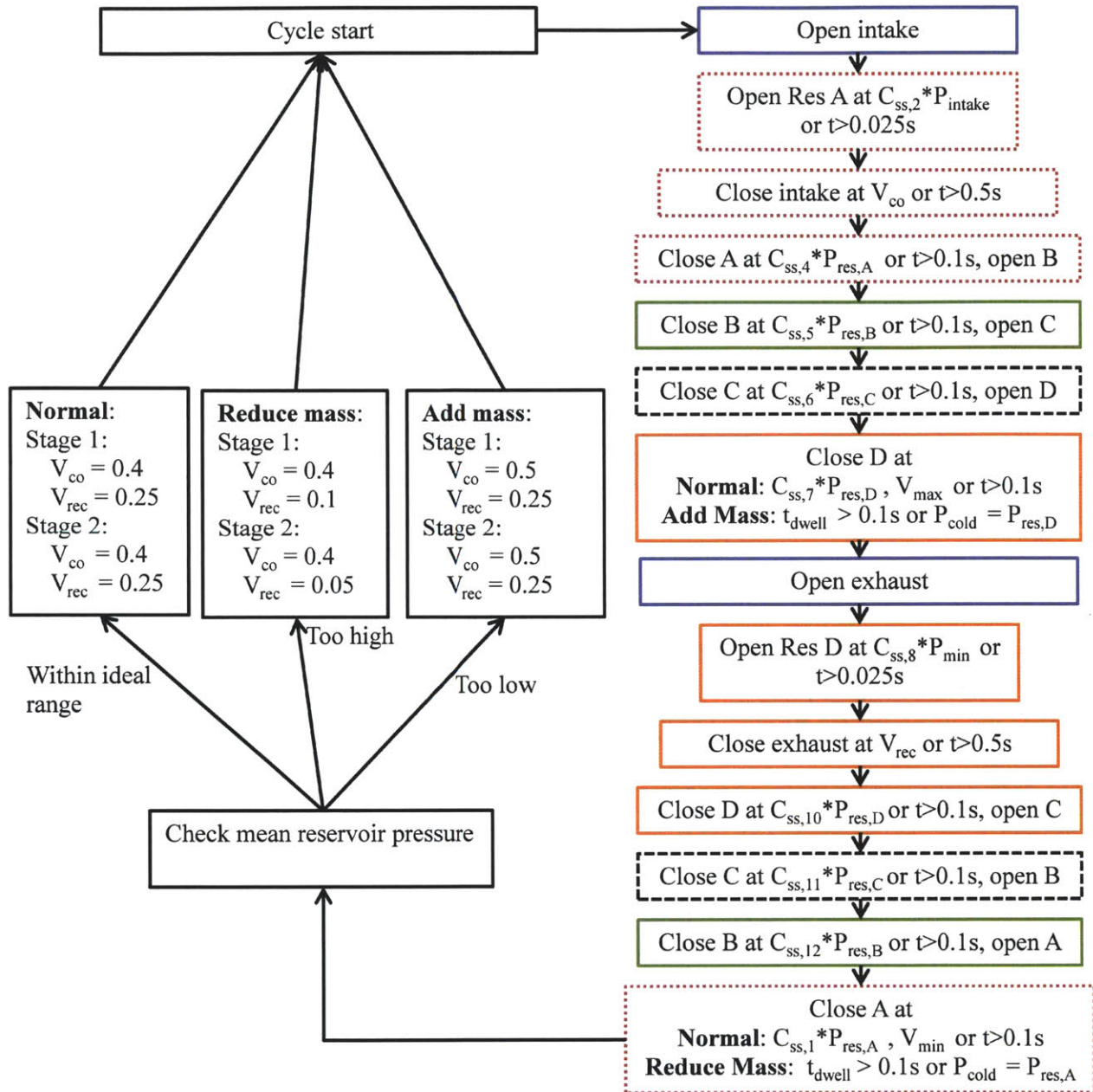


Figure 3.29 Control diagram for steady state expander operation. The colored boxes represent different processes of the expander during its operation (red is blow-in and intake, green is expansion, blue is blow-out and exhaust, yellow is recompression) while the non-colored boxes represent the controls taking place before or after different expander processes.

reservoir A valve should open. The reservoir A valve should close at $C_{ss,1} * P_{res,A}$, V_{min} , or after 0.1 seconds. Upon closing the reservoir A valve, the pressure in the reservoirs should be

compared to the ideal pressure. If the pressures are either too low or too high then the control scheme must adjust the cutoff or recompression volumes to add or reduce the mass in the reservoirs. Following this the intake valve should be opened to begin the next cycle. The switch states should be set at the values shown in Table 3.3. These values can be adjusted slightly for timing purposes if needed.

3.6 Expander startup and shut down

The operation of the expander has been established for the steady state, what remains to be established is the expander's behavior during the transient processes of starting up and shutting down. Since the piston is free to move within the cylinder, it is possible, through injudicious openings of the valves in the cylinder to rapidly accelerate and crash the piston into one end of the cylinder or the other possibly leading to damage in the expander. As a consequence, the startup and shut down procedures must insure against these piston crashes. One possible approach for startup is to fill each of the reservoirs directly from the compressor discharge. Control valves on each reservoir would open and would close when the reservoir approached the appropriate steady state pressure. This approach requires additional hardware for the expander such as the control valves themselves as well as additional plumbing to each of the reservoirs.

A second approach eliminates some of the valves and plumbing lines described in the previous approach. In this option, all reservoir valves would be open to the exhaust pressure so

Table 3.3 Switch states for expander operation. The switch states for all processes in the expander are shown.

Switch state	Switch state condition
$C_{ss,2}, C_{ss,4}, C_{ss,5}, C_{ss,6}, C_{ss,7}, C_{ss,8}, C_{ss,10}, C_{ss,11}, C_{ss,12}, C_{ss,1}$	0.92, 1.01, 1.01, 1.01, 1.01, 1.01, 1.3, 0.98, 0.98, 0.98, 0.98

that each reservoir is at the minimum cycle pressure. Then the two low pressure reservoirs would be closed. Then, with the bleed line attached to the high pressure reservoir, high pressure gas would fill both reservoirs A and B until both reservoirs were at the maximum pressure. At this point both reservoir valves would be closed and the bleed line valve would also be closed. The two high pressure reservoirs are now at the maximum pressure and the two low pressure reservoirs would be at the minimum pressure. The mean reservoir pressure is then greater than the ideal (5.5 pressure ratio). The pressure in the cylinder is the compressor discharge pressure. Following this pressurization, regular expander operation is initiated and the expander operates under the control algorithm described in Figure 3.29. The benefit of this startup method is that only two plumbing lines and two valves to the reservoirs are needed as opposed to four of each in the other option. However it does not completely eliminate any connection with the reservoirs.

The first stage expander was modeled using the second startup option described above. Similar to the example in section 3.5 of inappropriate reservoir pressures, the control algorithm allows the cycle to “heal” the reservoir pressures as shown by the indicator diagrams in Figures 3.30 through 3.32 and the reservoir pressure trace in Figure 3.33. In the first cycle of startup, the piston is barely able to move off of the bottom of the cylinder. However, there is enough movement to begin to pressurize the two low pressure reservoirs. The volumes displaced by subsequent cycles grow larger with each cycle as the pressures in the high pressure reservoirs decrease and the pressures in the low pressure reservoirs rise. After 100 cycles the reservoir pressures have distributed themselves. At this point the control system determines that the mean reservoir pressure is too large and the mass reduction control routine is initiated.

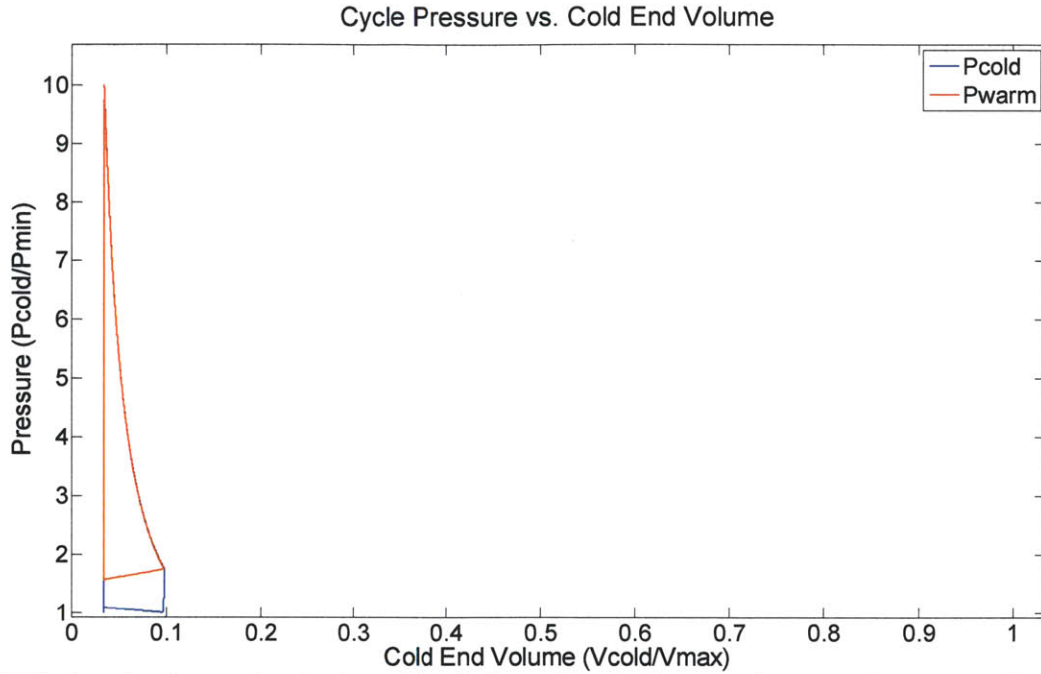


Figure 3.30 First cycle of expander start up. Due the large disparity between the reservoir pressures, the piston displacement is very restricted in the first cycle.

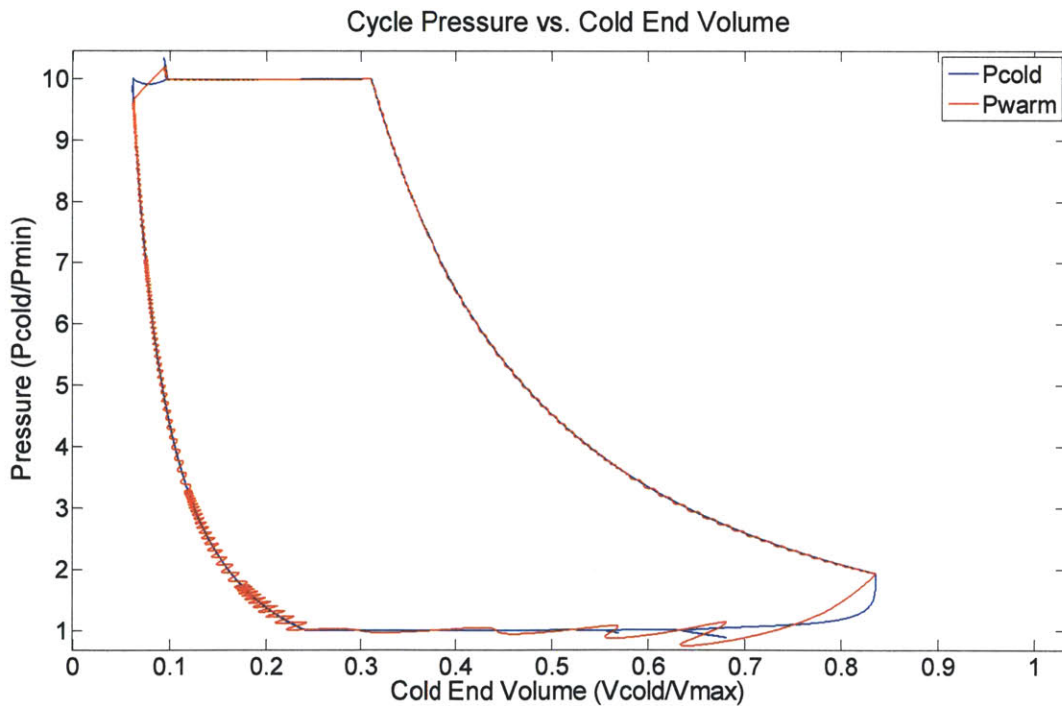


Figure 3.31 Expander startup after 10 cycles. The reservoir pressures are distributing in all reservoirs. However the mean pressure is too large so the reservoir mass reduction control scheme is initiated.

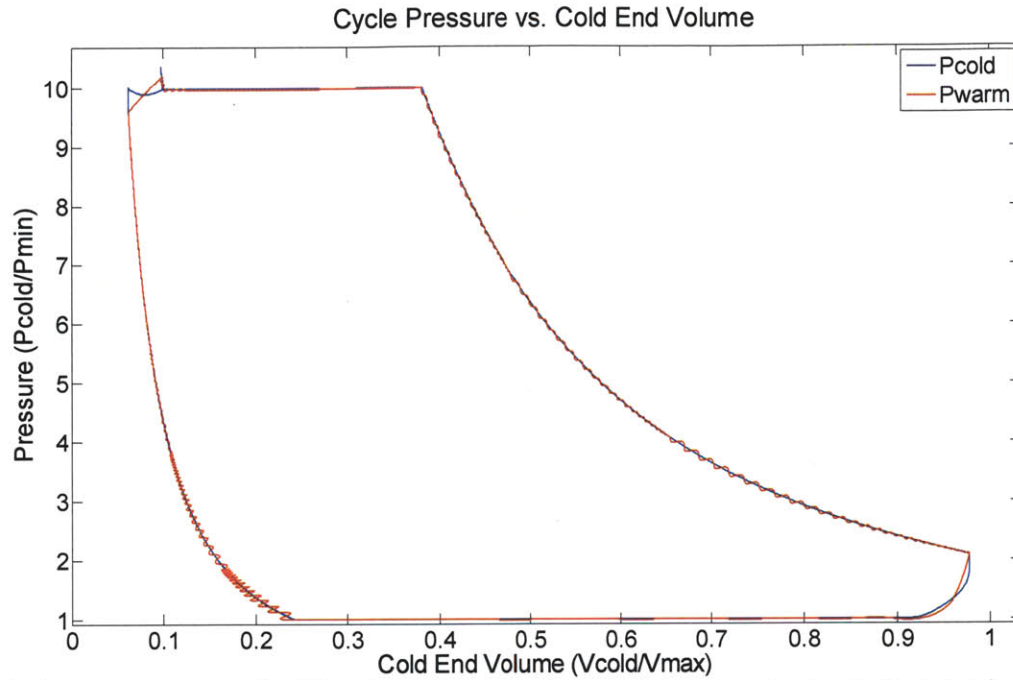


Figure 3.32 Expander startup after 20 cycles. The reservoir pressures are distributing in all reservoirs. However the mean pressure is too large so the reservoir mass reduction control scheme is initiated.

Figure 3.33 tracks the reservoir pressures during the first 175 cycles of startup. The figure shows that the reservoirs distribute to their operating pressures after roughly 30 cycles.

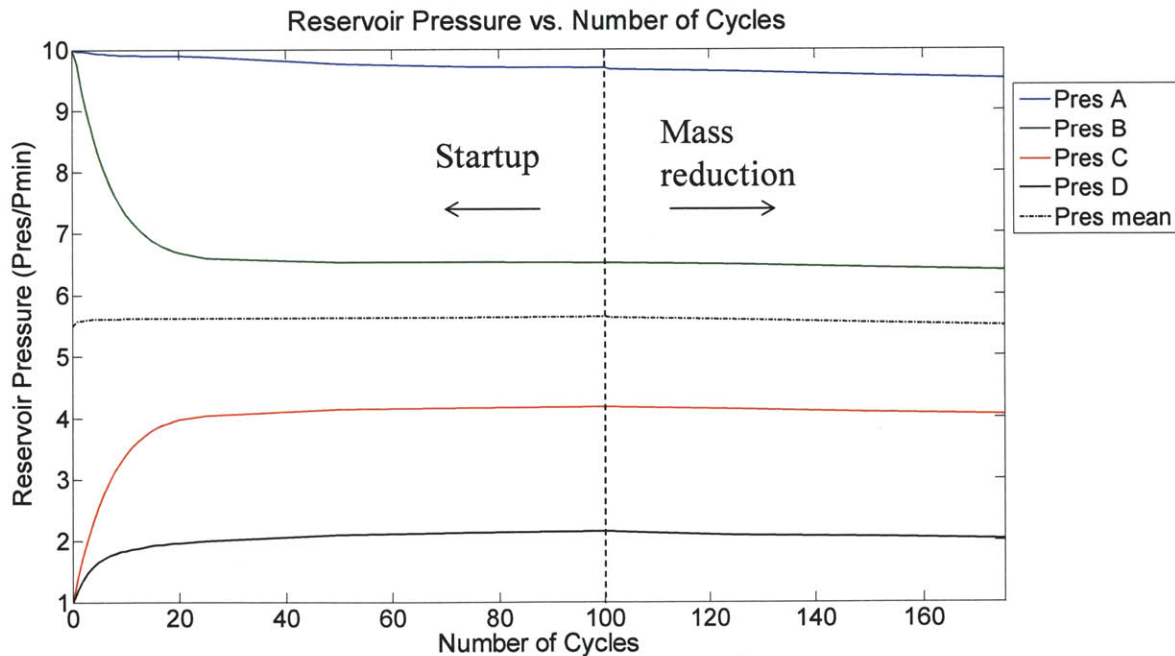


Figure 3.33 The reservoir pressures plotted over time for startup. The reservoir pressures as well as the mean reservoir pressure are plotted for each cycle as the expander approaches steady operation.

To shutdown the expander and leave it in a state to allow for disassembly the procedure is simpler than the startup procedure. To shut down the expander, the piston is set down on or nearly set down on the surface of the cylinder at the cold end of the expander. This can be achieved by reducing the recompression volume (V_{rec}) to zero or to a point where the piston reaches the bottom early into the recompression process to minimize the contact force. Once the piston is sitting on the bottom of the cylinder, the exhaust valve should be opened allowing flow out of the warm volume through the piston cylinder gap. Then, open each reservoir valve sequentially until all reservoirs are at the compressor suction pressure. At this point none of the reservoirs are pressurized and the piston is at rest. These valves should be left open in the case that any warming (to room temperature) of the gas remaining in the expander causes a pressure increase.

3.7 Chapter 3 Summary

In this chapter, the overly simplified model developed in Chapter 2 was extended to account for leakage past the floating piston and the inertia of the piston. This new model shows that there is a small but consistent helium flow past the piston from the cold to the warm volume for a piston that floats freely in the cylinder without contacting the warm end or cold end of the cylinder throughout operation.

A control algorithm intended for adding additional gas into the reservoirs was then modeled. The algorithm consisted of setting the piston down on the top of the cylinder during expansion for 100 milliseconds while holding the low pressure reservoir valve open. A model for this algorithm confirmed the effectiveness by showing that the mean reservoir pressure ratio can be increased from 4.0 to the target value of 4.95 in roughly 600 cycles for both stages.

Subsequently, a model was developed for the removal of gas from the reservoirs. In this algorithm the piston is set down on the bottom of the cylinder during recompression for 100 milliseconds while holding the high pressure reservoir open. The model for this algorithm confirmed the effectiveness by showing that the mean reservoir pressure ratio can be reduced from 5.5 to the target value of 5.05 in roughly 375 cycles for the first stage and 150 cycles for the second stage.

Both of these algorithms were then successfully incorporated into the controls for maintaining steady of the expander. These controls were based on a combination of the piston position as well as the pressure in the cylinder and the reservoir pressures. Additionally, the methods for startup and shut down of the expander were explained. This algorithm is comprehensive and allows for minimal losses due to leakage past the piston throughout operation.

Chapter 4: Conclusion

The previous prototype of the modified Collins cryocooler suffered a gradual reduction in the reservoir pressures during operation due to a flow of gas through the piston cylinder gap [7]. This deleterious effect is driven by a repeated contact of the piston with the cold end of the cylinder. This contact allows a large pressure difference to occur across the piston and hence drives a flow from the warm end to the cold end of the cylinder through the gap between the cylinder and the piston. This loss drove the reservoir pressures low enough in the prototype so that the expander would stop operation. To resolve this issue, the prototype was fitted with bleed lines from the compressor discharge port to the high pressure reservoir and from the low pressure reservoir to the compressor suction port. The flow through these bleed lines stabilized the pressures in the reservoirs but did not eliminate the leakage losses.

The goal of this thesis was to develop an algorithm for the control of the floating piston expander. Specifically, the purpose of the control algorithm was to mitigate the helium lost due to blow-by during operation. This would allow for the elimination of the bleed lines used and their associated losses.

A thermodynamic model of the expander was developed to understand how the expander performs when control parameters, the cutoff and recompression volumes, are changed. In this model the piston-cylinder gap was assumed to be perfectly sealed and the piston was assumed to

have zero mass. This study showed that, for this expander, there is a set range cutoff and recompression volumes that allow for the expander cycle to close and maximize the “area” swept in P-V space available to the expander. For these cutoff and recompression volume ranges, the model showed that the pressures in the intermediate pressure reservoirs (reservoirs B and C) were insensitive to the cutoff and recompression volumes. The dependence of the reservoir pressures on the total helium mass in the warm end of the expander was then studied. This showed that, in contrast to the previous result, the pressures in the intermediate pressure reservoirs were the most sensitive to the total helium mass in the warm volume.

The model was then extended to study the effects of the helium flow through the gap. This required that the inertia of the piston be implemented into the model so that a pressure drop across the piston could be observed. The study showed that, with no piston contact on the top or bottom of the cylinder, there will be a small net flow through the piston cylinder gap from the cold volume to the warm volume due to gravitational effects. The expander was then modeled to show that the control algorithm will effectively add helium to the reservoirs when the mean reservoir pressure is below the targeted value. The expander was also modeled to prove that the control algorithm will effectively remove helium from the reservoirs when the mean reservoir pressure is above the targeted value. These studies were integrated into a control algorithm for maintaining a net zero helium blow-by flow throughout the operation of the expander. When there is too much mass in the warm end (the mean reservoir pressure is too high), the recompression volume is reduced so that the piston contacts the bottom of the cylinder during recompression and helium flows from the high pressure reservoir, through the warm volume and the piston cylinder gap, and into the cold end of the cylinder. Similarly, when there is too little mass in the warm end (the mean reservoir pressure is too low), the cutoff volume is increased so

that the piston contacts the top of the cylinder during expansion and helium flows from the cold volume, through the gap, into the warm volume and then into the low pressure reservoir. The control algorithm developed here will minimize blow-by flow during expander operation. It will also eliminate the need for bleed lines to control the reservoir pressures.

Bibliography

- [1] Plachta, D and P. Kittel. "An updated zero boil-off cryogenic propellant storage analysis applied to upper stages or depots in an LEO environment." NASA Technical Report 2003-211691 (2003).
- [2] Barron, Randall F. Cryogenic Systems. New York: Oxford University Press, 1985.
- [3] Segado, M. A., C.L. Hannon and J. G. Brisson. "Collins Cryocooler Design for zero-boil-off storage of liquid hydrogen and oxygen in space." *Advances in Cryogenic Engineering*: Vol. 55, American Institute of Physics, New York, 2010. pp. 1377-1384.
- [4] Jones, R.E., Smith Jr., J.L., "Design and Testing of Experimental Free-Piston Cryogenic Expander," in *Advances in Cryogenic Engineering* 45, edited by Shu et al., Kluwer Academic/Plenum Publishers, New York, 2000, pp. 1485-1491.
- [5] Traum, M.J., Smith Jr., J.L., Brisson, J.G., Gerstmann, J., Hannon, C.L., "Electromagnetic Smart Valves for Cryogenic Applications," in *Advances in Cryogenic Engineering* 49A, edited by J Waynert et al., American Institute of Physics, Melville, New York, 2004, pp. 428-435.
- [6] Hannon, C.L., Krass B., Gerstmann, J., Chaudhry, G., Brisson, J.G., Smith Jr., J.L., "Modeling, Development and Testing of a Small-Scale Collins Type Cryocooler," in *Cryocoolers 14*, edited by S.D. Miller and R.G. Ross Jr., International Cryocooler Conference, Inc., Boulder, CO, 2007, pp. 477-485.
- [7] Chaudhry, G., "Modeling of a Floating Piston Expander employed in a 10 K Cryocooler," MIT Masters Thesis, 2005.
- [8] White, Frank M. Fluid Mechanics. New York, New York: McGraw Hill, 2008.
- [9] "Miniature and Subminiature Solenoid Valves." Gems Sensors and Controls. Accessed July 29, 2011. < http://www.gemssensors.com/Contact-Us/~media/GemsNA/CatalogPages/Updated%20Catalog%20Sections/J-Valves_05-16-2011opt.ashx>.
- [10] Incropera, Frank P. et. al. Fundamentals of Heat and Mass Transfer. Hoboken, New Jersey: John Wiley & Sons, 2007.
- [11] Fox, R.W. and McDonald, A.T. Introduction to Fluid Mechanics. New York, New York: John Wiley & Sons.

Appendix A

TIME DEPENDENT MODELING OF THE EXPANDER

Blow-in (process 1-2)

$$P_{c,2} = P_{c,1} + \frac{\gamma - 1}{V_{\text{tot}}} (K_{\text{intake}}(P_{\text{intake}} - P_c)c_p T_{\text{intake}})_{\text{in}} t_{\text{step}}$$

$$P_{w,2} = P_{c,2}$$

$$V_{w,2} = V_{w,1} \left(\frac{P_{w,2}}{P_{w,1}} \right)^{\frac{1}{\gamma}}$$

$$V_{c,2} = V_{\text{total}} - V_{w,2}$$

$$m_{c,2} = m_{c,1} + m_{c,\text{in}}$$

$$m_{w,2} = m_{w,1}$$

$$T_{c,2} = \frac{P_{c,2} V_{c,2}}{m_{c,2} R}$$

$$T_{w,2} = \frac{P_{w,2} V_{w,2}}{m_{w,2} R}$$

Intake (process 2-3)

$$P_{c,3} = P_{c,2} + \frac{\gamma - 1}{V_{\text{tot}}} [K_{\text{intake}}(P_{\text{intake}} - P_c)c_p T_{\text{intake}} - K_{\text{res,A}}(P_{w,1} - P_{\text{res,A}})c_p T_{w,1}] t_{\text{step}}$$

$$P_{w,3} = P_{c,3}$$

$$V_{c,3} = \frac{1}{P_{c,3}} [P_{c,2} V_{c,2} + (\gamma - 1)(-c_v T_{w,2}(m_{3,w} - m_{2,w}) + (K_{\text{intake}}(P_{\text{intake}} - P_c)c_p T_{\text{intake}}) t_{\text{step}} - (K_{\text{res,A}}(P_{w,1} - P_{\text{res,A}})c_p T_{w,2}) t_{\text{step}}]$$

$$V_{c,3} = V_{\text{total}} - V_{w,3}$$

$$m_{c,3} = m_{c,2} + m_{c,\text{in}}$$

$$m_{w,3} = m_{w,3} - m_{w,\text{out}}$$

$$T_{c,3} = \frac{P_{c,3} V_{c,3}}{m_{c,3} R}$$

$$T_{w,3} = \frac{P_{w,3} V_{w,3}}{m_{w,3} R}$$

First Expansion (process 3-4)

$$P_{w,4} = P_{w,3} + \frac{\gamma - 1}{V_{\text{tot}}} (K_{\text{res}} (P_{\text{res,A}} - P_{w,3}) c_p T_{\text{res,A}})_{\text{out}} t_{\text{step}}$$

$$P_{c,4} = P_{w,4}$$

$$V_{c,4} = V_{c,3} \left(\frac{P_{c,4}}{P_{c,3}} \right)^{\frac{1}{\gamma}}$$

$$V_{w,4} = V_{\text{total}} - V_{c,4}$$

$$m_{w,4} = m_{w,3} - m_{w,\text{out}}$$

$$m_{c,4} = m_{c,3}$$

$$T_{c,4} = \frac{P_{c,4} V_{c,4}}{m_{c,4} R}$$

$$T_{w,4} = \frac{P_{w,4} V_{w,4}}{m_{w,4} R}$$

Second Expansion (process 4-5)

$$P_{w,5} = P_{w,4} + \frac{\gamma - 1}{V_{\text{tot}}} (K_{\text{res}} (P_{\text{res,B}} - P_{w,4}) c_p T_{\text{res,B}})_{\text{out}} t_{\text{step}}$$

$$P_{c,5} = P_{w,5}$$

$$V_{c,5} = V_{c,4} \left(\frac{P_{c,5}}{P_{c,4}} \right)^{\frac{1}{\gamma}}$$

$$V_{w,5} = V_{\text{total}} - V_{c,5}$$

$$m_{w,5} = m_{w,4} - m_{w,\text{out}}$$

$$m_{c,5} = m_{c,4}$$

$$T_{c,5} = \frac{P_{c,5} V_{c,5}}{m_{c,5} R}$$

$$T_{w,5} = \frac{P_{w,5} V_{w,5}}{m_{w,5} R}$$

Third Expansion (process 5-6)

$$P_{w,6} = P_{w,5} + \frac{\gamma - 1}{V_{\text{tot}}} (K_{\text{res}} (P_{\text{res,C}} - P_{w,5}) c_p T_{\text{res,C}})_{\text{in}} t_{\text{step}}$$

$$P_{c,6} = P_{w,6}$$

$$V_{c,6} = V_{c,5} \left(\frac{P_{c,6}}{P_{c,5}} \right)^{\frac{1}{\gamma}}$$

$$V_{w,6} = V_{\text{total}} - V_{c,6}$$

$$m_{w,6} = m_{w,5} - m_{w,\text{out}}$$

$$m_{c,6} = m_{c,5}$$

$$T_{c,6} = \frac{P_{c,6} V_{c,6}}{m_{c,6} R}$$

$$T_{w,6} = \frac{P_{w,6} V_{w,6}}{m_{w,6} R}$$

Fourth Expansion (process 6-7)

$$P_{w,7} = P_{w,6} + \frac{\gamma - 1}{V_{\text{tot}}} (K_{\text{res}} (P_{\text{res,D}} - P_{w,6}) c_p T_{\text{res,D}})_{\text{out}} t_{\text{step}}$$

$$P_{c,7} = P_{w,7}$$

$$V_{c,7} = V_{c,6} \left(\frac{P_{c,7}}{P_{c,6}} \right)^{\frac{1}{\gamma}}$$

$$V_{w,7} = V_{\text{total}} - V_{c,7}$$

$$m_{w,7} = m_{w,6} - m_{w,\text{out}}$$

$$m_{c,7} = m_{c,6}$$

$$T_{c,7} = \frac{P_{c,7} V_{c,7}}{m_{c,7} R}$$

$$T_{w,7} = \frac{P_{w,7} V_{w,7}}{m_{w,7} R}$$

Blow-out (process 7-8)

$$P_{c,8} = P_{c,7} + \frac{\gamma - 1}{V_{\text{tot}}} (-K_{\text{exhaust}}(P_{c,7} - P_{\text{exhaust}})c_p T_{c,7})_{\text{out}} t_{\text{step}}$$

$$P_{w,8} = P_{c,8}$$

$$V_{w,8} = V_{w,7} \left(\frac{P_{w,8}}{P_{w,7}} \right)^{\frac{1}{\gamma}}$$

$$V_{c,8} = V_{\text{total}} - V_{w,8}$$

$$m_{c,8} = m_{c,7} - m_{c,\text{out}}$$

$$m_{w,8} = m_{w,7}$$

$$T_{c,8} = \frac{P_{c,8} V_{c,8}}{m_{c,8} R}$$

$$T_{w,8} = \frac{P_{w,8} V_{w,8}}{m_{w,8} R}$$

Exhaust (process 8-9)

$$P_{c,9} = P_{c,8} + \frac{\gamma - 1}{V_{\text{tot}}} [K_{\text{res,D}}(P_{\text{res,D}} - P_{w,8})c_p T_{\text{res,D}} - K_{\text{exhaust}}(P_{c,8} - P_{\text{exhaust}})c_p T_{c,8}] t_{\text{step}}$$

$$P_{w,9} = P_{c,9}$$

$$V_{w,9} = \frac{1}{P_{w,9}} [P_{w,8} V_{w,8} + (\gamma - 1)(-c_v T_{c,8}(m_{9,c} - m_{8,c}) - (K_{\text{exhaust}}(P_{c,8} - P_{\text{exhaust}})c_p T_{c,8}) t_{\text{step}}) \\ + (K_{\text{res,D}}(P_{\text{res,D}} - P_{w,8})c_p T_{\text{res,D}}) t_{\text{step}}]$$

$$V_{c,9} = V_{\text{total}} - V_{w,9}$$

$$m_{c,9} = m_{c,8} - m_{c,\text{out}}$$

$$m_{w,9} = m_{w,9} + m_{w,\text{in}}$$

$$T_{c,9} = \frac{P_{c,9}V_{c,9}}{m_{c,9}R}$$

$$T_{w,9} = \frac{P_{w,9}V_{w,9}}{m_{w,9}R}$$

First Recompression (process 9-10)

$$P_{w,10} = P_{w,9} + \frac{\gamma - 1}{V_{\text{tot}}} (K_{\text{res}}(P_{\text{res,D}} - P_{w,9})c_p T_{\text{res,D}})_{\text{in}} t_{\text{step}}$$

$$P_{c,10} = P_{w,10}$$

$$V_{c,10} = V_{c,9} \left(\frac{P_{c,10}}{P_{c,9}} \right)^{\frac{1}{\gamma}}$$

$$V_{w,10} = V_{\text{total}} - V_{c,10}$$

$$m_{w,10} = m_{w,9} + m_{w,\text{in}}$$

$$m_{c,10} = m_{c,9}$$

$$T_{c,10} = \frac{P_{c,10}V_{c,10}}{m_{c,10}R}$$

$$T_{w,10} = \frac{P_{w,10}V_{w,10}}{m_{w,10}R}$$

Second Recompression (process 10-11)

$$P_{w,11} = P_{w,10} + \frac{\gamma - 1}{V_{\text{tot}}} (K_{\text{res}}(P_{\text{res,C}} - P_{w,10})c_p T_{\text{res,C}})_{\text{in}} t_{\text{step}}$$

$$P_{c,11} = P_{w,11}$$

$$V_{c,11} = V_{c,10} \left(\frac{P_{c,11}}{P_{c,10}} \right)^{\frac{1}{\gamma}}$$

$$V_{w,11} = V_{\text{total}} - V_{c,11}$$

$$m_{w,11} = m_{w,10} + m_{w,\text{in}}$$

$$m_{c,11} = m_{c,10}$$

$$T_{c,11} = \frac{P_{c,11} V_{c,11}}{m_{c,11} R}$$

$$T_{w,11} = \frac{P_{w,11} V_{w,11}}{m_{w,11} R}$$

Third Recompression (process 11-12)

$$P_{w,12} = P_{w,11} + \frac{\gamma - 1}{V_{\text{tot}}} (K_{\text{res}} (P_{\text{res},B} - P_{w,11}) c_p T_{\text{res},B})_{\text{in}} t_{\text{step}}$$

$$P_{c,12} = P_{w,12}$$

$$V_{c,12} = V_{c,11} \left(\frac{P_{c,12}}{P_{c,11}} \right)^{\frac{1}{\gamma}}$$

$$V_{w,12} = V_{\text{total}} - V_{c,12}$$

$$m_{w,12} = m_{w,11} + m_{w,\text{in}}$$

$$m_{c,12} = m_{c,11}$$

$$T_{c,12} = \frac{P_{c,12} V_{c,12}}{m_{c,12} R}$$

$$T_{w,12} = \frac{P_{w,12} V_{w,12}}{m_{w,12} R}$$

Fourth Recompression (process 12-1)

$$P_{w,1} = P_{w,12} + \frac{\gamma - 1}{V_{\text{tot}}} (K_{\text{res}} (P_{\text{res},A} - P_{w,12}) c_p T_{\text{res},A})_{\text{in}} t_{\text{step}}$$

$$P_{c,1} = P_{w,1}$$

$$V_{c,1} = V_{c,12} \left(\frac{P_{c,1}}{P_{c,12}} \right)^{\frac{1}{\gamma}}$$

$$V_{w,1} = V_{\text{total}} - V_{c,1}$$

$$m_{w,1} = m_{w,12} + m_{w,\text{in}}$$

$$m_{c,1} = m_{c,12}$$

$$T_{c,1} = \frac{P_{c,1} V_{c,1}}{m_{c,1} R}$$

$$T_{w,1} = \frac{P_{w,1} V_{w,1}}{m_{w,1} R}$$

Appendix B

Table B.1 The nondimensional cutoff and recompression volumes for the indicator diagrams shown in Figure 2.2 are tabulated.

Cutoff Volume (V_{co}/V_{max})	0.3250	0.3355	0.3460	0.3566	0.3671	0.3776	0.3882	0.3987	0.4092	0.4198	0.4303	0.4408	0.4514	0.4619	0.4724										
Recompression Volume (V_{rec}/V_{max})	0.0000	0.0198	0.0396	0.0594	0.0792	0.0990	0.1188	0.1386	0.1584	0.1782	0.1980	0.2178	0.2377	0.2575	0.2773	0.2971	0.3169	0.3367	0.3565	0.3763	0.3961	0.4159	0.4357	0.4555	0.4753

The data points for the plots shown in Figure 2.5 and 2.6 are tabulated for each reservoir. In each table below the pressure of each reservoir is displayed for each cutoff and recompression volume in which an ideal, stable cycle was reached.

Table B.2 Reservoir A pressures and corresponding recompression and cutoff volumes.

Reservoir A pressure (Pres/Pmin)	Cutoff Volume (V_{co}/V_{max})														
	0.3250	0.3355	0.3460	0.3566	0.3671	0.3776	0.3882	0.3987	0.4092	0.4198	0.4303	0.4408	0.4514	0.4619	0.4724
0.0000	0	0	0	0	0	0	0	0	0	0	0	0	0	0	0
0.0198	0	0	9.373	0	9.686	0	0	0	0	0	0	0	0	0	0
0.0396	0	0	9.312	0	0	9.781	9.938	0	0	0	0	0	0	0	0
0.0594	0	0	0	9.405	0	0	9.88	0	0	0	0	0	0	0	0
0.0792	0	0	0	9.342	9.502	0	9.819	0	0	0	0	0	0	0	0
0.0990	0	9.035	0	9.274	0	9.594	9.758	9.92	0	0	0	0	0	0	0
0.1188	0	0	9.087	9.216	9.377	9.532	9.695	9.86	0	0	0	0	0	0	0
0.1386	0	0	9.035	9.149	9.307	9.466	9.632	9.797	9.964	0	0	0	0	0	0
0.1584	0	0	8.997	9.087	9.243	9.401	9.567	9.734	9.902	0	0	0	0	0	0
0.1782	0	0	0	0	9.166	9.337	9.501	9.67	9.839	0	0	0	0	0	0
0.1980	0	0	0	0	9.106	9.268	9.438	0	9.775	9.948	0	0	0	0	0
0.2178	0	0	0	0	9.036	9.196	9.365	0	9.71	9.886	0	0	0	0	0
0.2377	0	0	0	0	8.976	9.124	0	0	9.645	9.82	0	0	0	0	0
0.2575	0	0	0	0	0	9.057	9.236	0	9.577	9.755	9.932	0	0	0	0
0.2773	0	0	0	0	8.91	9	9.157	0	9.509	9.687	9.866	0	0	0	0
0.2971	0	0	0	0	0	8.935	9.095	9.262	9.435	9.618	9.801	0	0	0	0
0.3169	0	0	0	0	0	8.912	9.023	0	0	9.551	9.731	9.917	0	0	0
0.3367	0	0	0	0	0	8.863	8.961	9.114	9.286	9.479	9.662	9.85	0	0	0
0.3565	0	0	0	0	0	0	8.916	9.045	9.229	0	9.594	9.781	0	0	0
0.3763	0	0	0	0	0	0	8.892	8.964	9.148	9.328	9.522	9.713	9.906	0	0
0.3961	0	0	0	0	0	0	0	0	9.067	9.256	9.452	9.641	9.835	0	0
0.4159	0	0	0	0	0	0	0	0	0	0	9.374	9.567	9.764	0	0
0.4357	0	0	0	0	0	0	0	0	0	0	0	0	9.692	9.894	0
0.4555	0	0	0	0	0	0	0	0	0	0	0	0	0	9.819	0
0.4753	0	0	0	0	0	0	0	0	0	0	0	0	0	0	0

Table B.3 Reservoir B pressures and corresponding recompression and cutoff volumes.

Reservoir B pressure (Pres/Pmin)		Cutoff Volume (Vco/Vmax)														
		0.3250	0.3355	0.3460	0.3566	0.3671	0.3776	0.3882	0.3987	0.4092	0.4198	0.4303	0.4408	0.4514	0.4619	0.4724
Recompression Volume (Vrec/Vmax)	0.0000	0	0	0	0	0	0	0	0	0	0	0	0	0	0	0
	0.0198	0	0	6.024	0	6.091	0	0	0	0	0	0	0	0	0	0
	0.0396	0	0	6.013	0	0	6.116	6.15	0	0	0	0	0	0	0	0
	0.0594	0	0	0	6.037	0	0	6.141	0	0	0	0	0	0	0	0
	0.0792	0	0	0	6.026	6.061	0	6.131	0	0	0	0	0	0	0	0
	0.0990	0	5.979	0	6.015	0	6.085	6.121	6.157	0	0	0	0	0	0	0
	0.1188	0	0	5.985	6.005	6.041	6.075	6.111	6.147	0	0	0	0	0	0	0
	0.1386	0	0	5.979	5.994	6.029	6.064	6.101	6.137	6.174	0	0	0	0	0	0
	0.1584	0	0	5.975	5.985	6.018	6.053	6.09	6.127	6.164	0	0	0	0	0	0
	0.1782	0	0	0	0	6.004	6.042	6.078	6.116	6.154	0	0	0	0	0	0
	0.1980	0	0	0	0	5.993	6.03	6.068	0	6.143	6.182	0	0	0	0	0
	0.2178	0	0	0	0	5.981	6.017	6.055	0	6.132	6.172	0	0	0	0	0
	0.2377	0	0	0	0	5.973	6.004	0	0	6.122	6.161	0	0	0	0	0
	0.2575	0	0	0	0	0	5.992	6.034	0	6.11	6.15	6.19	0	0	0	0
	0.2773	0	0	0	0	5.965	5.983	6.019	0	6.098	6.139	6.179	0	0	0	0
	0.2971	0	0	0	0	0	5.972	6.009	6.046	6.086	6.127	6.169	0	0	0	0
	0.3169	0	0	0	0	0	5.97	5.995	0	0	6.116	6.156	6.198	0	0	0
	0.3367	0	0	0	0	0	5.963	5.985	6.02	6.059	6.103	6.145	6.187	0	0	0
	0.3565	0	0	0	0	0	0	5.978	6.008	6.05	0	6.133	6.176	0	0	0
	0.3763	0	0	0	0	0	0	5.976	5.993	6.035	6.076	6.121	6.164	6.209	0	0
0.3961	0	0	0	0	0	0	0	0	6.02	6.063	6.108	6.152	6.196	0	0	
0.4159	0	0	0	0	0	0	0	0	0	0	6.094	6.139	6.184	0	0	
0.4357	0	0	0	0	0	0	0	0	0	0	0	0	6.172	6.218	0	
0.4555	0	0	0	0	0	0	0	0	0	0	0	0	0	6.205	0	
0.4753	0	0	0	0	0	0	0	0	0	0	0	0	0	0	0	

Table B.4 Reservoir C pressures and corresponding recompression and cutoff volumes.

Reservoir C pressure (Pres/Pmin)	Cutoff Volume (Vco/Vmax)														
	0.3250	0.3355	0.3460	0.3566	0.3671	0.3776	0.3882	0.3987	0.4092	0.4198	0.4303	0.4408	0.4514	0.4619	0.4724
0.0000	0	0	0	0	0	0	0	0	0	0	0	0	0	0	0
0.0198	0	0	3.636	0	3.532	0	0	0	0	0	0	0	0	0	0
0.0396	0	0	3.657	0	0	3.502	3.45	0	0	0	0	0	0	0	0
0.0594	0	0	0	3.628	0	0	3.47	0	0	0	0	0	0	0	0
0.0792	0	0	0	3.65	3.596	0	3.492	0	0	0	0	0	0	0	0
0.0990	0	3.76	0	3.674	0	3.567	3.513	3.46	0	0	0	0	0	0	0
0.1188	0	0	3.741	3.694	3.641	3.589	3.535	3.481	0	0	0	0	0	0	0
0.1386	0	0	3.76	3.718	3.666	3.612	3.558	3.503	3.449	0	0	0	0	0	0
0.1584	0	0	3.775	3.741	3.688	3.635	3.581	3.525	3.47	0	0	0	0	0	0
0.1782	0	0	0	0	3.715	3.658	3.604	3.548	3.492	0	0	0	0	0	0
0.1980	0	0	0	0	3.737	3.683	3.626	0	3.515	3.458	0	0	0	0	0
0.2178	0	0	0	0	3.761	3.708	3.652	0	3.538	3.48	0	0	0	0	0
0.2377	0	0	0	0	3.783	3.733	0	0	3.561	3.503	0	0	0	0	0
0.2575	0	0	0	0	0	3.757	3.697	0	3.584	3.526	3.468	0	0	0	0
0.2773	0	0	0	0	3.808	3.777	3.725	0	3.608	3.55	3.491	0	0	0	0
0.2971	0	0	0	0	0	3.8	3.747	3.692	3.634	3.574	3.514	0	0	0	0
0.3169	0	0	0	0	0	3.809	3.772	0	0	3.597	3.538	3.477	0	0	0
0.3367	0	0	0	0	0	3.827	3.794	3.743	3.686	3.623	3.562	3.501	0	0	0
0.3565	0	0	0	0	0	0	3.811	3.768	3.707	0	3.586	3.525	0	0	0
0.3763	0	0	0	0	0	0	3.82	3.796	3.735	3.676	3.612	3.549	3.486	0	0
0.3961	0	0	0	0	0	0	0	0	3.763	3.701	3.636	3.574	3.511	0	0
0.4159	0	0	0	0	0	0	0	0	0	0	3.663	3.6	3.535	0	0
0.4357	0	0	0	0	0	0	0	0	0	0	0	0	3.561	3.495	0
0.4555	0	0	0	0	0	0	0	0	0	0	0	0	0	3.521	0
0.4753	0	0	0	0	0	0	0	0	0	0	0	0	0	0	0

Table B.5 Reservoir D pressures and corresponding recompression and cutoff volumes.

Reservoir D pressure (Pres/Pmin)		Cutoff Volume (Vco/Vmax)														
		0.3250	0.3355	0.3460	0.3566	0.3671	0.3776	0.3882	0.3987	0.4092	0.4198	0.4303	0.4408	0.4514	0.4619	0.4724
Recompression Volume (Vrec/Vmax)	0.0000	0	0	0	0	0	0	0	0	0	0	0	0	0	0	0
	0.0198	0	0	1.589	0	1.311	0	0	0	0	0	0	0	0	0	0
	0.0396	0	0	1.64	0	0	1.221	1.08	0	0	0	0	0	0	0	0
	0.0594	0	0	0	1.552	0	0	1.127	0	0	0	0	0	0	0	0
	0.0792	0	0	0	1.605	1.461	0	1.178	0	0	0	0	0	0	0	0
	0.0990	0	1.848	0	1.661	0	1.374	1.227	1.082	0	0	0	0	0	0	0
	0.1188	0	0	1.81	1.708	1.564	1.425	1.279	1.131	0	0	0	0	0	0	0
	0.1386	0	0	1.849	1.763	1.622	1.48	1.331	1.183	1.033	0	0	0	0	0	0
	0.1584	0	0	1.878	1.811	1.675	1.533	1.385	1.234	1.084	0	0	0	0	0	0
	0.1782	0	0	0	0	1.739	1.587	1.439	1.287	1.135	0	0	0	0	0	0
	0.1980	0	0	0	0	1.79	1.643	1.491	0	1.187	1.031	0	0	0	0	0
	0.2178	0	0	0	0	1.848	1.704	1.552	0	1.241	1.082	0	0	0	0	0
	0.2377	0	0	0	0	1.894	1.764	0	0	1.295	1.137	0	0	0	0	0
	0.2575	0	0	0	0	0	1.82	1.658	0	1.351	1.191	1.031	0	0	0	0
	0.2773	0	0	0	0	1.943	1.867	1.724	0	1.408	1.246	1.084	0	0	0	0
	0.2971	0	0	0	0	0	1.92	1.775	1.625	1.469	1.304	1.138	0	0	0	0
	0.3169	0	0	0	0	0	1.936	1.837	0	0	1.359	1.196	1.028	0	0	0
	0.3367	0	0	0	0	0	1.976	1.887	1.749	1.594	1.419	1.254	1.084	0	0	0
	0.3565	0	0	0	0	0	0	1.923	1.807	1.64	0	1.31	1.14	0	0	0
	0.3763	0	0	0	0	0	0	1.94	1.875	1.709	1.546	1.37	1.196	1.02	0	0
0.3961	0	0	0	0	0	0	0	0	1.778	1.607	1.429	1.257	1.08	0	0	
0.4159	0	0	0	0	0	0	0	0	0	0	1.494	1.319	1.139	0	0	
0.4357	0	0	0	0	0	0	0	0	0	0	0	0	1.199	1.015	0	
0.4555	0	0	0	0	0	0	0	0	0	0	0	0	0	1.077	0	
0.4753	0	0	0	0	0	0	0	0	0	0	0	0	0	0	0	

Appendix C

The assumptions used in the model described in Chapter 2 are tabulated below. Included are the initial properties of each reservoir as well as the warm and cold volumes as well as the flow coefficients for all of the valves in the expander.

Table C.1 Assumptions applying to the pressure reservoirs

Variable/Property	Reservoir A	Reservoir B	Reservoir C	Reservoir D
Temperature	300 K	300 K	300 K	300 K
Pressure (for study in section 2.3)	0.5 MPa	0.5 MPa	0.5 MPa	0.5 MPa
Pressure (for study in section 2.4)	Range from 1.5 to 8.5 MPa with each reservoir at equal pressure when initialized			
Volume	5 Liters	5 Liters	5 Liters	5 Liters
Valve flow coefficient (K)	10^{-7} m-s	10^{-7} m-s	10^{-7} m-s	10^{-7} m-s

Table C.2 Assumptions applying to the expander intake, expander exhaust, the warm volume, and the cold volume.

Variable/Property	Intake	Exhaust	Warm Volume	Cold Volume
Temperature	300 K	300 K	300 K	300 K
Pressure	1 MPa	0.1 MPa	$P_{res,A}$	$P_{res,A}$
Volume	N/A	N/A	$7.28E-6$ m ³	0.0001 m ³
Valve flow coefficient (K)	10^{-6} m-s	10^{-6} m-s	N/A	N/A

Piston motion function

```
function [xnew velnew ap tstep]=piston_motion(delPp, vel, xcl, t_step,...
    mp, Ap, Asurf, gap, xlim, xclc)
g=9.81;
dPgun=0.207e5;%Gunaranjan Stiction pressure (3 psi)
Dgun=0.0244;%Gunaranjan piston diameter (0.96 in)
Dp=sqrt(4/pi*Ap);
Fvisc=dPgun*(Dgun/Dp)*Ap;
Fvisc=Fvisc/50;
if vel>0
    ap=1/mp*(delPp*Ap-mp*g-Fvisc);
elseif vel<0
    ap=1/mp*(delPp*Ap-mp*g+Fvisc);
elseif abs(delPp*Ap-mp*g)<Fvisc
    ap=0;
else
    ap=1/mp*(sign(delPp*Ap-mp*g)*(abs(delPp*Ap-mp*g)-Fvisc));
end
velnew=vel+ap*t_step;
xnew=xcl+vel*t_step+0.5*ap*t_step^2;
ts=0;
tstep=t_step;
if abs(sign(vel)-sign(ap))<=1
    ts=t_step;
else
    ts=-vel/ap;
    if ts==0
        ts=t_step;
    end
end
if ts<t_step
    tstep=ts;
    velnew=0;
    xnew=xcl+vel*tstep+0.5*ap*tstep^2;
end
if xnew>xlim
    xnew=xlim;
    velnew=0;
elseif xnew<xclc
    xnew=xclc;
    velnew=0;
end
end
```

Leakage flow (blow-by) function

```
function mblo=blowby(delP,Pup, Tup, time)
R=2078;
D=0.0873;
L=0.0254; %1 in seal on warm end of piston
gap=0.0005*0.0254;
visc=1.85e-5; %Pa*s. Setting average viscosity
dt=time;
```



```

Vrec_SS=2.5e-5;
%Vrec=Vrec_rat*Vmax;
V_RECOMP=1;
for rit=1:length(Pres_init);
    %for V_CO=1:length(Vco)
    %<<<UNCOMMENT THIS FOR LOOP FOR MULTIPLE CUTOFF VOLUMES
    tic
    %for V_RECOMP=1:length(Vrec)
    %<<<UNCOMMENT THIS FOR LOOP FOR MULTIPLE RECOMPRESSION VOLUMES
        %<<<<<<<<SETTING INITIAL CYCLE STATE
        cutoff_check=0;
        recomp_check=0;
        Vres(:)=Vres_init;
        Pres(:)=[9.0e5 6.0e5 3.5e5 1.5e5];
        Pres_aveInit=sum(Pres(:))/4;

        Pplenum=Pmax;
        Tplenum=Tintake;
        Tres=320; %<<<<NOTE ALL TEMPS ARE EQUAL
        Thx=(Tplenum+300)/2;
        Tintake=Tplenum;
        mres(:)=Pres.*Vres/(R*Tres);
        Res_dens(:)=mres(:)./Vres(:);
        dPpiston(1)=0;%10e3;
        Pw(1)=Pres(1);%Pres(1);
        Pc(1)=Pw(1)+dPpiston(1);
        Vc(1)=Vclc; Vw(1)=Vmax+Vclw+Vclc-Vc(1);
        Xc(1)=Vc(1)/(pi/4*D^2); Xw(1)=Vw(1)/(pi/4*D^2);
        Vp(1)=0; %accel(1)=1/m_piston*(dPpiston(1)*Ap-m_piston*grav);
        accel(1)=0;
        Tw(1)=400;%Tres;
        Tc(1)=100;%Tres;
        mw(1)=Pw(1)*Vw(1)/(R*Tw(1));
        mc(1)=Pc(1)*Vc(1)/(R*Tc(1));
        hw(1)=cp*Tw(1); hc(1)=cp*Tc(1);
        uw(1)=cv*Tw(1); uc(1)=cv*Tc(1);
        totmass_iter(1,1)=mw(1)+sum(mres);
        totmass_iter(2,1)=mc(1);
        mw_tot(1,V_RECOMP)=mw(1)+sum(mres);
        Twave=Tw(1); Tcave=Tc(1);
    for iter=1:ITERATIONS
        Pres_aveInit
        if Pres_aveInit<(0.5*(Pmax/Pmin)*Pmin-5e3) && iter>100 && CNTRL1==1
            increase=1;
            Vco=5e-5;
            reduce=0;
            Vrec=Vrec_SS;
            tdwell_inc=0;
        elseif Pres_aveInit>(0.5*(Pmax/Pmin)*Pmin+5e3) && iter>100 && CNTRL2==1
            reduce=1;
            if STAGE==1
                Vrec=1e-5;
            else
                Vrec=0.5e-5;
            end
            increase=0;
            Vco=3.75e-5;

```



```

        mcin=0;
    end
    mwout=valveflow(Pw(x-1), Pres(RES), Tw(x-1), Pw(x-1)...
        / (R*Tw(x-1)), dt, 1);
    mwout=mwout*mdotadjust;%increasing valve resistance
    if Pw(x-1) - Pres(RES) < 10
        mwout=0;
    end
    if dPpiston(x-1) > 0
        Pupst=Pc(x-1);
        Tupst=(Tcave-Twave)/L*(0.0254)+Twave;
    else
        Pupst=Pw(x-1);
        Tupst=Tw(x-1);
    end
    mblo=blowby(dPpiston(x-1), Pupst, Tupst, dt);
    blo(x)=mblo;
    mw(x)=mw(x-1)+mblo-mwout;
    mc(x)=mc(x-1)+mcin-mblo;
    if dPpiston(x-1) > 0
        Pc(x)=(1/Vc(x))*(Pc(x-1)*Vc(x-1)+(gam-1)*(-Pc(x-1)...
            *(Vc(x)-Vc(x-1))+mcin*cp*Tintake-mblo*cp*Tc(x-1)));
        Pw(x)=(1/Vw(x))*(Pw(x-1)*Vw(x-1)+(gam-1)*(-Pw(x-1)...
            *(Vw(x)-Vw(x-1))+mblo*cp*Twave-mwout*cp*Tw(x-1)));
    else
        mblo=-mblo;%recall that flow up piston shows mblo>0
        Pc(x)=(1/Vc(x))*(Pc(x-1)*Vc(x-1)+(gam-1)*(-Pc(x-1)...
            *(Vc(x)-Vc(x-1))+mcin*cp*Tintake+mblo*cp*Tcave));
        Pw(x)=(1/Vw(x))*(Pw(x-1)*Vw(x-1)+(gam-1)*(-Pw(x-1)...
            *(Vw(x)-Vw(x-1))-mblo*cp*Tw(x-1)-mwout*cp*Tw(x-1)));
    end
else
    display('Bad Intake');
    [xc Vpc acp dt]=piston_motion(dPpiston(x-1), Vp(x-1), Xc(x-1), ...
        (dt), m_piston, Ap, Ap_surf, gap, xlimit, Vclc/(pi/4*D^2));
    Xc(x)=xc; Vp(x)=Vpc; accel(x)=acp;
    Vc(x)=Xc(x)*(pi/4)*D^2;
    Vw(x)=(Vmax+Vclc+Vclw)-Vc(x);
    Xw(x)=Vw(x)/(pi/4*D^2);
    mp_in=mdot_plen*dt;
    mcin=mdot_c_in*dt;
    mwin=valveflow(Pres(RES), Pw(x-1), Tres, res_dens, dt, 1);
    mwin=mwin*mdotadjust;%increasing valve resistance
    if Pplenium-Pc(x-1) < 100
        mcin=0;
    end
    if Pres(RES) - Pw(x-1) < 10
        mwin=0;
    end
    if dPpiston(x-1) > 0
        Pupst=Pc(x-1);
        Tupst=(Tcave-Twave)/L*(0.0254)+Twave;
    else
        Pupst=Pw(x-1);
        Tupst=Tw(x-1);
    end
    mblo=blowby(dPpiston(x-1), Pupst, Tupst, dt);

```



```

end
Xc(y)=xc; Vp(y)=Vpc; accel(y)=acp;
Vc(y)=Xc(y)*(pi/4)*D^2;
Vw(y)=(Vmax+Vclc+Vclw)-Vc(y);
Xw(y)=Vw(y)/(pi/4*D^2);
if dPpiston(y-1)>0
    Pupst=Pc(y-1);
    Tupst=(Tcave-Twave)/L*(0.0254)+Twave;
else
    Pupst=Pw(y-1);
    Tupst=Tw(y-1);
end
mblo=blowby(dPpiston(y-1),Pupst, Tupst,dt);
blo(y)=mblo;
mw(y)=mw(y-1)+mblo-mwout;
mc(y)=mc(y-1)-mblo;
if dPpiston(y-1)>0
    Pc(y)=(1/Vc(y))*(Pc(y-1)*Vc(y-1)+(gam-1)*(-Pc(y-1)...
        *(Vc(y)-Vc(y-1))-mblo*cp*Tc(y-1)));
    Pw(y)=(1/Vw(y))*(Pw(y-1)*Vw(y-1)+(gam-1)*(-Pw(y-1)...
        *(Vw(y)-Vw(y-1))+mblo*cp*Twave-mwout*cp*Tw(y-1)));
else
    mblo=-mblo;%recall that flow up piston shows mblo>0
    Pc(y)=(1/Vc(y))*(Pc(y-1)*Vc(y-1)+(gam-1)*(-Pc(y-1)...
        *(Vc(y)-Vc(y-1))+mblo*cp*Tcave));
    Pw(y)=(1/Vw(y))*(Pw(y-1)*Vw(y-1)+(gam-1)*(-Pw(y-1)...
        *(Vw(y)-Vw(y-1))-mblo*cp*Tw(y-1)-mwout*cp*Tw(y-1)));
end
else
display('Bad Expansion');
[xc Vpc acp dt]=piston_motion(dPpiston(y-1),Vp(y-1),Xc(y-1),...
    (dt), m_piston, Ap, Ap_surf, gap, xlimit, Vclc/(pi/4*D^2));
mwin=valveflow(Pres(RES),Pw(y-1),Tres,res_dens,dt,1);
mwin=mwin*mdotadjust;%increasing valve resistance
if abs(Pres(RES)-Pw(y-1))<10
    mwin=0;
end
Xc(y)=xc; Vp(y)=Vpc; accel(y)=acp;
Vc(y)=Xc(y)*(pi/4)*D^2;
Vw(y)=(Vmax+Vclc+Vclw)-Vc(y);
Xw(y)=Vw(y)/(pi/4*D^2);
if dPpiston(y-1)>0
    Pupst=Pc(y-1);
    Tupst=(Tcave-Twave)/L*(0.0254)+Twave;
else
    Pupst=Pw(y-1);
    Tupst=Tw(y-1);
end
mblo=blowby(dPpiston(y-1),Pupst, Tupst,dt);
blo(y)=mblo;
mw(y)=mw(y-1)+mwin+mblo;
mc(y)=mc(y-1)-mblo;
if dPpiston(y-1)>0
    Pc(y)=(1/Vc(y))*(Pc(y-1)*Vc(y-1)+(gam-1)*(-Pc(y-1)...
        *(Vc(y)-Vc(y-1))-mblo*cp*Tc(y-1)));
    Pw(y)=(1/Vw(y))*(Pw(y-1)*Vw(y-1)+(gam-1)*(-Pw(y-1)...
        *(Vw(y)-Vw(y-1))+mblo*cp*Twave+mwin*cp*Tres));

```

```

else
    mblo=-mblo;%recall that flow up piston shows mblo>0
    Pc(y)=(1/Vc(y))*(Pc(y-1)*Vc(y-1)+(gam-1)...
        *(-Pc(y-1)*(Vc(y)-Vc(y-1))+mblo*cp*Tcave));
    Pw(y)=(1/Vw(y))*(Pw(y-1)*Vw(y-1)+(gam-1)*(-Pw(y-1)...
        *(Vw(y)-Vw(y-1))-mblo*cp*Tw(y-1)+mwin*cp*Tres));
end
end
Tc(y)=Pc(y)*Vc(y)/(mc(y)*R);
Tw(y)=Pw(y)*Vw(y)/(mw(y)*R);
if dPw_exp<0
    mres(RES)=mres(RES)-mwin;
else
    mres(RES)=mres(RES)+mwout;
end
Pres(RES)=mres(RES)*R*Tres/Vres(RES);
%<<<<<<<HEX FLOW ADAPTED CHAUDHRY THESIS FOR ESTIMATIONS
mdot_hx1 = sqrt((Pmax^2 - Pplenum^2)/(3.232e15*f*Thx));
mdot_hx2 = (Pmax^2 - Pplenum^2)/(2.063e10*Thx);
dPc_int=Pplenum-Pc(y-1);
mdot_plen=min(mdot_hx1,mdot_hx2);
if Pplenum>Pmax
    mdot_plen=0;
end
mdot_plen=2*mdot_plen;
mp_in=mdot_plen*dt;
Pplenum=Pplenum + (mp_in)*R*Tplenum/Vplenum;
dPpiston(y)=Pc(y)-Pw(y);
if (y-checkplace)>10000
    display('Update');
    Vc(y)
    Pw(y)
    checkplace=y;
end
if RES==1
    C=1.01;
elseif RES==2
    C=1.01;%1.02;
elseif RES==3
    C=1.01;%1.03;
else
    C=1.01;%1.05;
end
time(y)=time(y-1)+dt;
if RES<NUMRES
    if (time(y)-time(xswitch))>=0.1 || Pw(y)<=C*Pres(RES)
        xswitch=y;
        res_switch_points(RES)=y;
        RES=RES+1;
    end
else
    if (time(y)-time(xswitch))>=0.1 || Pw(y)<=C*Pres(RES) || ...
        Vc(y)>=(Vmax+Vclc)
        if increase==0
            break;
        elseif Pres_aveInit>=0.5e6
            break;
        end
    end
end

```



```

if Pc(j-1)-Pmin<10
    mcout=0;
end
mwin=valveflow(Pres(NUMRES),Pw(j-1),Tres,...
    Pres(NUMRES)/(R*Tres),dt,1);
mwin=mwin*mdotadjust;%<increasing valve resistance
if abs(Pres(NUMRES)-Pw(j-1))<100
    mwin=0;
end
Xc(j)=xc; Vp(j)=Vpc; accel(j)=acp;
Vc(j)=Xc(j)*(pi/4)*D^2;
Vw(j)=(Vmax+Vclc+Vclw)-Vc(j);
Xw(j)=Vw(j)/(pi/4*D^2);
if dPpiston(j-1)>0
    Pupst=Pc(j-1);
    Tupst=(Tcave-Twave)/L*(0.0254)+Twave;
else
    Pupst=Pw(j-1);
    Tupst=Tw(j-1);
end
mblo=blowby(dPpiston(j-1),Pupst, Tupst,dt);
blo(j)=mblo;
mw(j)=mw(j-1)+mblo+mwin;
mc(j)=mc(j-1)-mcout-mblo;
if dPpiston(j-1)>0
    Pc(j)=(1/Vc(j))*(Pc(j-1)*Vc(j-1)+(gam-1)*(-Pc(j-1)...
        *(Vc(j)-Vc(j-1))-mcout*cp*Tc(j-1)-mblo*cp*Tc(j-1)));
    Pw(j)=(1/Vw(j))*(Pw(j-1)*Vw(j-1)+(gam-1)*(-Pw(j-1)...
        *(Vw(j)-Vw(j-1))+mblo*cp*Twave+mwin*cp*Tres));
else
    mblo=-mblo;%recall that flow up piston shows mblo>0
    Pc(j)=(1/Vc(j))*(Pc(j-1)*Vc(j-1)+(gam-1)*(-Pc(j-1)...
        *(Vc(j)-Vc(j-1))-mcout*cp*Tc(j-1)+mblo*cp*Tcave));
    Pw(j)=(1/Vw(j))*(Pw(j-1)*Vw(j-1)+(gam-1)*(-Pw(j-1)...
        *(Vw(j)-Vw(j-1))-mblo*cp*Tw(j-1)+mwin*cp*Tres));
end
else
display('Bad Exhaust');
[xc Vpc acp dt]=piston_motion(dPpiston(j-1),Vp(j-1),Xc(j-1),...
    (dt), m_piston, Ap, Ap_surf, gap, xlimit, Vclc/(pi/4*D^2));
mwout=valveflow(Pw(j-1),Pres(NUMRES),Tw(j-1),...
    Pw(j-1)/(R*Tw(j-1)),dt,1);
mwout=mwout*mdotadjust;%<<increasing valve resistance
if abs(Pw(j-1)-Pres(RES))<10
    mwout=0;
end
mcout=mdot_c_out*dt;
if Pc(j-1)-Pmin<10
    mcout=0;
end
Xc(j)=xc; Vp(j)=Vpc; accel(j)=acp;
Vc(j)=Xc(j)*(pi/4)*D^2;
Vw(j)=(Vmax+Vclc+Vclw)-Vc(j);
Xw(j)=Vw(j)/(pi/4*D^2);

if dPpiston(j-1)>0
    Pupst=Pc(j-1);

```



```

mp_in=mdot_plen*dt;
Pplenum=Pplenum + (mp_in)*R*Tplenum/Vplenum;

time(n)=time(n-1)+dt;
dPpiston(n)=Pc(n)-Pw(n);
%Switch Controls from Chaudhry Thesis
if RES==4 || RES==3
    C=0.98;
else
    C=0.98;
end
if RES>1
    if (time(n)-time(xswitch))>=0.1 || Pw(n)>=C*Pres(RES)
        xswitch=n;
        res_switch_points(1+2*NUMRES-RES)=n;
        RES=RES-1;
    end
else
    if (time(n)-time(xswitch))>=0.1 || Pw(n)>=C*Pres(RES)
        if reduce==0
            break;
        elseif Pres_aveInit<0.5e6
            break;
        elseif Pc(y)>=0.98*Pres(NUMRES) || tdwell_red>=dwell_red
            break;
        else
            tdwell_red=tdwell_red+dt;
        end
    end
end
Pwrec=Pw(n);
n=n+1;
end
res_switch_points(1+2*NUMRES-RES)=n;
Pres_int((NUMRES+1):(2*NUMRES),iter)=[Pres(1);Pres(2);Pres(3);Pres(4)];

if iter>100 && tdwell_red>0
    redcnt=redcnt+1;
elseif iter>100 && tdwell_inc>0
    incnt=incnt+1;
end
%STORING CYCLES. redcnt and incnt can be used to specifically store
%cycles in which helium mass is being added or removed
if iter==1 || iter==101 || rem(iter,100)==0 || rem(iter,25)==0
    bank=bank+1;
    Pc_iter(1:n,bank)=Pc(1:n);
    Pw_iter(1:n,bank)=Pw(1:n);
    mc_iter(1:n,bank)=mc(1:n);
    mw_iter(1:n,bank)=mw(1:n);
    Tc_iter(1:n,bank)=Tc(1:n);
    Tw_iter(1:n,bank)=Tw(1:n);
    Vc_iter(1:n,bank)=Vc(1:n);
    Pres_iter(1:4,bank)=[(Pres_int(1,iter)+Pres_int(5,iter))/2;...
        (Pres_int(2,iter)+Pres_int(6,iter))/2; (Pres_int(3,iter)...
        +Pres_int(7,iter))/2; (Pres_int(4,iter)+Pres_int(8,iter))/2];
    Pres_iter(6,bank)=(sum(Pres_int(1:8,iter)))/8;
end

```

```

Pres_iter(5,bank)=Pres_aveInit;
totmass_iter(1,1+bank)=sum(mres(:))+mw(n);
totmass_iter(2,1+bank)=mc(n);
blo_iter(1:n,bank)=blo(1:n);
dPpiston_iter(1:n,bank)=dPpiston(1:n);
process_switch_iter(1:6,bank)=[i; x; y; z; j; n];
res_switch_iter(1:8,bank)=res_switch_points(1:8);
time_iter(1:n,bank)=time(1:n);
accel_iter(1:n,bank)=accel(1:n);
Vp_iter(1:n,bank)=Vp(1:n);
tdwell_iter(1:2,bank)=[tdwell_inc; tdwell_red];
iter_cnt(bank)=iter;
Twave_iter(bank)=Twave;
Tcave_iter(bank)=Tcave;
end
if iter<ITERATIONS
    Twave=trapz(time(1:n),Tw(1:n))/time(n);
    Tcave=trapz(time(1:n),Tc(1:n))/time(n);
    Pw(1)=Pw(n); Pc(1)=Pc(n);
    Vc(1)=Vc(n); Vw(1)=Vmax+Vclw+Vclc-Vc(1);
    Vp(1)=Vp(n-1); accel(1)=accel(n-1);
    dPpiston(1)=dPpiston(n);
    mblo=0;
    tdwell_red=0; tdwell_inc=0;
    Xc(1)=Xc(n); Xw(1)=Xw(n);
    Tw(1)=Tw(n); Tc(1)=Tc(n);
    mw(1)=mw(n);
    mc(1)=mc(n);
    hw(1)=cp*Tw(1); hc(1)=cp*Tc(1);
    uw(1)=cv*Tw(1); uc(1)=cv*Tc(1);
    time(1)=0;
    cutoff_check=0;
    recomp_check=0;
    Pw(2:end)=0; Pc(2:end)=0; Vc(2:end)=0; Vw(2:end)=0;
    Tw(2:end)=0; Tc(2:end)=0; mw(2:end)=0; mc(2:end)=0;
    hw(2:end)=0; hc(2:end)=0; uw(2:end)=0; uc(2:end)=0;
    Pres_aveInit=sum(Pres_int(1:8,iter))/8;
end
end
pv_plot=plot(Vc(1:n)./(Vmax+Vclc),Pc(1:n)./Pmin,'-b',...
    Vc(1:n)./(Vmax+Vclc),Pw(1:n)./Pmin,'-r');
set(pv_plot,'LineWidth',2);
xlim([0 (Vmax+2*Vclw)/(Vmax+Vclc)]);
ylim([0.98*Pmin/Pmin 1.02*Pmax/Pmin]);
xlabel('Cold End Volume (Vcold/Vmax)','fontsize',25);
ylabel('Pressure (Pcold/Pmin)','fontsize',25);
title('Cycle Pressure vs. Cold End Volume','fontsize',27);
LEG=legend('Pcold','Pwarm');
set(LEG,'fontsize',24);
set(gca,'fontsize',24);
display('FINISHED');
end

```